

**DEFINING CDK4 INHIBITOR-INDUCED SENESENCE AFTER GROWTH ARREST:
A NEW TRANSITION WITH CLINICAL IMPLICATIONS**

by

Mary Elizabeth Klein

A Dissertation

Presented to the Faculty of the Louis V. Gerstner, Jr.

Graduate School of Biomedical Sciences,

Memorial Sloan Kettering Cancer Center

In Partial Fulfillment of the Requirements for the Degree of

Doctor of Philosophy

New York, NY

September 2018

Andrew Koff, PhD
Dissertation Mentor

Date

Copyright by Mary E. Klein 2018

DEDICATION

To my family, whose support, encouragement, and love is immeasurable.

ABSTRACT

With the war on cancer declared almost fifty years ago, a mechanistic understanding of the processes underlying the duplication and segregation of DNA was long considered a useful area for the identification of druggable targets for therapy. Today, specific CDK4/6 inhibitors are among a new generation of therapeutics being broadly applied to the treatment of a variety of human malignancies. *In vitro*, many Rb-positive cell lines exit the cell cycle after CDK4/6 inhibition into quiescence or senescence. The down-regulation of MDM2 drives CDK4 inhibitor-induced senescence in many cell lines derived from multiple types of cancer. In well-differentiated and dedifferentiated liposarcoma, the clinical success of CDK4/6 inhibitors was associated with loss of MDM2 protein after treatment.

In my thesis work, I discovered that the decision of a cell to senesce in response to CDK4/6 inhibition follows the decision of cell cycle exit. This transition, which I called senescence after growth arrest (SAGA), is triggered in CDK4 inhibitor-induced quiescent cells by enhanced turnover of MDM2 protein. In cell lines, PDLIM7 can prevent MDM2 turnover in cells that remain quiescent, but is sequestered away from MDM2 by association with CDH18 in cells that undergo senescence. Remarkably, a retrospective analysis of a clinical trial for the CDK4/6 inhibitor palbociclib revealed that progression free and overall survival were significantly extended in patients whose tumors were CDH18-positive prior to therapy. This supports the notion that SAGA contributes to the clinical efficacy of CDK4/6 inhibitors.

In parallel, I used my discovery of SAGA to design a system where I could identify other transcriptional changes that occur as cells become senescent. Specifically, I created a cell line with stable integration of a doxycycline-inducible promoter that drives expression of MDM2. I showed that when treated with both doxycycline and a CDK4/6 inhibitor, these cells are growth arrested but cannot become senescent. Upon removal of doxycycline, MDM2 is turned over and the cells enter into senescence. The synchronous nature of this system allowed me to find that individual phenotypes of a senescent cell are temporally separated, and I uncovered distinct

transcriptional programs coincident with the acquisition of these hallmarks of senescence. One such finding was that a subset of the senescence-associated secretory program (SASP) is transcribed coincident with the occurrence of irreversible growth arrest. Knockdown of specific SASP factors, including ANGPTL4, prevented the induction of irreversible growth arrest if lowered in a quiescent cell. This work highlights the importance of understanding not only biological endpoints but also the specific transitions between such endpoints, and yields unprecedented insight into how cells enter into senescence after growth arrest.

ACKNOWLEDGEMENTS

“Extraordinary lives are built by dancing along the edge of our comfort zones, and leaving them whenever possible.” – Unknown

Andy, perhaps the greatest lesson you have taught me is that sometimes you have to jump off the cliff. Thank you for giving me the freedom to jump and the support that made me unafraid to fall. Without your mentorship, guidance, and discussions, I never would have had the opportunity or the inspiration to ask the crazy questions. Thank you for always challenging my ideas when I thought I was right, and encouraging me when I was sure everything was going wrong. Your passion for science is contagious, and I am so glad I showed up in your office with my yellow notepad six years ago. A truly wonderful boss is hard to find but impossible to forget.

I have the deepest appreciation for all the scientists who have guided me throughout my PhD. To my committee, Mary and Xiaolan, thank you for all your suggestions, advice, discussions, and support in and outside of thesis meetings. John, thank you for agreeing to chair not only my thesis committee, but also my proposal exam so many years ago, and thank you Greg for your willingness to serve as an external advisor. Thank you Bill for countless discussions on how we can translate basic science into the clinic and the hard work of you, Mark, and Ellie to obtain the clinical samples and records needed. I am so grateful to Cristina, Afsar, Katia, Li-Xuan, and my clinical mentor Maura, for not only providing their incredible expertise to my projects, but also for taking the time to teach a graduate student what underlies their mastery and giving me so many tools I can use in the future.

To everyone in the Koff lab, thank you for being a part of my journey. My work stands on the shoulders of the giants that came before me and would not have been possible without the foundation laid by Aimee, David, and Marta. As a part of the lab, I have had the great fortune to work alongside colleagues I admire who are also friends I trust. To Marta- thank you for your

undying optimism when I needed it most. Being your baymate for 4 years made me a more thoughtful and passionate scientist, and I could not ask for a more amazing friend to share this experience with. To Jossie- thank you for all the smiles and laughs, coming into work with you brightened every day and I'm glad we had the opportunity to grow as scientists together. To Caroline- thank you for celebrating my successes as if they were your own, even when I wasn't sure they should be celebrated. You have made my last year in lab so special, and it has been my great pleasure to sit beside you.

Thank you to all my friends in New York, Pennsylvania, Arizona, and beyond for reminding me that there is life outside the laboratory. The memories I have made in the last six years are some of my fondest, and I'm glad to have gone on this crazy ride with all of you.

I am forever grateful for the love of my family. To my mom who is my biggest cheerleader and the most supportive person I know, to my dad who always taught me to reach higher and pursue my dreams, and to my sister who is always a phone call and last minute plane ride away when I need an escape, thank you for all that you do for me.

Finally, thank you Scott for standing beside me no matter what research or life threw at us. I do not know how getting through the PhD lows would have been possible without you; and I certainly know the successes would not have been nearly as high if I did not have you to share them with. Your love, kindness, and generosity makes me a better person, and I am so glad you are my partner in science and in life. The completion of our PhDs signals the bittersweet end of one chapter, and the beginning of so much more.

TABLE OF CONTENTS

LIST OF TABLES	xi
LIST OF FIGURES	xii
LIST OF ABBREVIATIONS	xiv
CHAPTER 1: INTRODUCTION.....	1
Mechanism of action of CDK4/6 inhibitors	1
A brief history of cancer therapy.....	1
The importance of cyclin D-CDK4/6 in the cell cycle.....	2
CDK4/6 inhibitors: A trio of compounds with distinct advantages	3
The mechanism of action of CDK4/6 inhibitors may not be as simple as once thought	6
CDK4/6 in the tumor microenvironment	11
The impact of CDK4/6 inhibitors on cellular metabolism	13
The outcome of CDK4/6 inhibition can be quiescence or senescence.....	15
Cellular Senescence	17
Defining senescence	17
Pathways into senescence.....	19
Thesis Objectives	21
CHAPTER 2: MATERIALS AND METHODS.....	23
Cell lines.....	23
Lentivirus constructs	23
Real-time quantitative PCR.....	23
Immunoblots.....	26
Immunoprecipitation	26
Senescence Assays	26
Immunofluorescence	27
CRISPR/Cas9	28
Immunohistochemistry	28
Patient Sample Usage.....	29
Statistical analysis	29
RNA sequencing.....	29
Heatmap generation and gene set enrichment analysis	33

CHAPTER 3: PDLIM7 AND CDH18 DEPENDENT REGULATION OF MDM2 IS A CLINICALLY RELEVANT MECHANISM OF ACTION FOR CDK4 INHIBITORS	34
Introduction	34
Well-differentiated and dedifferentiated liposarcoma	34
WD/DDLS cell lines undergo quiescence or senescence after CDK4 inhibition.....	35
Changes in MDM2 expression underlie the decision between quiescence and senescence	35
Changes in MDM2 expression associate with WD/DDLS patient outcome.....	36
Known regulators of MDM2	36
Results	37
MDM2 turnover is increased in cells that undergo senescence	37
HAUSP dissociates from MDM2 as cells exit the cell cycle	41
PDLIM7 knockdown allows PD0332991 to induce senescence in non-responder cells	45
Co-knockdown of PDLIM7 and HAUSP is sufficient to induce senescence in LS8107 cells	45
The association of PDLIM7 with MDM2 is cell line and condition dependent	50
The cytosolic distribution of PDLIM7 is cell line and condition dependent	50
PDLIM7 is associated with CDH18 in foci.....	54
Knockout of CDH18 prevents PD0332991 induced MDM2 turnover and senescence	59
CDH18 is expressed at higher levels in responder cells than non-responder cells	64
CDH18 expression correlates with extended progression free and overall survival in WD/DDLS patients treated with palbociclib	64
Discussion	73
When one pathway isn't enough: the context dependent regulation of MDM2.....	73
Beyond the plasma membrane: intracellular cadherin expression	75
From bedside to bench and back again: SAGA is a clinically relevant mechanism	77
 CHAPTER 4: CDK4 INHIBITORS DRIVE SENESCENCE AFTER GROWTH ARREST	 80
Introduction	80
Quiescence vs. senescence	80
Results	83
CDK4 inhibition drives senescence after growth arrest	83
LS8817 ^{TetONFMDM2} system allows for the separation of senescence phenotypes over time.....	88
Discussion	93
SAGA separates cell cycle exit from entry into and deepening of senescence.....	93
Potential applications of the LS8817 ^{TetONFMDM2} system	94

CHAPTER 5: PROFILING THE TEMPORAL DYNAMICS OF GENE TRANSCRIPTION DURING CDK4 INHIBITOR-INDUCED SENESCENCE	97
Introduction	97
The tripartite phenotype defining senescence	97
Challenges of profiling senescence	97
Results	99
Profiling transcriptional changes as cells progress into senescence.....	99
Gene changes associated with entry into and early senescence	102
A senescence-associated secretory program arises coincident with irreversible growth arrest	105
Knockdown of ANGPTL4 blocks CDK4 inhibitor induced irreversible cell cycle exit.....	111
Knockdown of ANGPTL4 suggests the presence of multiple, parallel SASP pathways.....	111
Discussion	113
Transcriptional changes: an evolution over time.....	113
The complex actions and regulation of the SASP	115
Functions of ANGPTL4	117
Senescence: one state or many pathways?	119
 CHAPTER 6: DISCUSSION	 122
Senescence after growth arrest links MDM2 regulation to therapeutic outcomes in cancer	123
Quiescence is an actively inactive state	127
Exploiting senescence after growth arrest to combat age-associated pathologies	130
 REFERENCES.....	 134

LIST OF TABLES

Table 1.1. Drug characteristics of CDK4/6 inhibitors.....	4
Table 1.2. IC50 of CDK4/6 inhibitors in cell free assays.....	5
Table 1.3. List of ongoing clinical trials with CDK4/6 inhibitors in combination with one or more other therapies.....	8
Table 2.1. shRNA sequences.....	24
Table 2.2. Primer sequences for RT-qPCR analysis.....	25
Table 3.1. Patient characteristics based on CDH18 status.....	71
Table 5.1. Genes implicated previously in the SASP.....	106

LIST OF FIGURES

Figure 1.1. Cytostatic growth arrest after CDK4/6 inhibition.....	10
Figure 1.2. CDK4/6 inhibitor induced immunologic changes.....	12
Figure 1.3. Metabolic consequences of CDK4/6 inhibition.....	14
Figure 1.4. Possible outcomes of cell cycle exit.....	16
Figure 1.5. Keywords associated with publications pertaining to senescence.....	18
Figure 1.6. Triggers of senescence.....	20
Figure 3.1. Known mechanisms that can affect MDM2 ubiquitin dependent turnover.....	38
Figure 3.2. PD0332991 induces accelerated MDM2 turnover in LS8817 cells.....	39
Figure 3.3. MG132 causes accumulation of MDM2 protein in responder cells treated with PD0332991....	40
Figure 3.4. Mutating the E3 ligase domain of MDM2 prevents PD0332991 induced turnover.....	42
Figure 3.5. HAUSP dissociates from MDM2 after treatment with PD0332991.....	43
Figure 3.6. PDLIM7 knockdown allows PD0332991 to induce MDM2 down regulation and accumulation of SA-β-Gal in responder cell lines.....	44
Figure 3.7. shRNA knockdown screen targeting known regulators of MDM2.....	46
Figure 3.8. PDLIM7 knockdown allows PD0332991 to induce accumulation of SA-β-Gal in non-responder LS8313 cells and can be rescued by expression of a wobble mutant PDLIM7.....	47
Figure 3.9. PDLIM7 knockdown allows PD0332991 to induce senescence in LS8107 cells.....	48
Figure 3.10. PDLIM7 knockdown allows PD0332991 to induce MDM2 down-regulation in LS8107 cells.	49
Figure 3.11. PDLIM7 and HAUSP co-knockdown induces accumulation of SA-β-Gal in non-responder LS8107 cells.....	51
Figure 3.12. The association of PDLIM7 and MDM2 is cell line and condition dependent.....	52
Figure 3.13. PDLIM7 is located in foci in LS8817 cells.....	53
Figure 3.14. Immunofluorescence staining of cytoskeletal elements in LS8817 and LS8107 cells.....	55
Figure 3.15. Immunofluorescence staining of pan-cadherin in a variety of cell lines.....	56
Figure 3.16. PDLIM7 is associated with pan-cadherin foci in a cell line and condition dependent manner.	57
Figure 3.17. Knocking down CDH18 can reduce the appearance of pan-cadherin foci in LS8817 cells.....	58
Figure 3.18. Generation of CDH18 knockout cell lines.....	60
Figure 3.19. PDLIM7 is associated with CDH18 in foci in LS8817 cells.....	61
Figure 3.20. Knockout of CDH18 prevents CDK4 inhibitor induced senescence in LS8817 cells.....	62
Figure 3.21. Knockout of CDH18 prevents CDK4 inhibitor induced MDM2 turnover in LS8817 cells.....	63
Figure 3.22. CDH18, PDLIM7, MDM2 and CDK4 protein expression levels.....	65
Figure 3.23. CDH18 detection by immunohistochemistry.....	67
Figure 3.24. CDH18 expression and characteristics of the patient samples used in this study.....	68

Figure 3.25. CDH18 expression can stratify WD/DDLS patient response to palbociclib monotherapy.....	69
Figure 3.26. Other clinical factors do not stratify patient response to palbociclib monotherapy.....	70
Figure 3.27. CDH18 expression can stratify DDLS patient response to palbociclib monotherapy.....	72
Figure 3.28. Mechanisms underlying CDK4 inhibitor induced quiescence and senescence.....	79
Figure 4.1. Models of the relationship between senescence and quiescence.....	82
Figure 4.2. Knockdown of MDM2 drives senescence after growth arrest.....	84
Figure 4.3. Plasmid map of TetON FLAG-MDM2.....	85
Figure 4.4. Expression of FLAG-MDM2 in LS8817 ^{TetONFMDM2} cells is controlled by doxycycline.....	86
Figure 4.5. LS8817 ^{TetONFMDM2} cells can be induced to enter a stable quiescent or senescent state by PD0332991.....	87
Figure 4.6. The TetONFMDM2 system is not PD0332991 or cell line dependent.....	89
Figure 4.7. LS8817 ^{TetONFMDM2} cells acquire hallmarks of senescence over time.....	90
Figure 4.8. LS8817 ^{TetONFMDM2} system offers sharper resolution of the acquisition of senescence hallmarks.....	91
Figure 4.9. LS8817 ^{TetONFMDM2} cells become irreversibly arrested 14 days after doxycycline removal.....	92
Figure 4.10. Illustration of LS8817 ^{TetONFMDM2} system and phenotype acquisition over time.....	95
Figure 5.1. Principle component analysis of LS8817 ^{TetONFMDM2} cells across the time course.....	100
Figure 5.2. Hierarchical cluster analysis of gene expression changes across the time course.....	101
Figure 5.3. Heatmap of gene expression changes during the progression of senescence after growth arrest.	103
Figure 5.4. Gene ontology terms identified by gene set enrichment analysis across the time course.....	104
Figure 5.5. Hierarchical cluster analysis of SASP genes across the time course.....	107
Figure 5.6. TRANSFAC analysis of the 37 SASP genes.....	109
Figure 5.7. Expression levels of 13 SASP genes from Cluster 1 in additional senescence data sets.....	110
Figure 5.8. Evaluating senescence hallmarks after knockdown of conserved SASP.....	112
Figure 5.9. RT-qPCR of SASP genes after knockdown of ANGPTL4 reveals a bimodal response.....	114
Figure 5.10. Illustration of the pathways to senescence.....	121
Figure 6.1. Possible physiological consequences of exiting quiescence.....	128
Figure 6.2. Countering the senescence burden by preventing SAGA.....	132

LIST OF ABBREVIATIONS

CDK	Cyclin-dependent kinase
Rb	Retinoblastoma protein
MDM2	Mouse double minute 2
PDLIM7	PDZ and LIM domain 7
CDH18	Cadherin 18
WD/DDLS	Well-differentiated and dedifferentiated liposarcoma
NSCLC	Non-small cell lung cancer
shRNA	Short-hairpin RNA
RT-qPCR	Real-time quantitative polymerase chain reaction
PFS	Progression free survival
OS	Overall survival
PD	PD0322991 or palbociclib, CDK4/6 inhibitor
Dox	Doxycycline
SA-β-Gal	Senescence-associated beta-galactosidase
SAHF	Senescence-associated heterochromatic foci
SASP	Senescence-associated secretory program
ROS	Reactive oxygen species
SAGA	Senescence after growth arrest

CHAPTER 1: INTRODUCTION

Mechanism of action of CDK4/6 inhibitors

A brief history of cancer therapy

Cancer is an ancient disease, with documentation from as early as 3000 BCE describing a tumor as a grave malignancy with no treatment [1]. While significant advances have been made, many of the earliest treatments developed, including aggressive surgeries and cytotoxic agents, are still the standards of care today [2, 3]. By 1970, as medicine was advancing and mortality rates from treatable and preventable diseases were dropping, cancer became, and remains today, the second leading cause of death in the United States [4]. This prompted the National Cancer Act of 1971, which signified the nation's renewed commitment to the 'war on cancer'.

In the almost 50 years since, we have gained considerable understanding of the genetic and molecular basis of many types of cancer. Tumor growth and progression generally requires sustained proliferative signaling, loss of growth suppression, avoidance of immune destruction, replicative immortality, tumor promoting inflammation, invasion and metastasis, angiogenesis, resistance to cell death, and perturbed cellular energetics [5]. Underlying these activities are genome instability, DNA mutations, and epigenetic alterations.

The identification of oncogenes and tumor suppressors, combined with revolutions in sequencing, has led to a significant increase in the number of targeted therapies that have been developed and employed in clinical trials for patients with druggable 'driver' mutations [6, 7]. Other clinical strategies aim to treat not just the tumor cell, but also the microenvironment by blocking angiogenesis, limiting inflammation, or harnessing the power of the immune system [8, 9]. In all cases, it is clear that successful treatment of tumors will require knowledge of the molecular mechanisms underlying response in order to predict which patients will respond to treatment and to develop rational combination therapies that will yield maximal clinical benefit.

The importance of cyclin D-CDK4/6 in the cell cycle

Due to the ability of tumor cells to evade growth suppression and maintain proliferation, a mechanistic understanding of the processes underlying the duplication and segregation of DNA was long considered a useful area for the identification of druggable targets for therapy. In the 1990s, the cyclin/cyclin-dependent kinase (CDK) holoenzyme was identified as a key driver of a number of mammalian cell cycle transitions, and the first non-specific CDK inhibitors were evaluated in the clinic over the next ten years. Such pan-CDK inhibitors had limited success, due in part to dose limiting toxicities [10]. Today, specific inhibitors that target CDK4 and CDK6 including palbociclib, abemaciclib and ribociclib are available. These have more limited toxicities, which allows for broad use to treat a variety of neoplasms. Currently, CDK4/6 inhibitors are being employed both as single agents and in combination with signaling pathway inhibitors in numerous clinical trials to evaluate their efficacy (Klein et al, *Cancer Cell* 2018). An understanding of how these inhibitors exert their anti-tumorigenic effects will aid in determining how to use them effectively in the future.

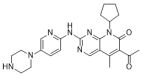
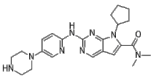
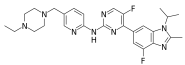
CDK4/6 activity bridges multiple extracellular signaling pathways to the cell cycle [11]. Both non-immortal non-transformed cells and many transformed tumor cells commit irreversibly to the mitotic cell cycle in the G₁ phase. Commitment depends on the phosphorylation and inactivation of the retinoblastoma tumor suppressor protein, Rb. The growth suppressive properties of Rb are largely, but not completely, associated with its binding to the transcription factor E2F and repressing transcription at target promoters [12-14]. Phosphorylation of Rb destabilizes its interaction with E2F and other transcriptional regulators. In normal cells, the phosphorylation of Rb is typically carried out by the sequential actions of the CDK4 or CDK6 kinases in complex with a positive regulatory D-type cyclin subunit, followed by cyclin E/CDK2 complexes [15, 16]. Additionally, extracellular signals regulate the expression of cyclins and CDK inhibitors, like p16^{Ink4a}, p21^{Cip1}, and p27^{Kip1}, the first of which inhibits the CDK4/6 kinases whereas the latter two inhibit the CDK2 kinase [11].

In virtually all human cancer cells, this circuit is dysregulated by either overexpression of cyclin D1, loss of p16^{Ink4a}, the mutation of CDK4 to an Ink4-refractory state, or the loss of Rb itself [12]. This not only affects how the cell responds to extracellular signals, but also can affect the requirement for sequential ordered phosphorylation by the CDKs during inactivation of Rb. Importantly, while the viability of CDK4 null mice reveals that loss of CDK4 is dispensable for the proliferation of many cell types, crossing cancer prone models of mice into a CDK4 or cyclin D1 deficient background prevents or delays tumor formation, demonstrating the importance of this enzyme complex for tumor growth in multiple models [17-25]. This suggests that CDK4-specific inhibitors might be beneficial for the treatment of a variety of tumors.

CDK4/6 inhibitors: A trio of compounds with distinct advantages

Palbociclib was the first CDK4/6 inhibitor to demonstrate clinical efficacy [26], and two others soon followed. Ribociclib is structurally similar to palbociclib, and abemaciclib is significantly less similar to either one (**Table 1.1**). *In vitro* studies using cyclin D1/CDK4 and various cyclin D/CDK6 kinase complexes determined that palbociclib has similar potency on cyclin D1/CDK4 and cyclin D2/CDK6 [27]. In contrast, abemaciclib and ribociclib are both more potent against CDK4 than CDK6 [28, 29]. Abemaciclib also has modest activity, relative to its CDK4 inhibitory activity, against cyclin T1/CDK9, cyclin E2/CDK2, p25/CDK5 and p35/CDK5 [28] (**Table 1.2**). However, these drugs are remarkably specific in their ability to inhibit the proliferation of Rb-positive tumor cells, but not Rb-negative tumor cells [30, 31], suggesting that these differences in the *in vitro* profiles may not correlate with their *in vivo* activity.

All three CDK4/6 inhibitors are administered orally, but have differing pharmacokinetics (**Table 1.1**). Both palbociclib and ribociclib are dosed once daily whereas abemaciclib is dosed twice daily. Ribociclib is notable for achieving high maximum plasma concentrations (exceeding 2 µg/mL) with a long half-life. This may translate to higher cerebrospinal fluid concentrations for ribociclib compared to palbociclib and abemaciclib as noted in mouse models [32-34].

	Structure	IC ₅₀ in cell free assay	C _{max} (nM)	t _{max} (hr)	t _{1/2} (hr)	K _{p,uu} in mouse models	Toxicities in phase 3 trials	Dosing schedule
Palbociclib (PD0332991)		CDK4 (11 nM) CDK6 (15 nM)	200-260	4-8	28	0.01	Neutropenia	125 mg PO daily for 21 out of every 28 days (in combination with hormone therapy)
Ribociclib (LEE011)		CDK4 (10 nM) CDK6 (39 nM)	4,000-7,000	2-5	30-50	0.12	Neutropenia	600 mg PO daily for 21 out of every 28 days (in combination with hormone therapy)
Abemaciclib (LY2835219)		CDK4 (2 nM) CDK6 (9.9 nM)	500-600	4	NR (21 hr for a single dose)	0.03	GI distress, neutropenia (not dose-limiting)	200 mg PO daily continuously (as a monotherapy)

NR = not reported

Table 1.1. Drug characteristics of CDK4/6 inhibitors

CDK family kinase complex	IC ₅₀ (nM) by cell free assay		
	Palbociclib	Ribociclib	Abemaciclib
CDK4/CyclinD1	11	8	2
CDK4/CyclinD3	9	NR	NR
CDK6/CyclinD1	NR	NR	9.9
CDK6/CyclinD2	15	NR	NR
CDK6/CyclinD3	NR	39	NR
CDK1/CyclinB	>10 μ M	>1.5 μ M	1,627
CDK2/CyclinA	>10 μ M	>1.5 μ M	NR
CDK2/CyclinE2	>10 μ M	>1.5 μ M	504
CDK5/p25	>10 μ M	>1.5 μ M	355
CDK5/p35	NR	>1.5 μ M	287
CDK7/CyclinH1	NR	>1.5 μ M	3,910
CDK9/CyclinT1	NR	1510	57
References	Fry et al 2004	Tripathy et al 2017	Gelbert et al 2014

NR = not reported

Table 1.2. IC₅₀ of CDK4/6 inhibitors in cell free assays

Additionally, there are marked differences in the toxicity profiles of the inhibitors for reasons that are not completely clear. Grade 3-4 neutropenia is observed in approximately 60% of patients taking palbociclib and ribociclib [10, 35]. Abemaciclib appears to be better tolerated overall, with only 55% of patients experiencing severe adverse events (as compared to 70-80% with ribociclib and palbociclib), and only 21% have grade 3-4 neutropenia. However, 10% of patients treated with abemaciclib develop grade 3 diarrhea, which is very rare with the other two inhibitors [10, 35]. Due to the significant myelotoxicity of palbociclib and ribociclib, both drugs require dose-interruption and are administered on a three-weeks-on, one-week-off schedule to allow bone marrow recovery. In contrast, abemaciclib is dosed continuously.

Preclinical studies of CDK4/6 inhibitors have evaluated their potential as a single agent in over 30 different cancer subtypes with diverse driver mutations (reviewed in [36]). In addition, their effectiveness in combination with targeted signaling pathway inhibitors and cytotoxic therapies is being evaluated in numerous clinical trials (**Table 1.3**). Pioneering trials have shown promising clinical efficacy for Rb-positive patients and led to approval for this class of compounds. However, there is a subset of patients that obtain no clinical benefit in each trial, and predictors of response have not emerged [10]. Therefore, to optimize clinical benefit with CDK4/6 inhibitors, it will be critical to determine the cellular mechanisms by which they act.

The mechanism of action of CDK4/6 inhibitors may not be as simple as once thought

The simplest explanation for the success of CDK4/6 inhibitors in the clinic is their ability to induce growth arrest. Hypothetically, all Rb-positive tumor cells treated with CDK4/6 inhibitors could undergo G₀-G₁ cell cycle exit, leading to a cytostatic clinical response in all patients. In support of this model, intrinsic and acquired resistance to CDK4/6 inhibitors *in vitro* is often found to involve G₁ bypass mechanisms such as non-canonical cyclin D1-CDK2 complex formation, amplification of cyclin E1, amplification of CDK6, loss of Rb, or loss of p16^{Ink4a} [37-41].

	Combination	Dosing schedule	Disease	Phase	Identifier
Palbociclib	Trastuzumab-DM1 (HER2 antibody)	Palbociclib days 5-18 (21 day cycle) Trastuzumab day 1	HER2 ⁺ breast cancer	Ib	NCT1976169
	Tucatinib (HER2i) + Letrozole (aromatasei)	Palbociclib days 1-21 (28 day cycle) Letrozole and Tucatinib days 1-28	HR ⁺ , HER2 ⁺ breast cancer	Ib/II	NCT03054363
	Anastrozole (aromatasei) + Trastuzumab + Pertuzumab (HER2i)	Palbociclib days 1-21 (28 day cycle) Anastrozole days 1-28 Trastuzumab and Pertuzumab once every 21 days	HR ⁺ , HER2 ⁺ breast cancer	I/II	NCT03304080
	Bazedoxifene (ER modulator)	Not stated	HR ⁺ breast cancer	Ib/II	NCT02448771
	SAR439859 (ER degrader)	Palbociclib days 1-21 (28 day cycle) SAR439859 days 1-28	ER ⁺ breast cancer	I/II	NCT03284957
	GDC-0810 (ER downregulator)	Palbociclib days 1-21 (28 day cycle) GDC-0810 days 1-28	ER ⁺ /HER2 ⁺ breast cancer	I/II	NCT01823835
	Gedatolisib (PI3K/mTORi) + Fulvestrant (ER antagonist)	Palbociclib days 1-21 (28 day cycle) Gedatolisib days 1, 7, 14, 21; Fulvestrant day 1	ER ⁺ /HER2 ⁺ breast cancer	I	NCT02626507
	Gedatolisib (PI3K/mTORi)	Palbociclib days 1-21 (28 day cycle) Gedatolisib days 1, 7, 14, and 21	Solid tumors	I	NCT03065062
	Copanlisib (PI3Ki) + Letrozole	Palbociclib days 1-21 (28 day cycle) Copanlisib days 1, 8, and 15; Letrozole days 1-28	HR ⁺ , HER2 ⁺ breast cancer	Ib/II	NCT03128619
	GDC-0077 (PI3Ki) + Letrozole	Palbociclib days 1-21 (28 day cycle) GDC-0077 and Letrozole days 1-28	PIK3CA mutant, HR ⁺ , HER2 ⁺ breast cancer	I/II	NCT03006172
	AZD2014 (mTORC1/2i) +Fulvestrant	Not stated	ER ⁺ breast cancer	I/II	NCT02599714
	Everolimus (mTORi) + Exemestane (aromatasei)	Palbociclib days 1-21 (28 day cycle) Everolimus and Exemestane days 1-28	ER ⁺ , HER2 ⁺ breast cancer	Ib/IIa	NCT02871791
	PD-0325901 (MEKi)	Palbociclib and PD-0325901 days 1-21 (28 day cycle)	KRAS mutant non-small cell lung cancer, solid tumors	I/II	NCT02022982
	Binimetinib (MEKi)	Palbociclib days 1-21 (28 day cycle) Binimetinib days 1-28	KRAS mutant non-small cell lung cancer	I/II	NCT03170206
	Neratinib (pan-ERBBi)	Palbociclib and Neratinib days 1-21 (28 day cycle)	EGFR, HER2/3/4 amplified/mutated advanced cancers	I	NCT03065387
	Ibrutinib (BTKi)	Palbociclib days 1-21 (28 day cycle) Ibrutinib days 1-28	Mantle cell lymphoma	I	NCT02159775
	Erdafitinib (FGFRi) + Fulvestrant	Palbociclib days 1-21 (28 day cycle) Erdafitinib days 1-28; Fulvestrant day 1	ER ⁺ /HER2 ⁺ /FGFR amplified breast cancer	I	NCT03238196
	Cetuximab (EGFRi)	Palbociclib days 1-21 (28 day cycle) Cetuximab once weekly	Squamous cell carcinoma of the head and neck	II	NCT02499120
	Sorafenib (RTKi) OR Decitabine OR Dexamethasone	Palbociclib days 1-21 (28 day cycle); Sorafenib days 1-28 Palbociclib days 1-7 (28 day cycle); Decitabine days 8-12 Palbociclib days 1-21 (28 day cycle); Dexamethasone days 1-4 and days 15-18	Relapsed and refractory leukemias	I	NCT03132454
	Bicalutamide (anti-androgen)	Palbociclib days 1-21 (28 day cycle) Bicalutamide days 1-28	AR ⁺ breast cancer	I/II	NCT02605486
	Anastrozole (aromatasei)	Palbociclib days 1-21 (28 day cycle) Anastrozole days 1-28	HER2 ⁺ breast cancer	II	NCT02942355
	Tamoxifen (anti-mitotic)	Palbociclib days 1-21 (28 day cycle) Tamoxifen days 1-28	HR ⁺ , HER2 ⁺ breast cancer	II	NCT02668666
	Cisplatin OR Carboplatin	Palbociclib days 2-22 (28 day cycle) Cisplatin or carboplatin day 1	Advanced solid tumors	I	NCT02897375
	Carboplatin	Palbociclib days 1-14 (21 day cycle) Carboplatin day 1	Squamous cell carcinoma of the head and neck	II	NCT03194373
	5-FU (nucleotide analog) + Oxaliplatin (platinum-based)	Palbociclib days 1-7 (14 day cycle) 5-fu/Oxaliplatin day 8	Advanced solid tumors	I	NCT01522989
	Bortezomib (proteasomei)	Palbociclib days 1-12 (21 day cycle) Bortezomib days 8,11,15,18	Mantle cell lymphoma	I	NCT01111188
	Paclitaxel (anti-mitotic)	Palbociclib days 1-21 (28 day cycle) Paclitaxel days 1, 8, 15	Pancreatic ductal adenocarcinoma	I	NCT02501902
	Paclitaxel	Not stated	Advanced breast cancer	I	NCT01320592
Avelumab (anti PD-L1) + Fulvestrant	Palbociclib days 2-22 (28 day cycle) Avelumab once every two weeks; Fulvestrant day 1	ER ⁺ /HER2 ⁺ metastatic breast cancer	II	NCT03147287	

Table 1.3. List of ongoing clinical trials with CDK4/6 inhibitors in combination with one or more other therapies

	Combination	Dosing schedule	Disease	Phase	Identifier	
Ribociclib	Trastuzumab (HER2 antibody)	Ribociclib days 5-18 (21 day cycle); Trastuzumab day 1	HER2 ⁺ breast cancer	I/II	NCT02657343	
	LSZ102 (ER degrader)	Not stated	ER ⁺ breast cancer	I	NCT02734615	
	Everolimus (mTORi)	Ribociclib days 1-21 (28 day cycle) Everolimus days 1-28	Pancreatic adenocarcinoma	I/II	NCT02985125	
	Everolimus + Letrozole	All drugs days 1-28 (28 day cycle)	Endometrial cancer	II	NCT03008408	
	Everolimus	Ribociclib days 1-21 (28 day cycle) Everolimus days 1-28	Dedifferentiated liposarcoma and Leiomyosarcoma	II	NCT03114527	
	Everolimus	Ribociclib days 1-21 (28 day cycle) Everolimus days 1-28	Neuroendocrine tumors	II	NCT03070301	
	Everolimus + Exemestane (aromatasei)	Ribociclib days 1-21 (28 day cycle) Everolimus + Exemestane days 1-28	HR ⁺ , HER2 ⁻ breast cancer	I	NCT01857193	
	BLY719 (PI3Ki) + Letrozole	Ribociclib days 1-21 (28 day cycle) BLY719 + Letrozole days 1-28	ER ⁺ breast cancer	I	NCT01872260	
	BLY719 OR BKM120 (pan-PI3Ki) + Fulvestrant	Ribociclib days 1-21 (28 day cycle) BLY719 or BKM120 days 1-28; Fulvestrant day 1	ER ⁺ /HER2 ⁻ breast cancer	I/II	NCT02088684	
	Trametinib (MEKi)	Not stated	Advanced solid tumors	I/II	NCT02703571	
	MEK162 (MEKi)	Ribociclib days 1-21 (28 day cycle) MEK162 days 1-28	NRAS mutant melanoma	Ib/II	NCT01781572	
	LGX818 (RAFi) + MEK162	Ribociclib days 1-21 (28 day cycle) LGX818 + MEK162 days 1-28	BRAF dependent advanced solid tumors	I/II	NCT01543698	
	EGF816 (EGFRi)	Not stated	EGFR mutant non-small cell lung cancer	I	NCT03333343	
	Ceritinib (ALKi)	Not stated	ALK positive non-small cell lung cancer	I	NCT02292550	
	Enzalutamide (anti-androgen)	Ribociclib days 1-21 (28 day cycle); Enzalutamide days 1-28	Prostate Cancer	I/II	NCT02555189	
	Bicalutamide (anti-androgen)	Ribociclib days 1-21 (28 day cycle) Bicalutamide days 1-28	AR ⁺ triple negative breast cancer	I/II	NCT03090165	
	Carboplatin + Paclitaxel (anti-mitotic)	Ribociclib days 1-4, 8-11, 15-18 (28 day cycle) Paclitaxel + carboplatin days 1, 8, 15	Ovarian cancer	I	NCT03056833	
	Paclitaxel	Not stated	Advanced breast cancer	I	NCT02599363	
	Doxorubicin	Ribociclib days 1-7 (21 day cycle) Doxorubicin day 10	Advanced soft tissue sarcoma	I	NCT03009201	
	Tamoxifen (anti-mitotic)	Ribociclib days 1-21 (28 day cycle) Tamoxifen days 1-28	ER ⁺ , HER2 ⁻ breast cancer	I	NCT02586675	
	Gemcitabine (nucleotide analog)	Ribociclib days 8-14 (21 day cycle) Gemcitabine days 1, 8	Advanced solid tumors	I	NCT03237390	
	Docetaxel (anti-mitotic) + Prednisone	Ribociclib days 2-14 (21 day cycle) Docetaxel and Prednisone days 1-21	Prostate cancer	I/II	NCT02494921	
	PDR001 (anti-PD1 antibody) ± Fulvestrant	Ribociclib days 1-21 (28 day cycle) PDR001 days 1-28	HR ⁺ , HER2 ⁻ breast and ovarian cancer	I	NCT03294694	
	Abemaciclib	LY3023414 (PI3K/mTORi)	Not stated	Pancreatic ductal adenocarcinoma	II	NCT02981342
		LY3214996 (ERK1/2i)	Not stated	Advanced solid tumors	I	NCT02857270
		Ramucirumab (anti-VEGFR2)	Abemaciclib days 1-28 (28 day cycle) Ramucirumab days 1, 15	Advanced solid tumors and lymphoma	I	NCT02745769
Xentuzumab (IGF1/2i)		Abemaciclib daily, Xentuzumab once a week	Advanced solid tumors, HR ⁺ breast cancer	I	NCT03099174	
LY3039478 (Notchi)		Both drugs daily	Advanced solid tumors	Ib	NCT02787495	
Exemestane (aromatasei) OR Exemestane + Everolimus OR LY3032414 + Fulvestrant OR Letrozole (aromatasei) OR Anastrozole (aromatasei) OR Tamoxifen (anti-mitotic) OR Trastuzumab (HER2 antibody)		All drugs daily	Metastatic breast cancer	Ib	NCT02057133	
Anastrozole OR Letrozole		All drugs daily	HR ⁺ , HER2 ⁻ breast cancer	III	NCT02246621	
Tamoxifen		Both drugs daily	HR ⁺ , HER2 ⁻ breast cancer	II	NCT02747004	
Premetrexed (anti-folate) OR Gemcitabine OR Ramucirumab OR LY3023414 OR Pembrolizumab (PD-1i)		Abemaciclib daily (21 day cycle) Premetrexed day 1 Gemcitabine days 1, 8 Ramucirumab days 1, 8 Pembrolizumab day 1	Non-small cell lung cancer	I	NCT02079636	

Table 1.3. List of ongoing clinical trials with CDK4/6 inhibitors in combination with one or more other therapies

Similarly, mutations in p16^{Ink4a}, up-regulated expression of cyclin D1 or other D-type cyclins, and upregulation of CDK4 or CDK6 in cell lines and xenografts can be linked to intrinsic and acquired resistance to signaling pathway inhibitors against estrogen, RAF, EGFR, PI3K, and others [42-44]. In some of these models, resistance can be overcome or delayed by combining CDK4/6 inhibitors [45-49]. Thus, one explanation for the increased therapeutic efficiency of combining CDK4/6 inhibitors and targeted therapies is through enforcing a more durable cell cycle exit (**Figure 1.1**).

However, not all Rb-positive tumors respond to CDK4/6 inhibition in the clinic. Multiple trials investigating CDK4/6 inhibitors as a single-agent or in combination with anti-hormone therapies and signaling pathway inhibitors have consistently shown that while a subset of patients achieve durable clinical responses, there is always a group of patients that do not respond [35, 50-54]. This is the case in well-differentiated and dedifferentiated liposarcoma, where approximately a third of patients progress in the first 12 weeks while on palbociclib, despite evidence that Rb phosphorylation is lost in the tumor after drug treatment [55-57]. Furthermore, if cytostatic cell exit was the only mechanism of action, it would follow that the avenues of resistance seen in cell lines would be able to predict clinical outcome in patients. Yet no such correlation between the expression of cyclin D, cyclin E, or p16 and clinical response has been seen in patients in clinical trials with any of the three CDK4/6 inhibitors [58, 59]. Recently, analysis of 560 endometrial cancer cell lines revealed a profile of cyclin D activation that correlated with sensitivity to CDK4/6 inhibitors *in vitro* [41]. It remains to be determined if such a profile will have improved success over individual markers at identifying patients that will respond clinically. However, failure thus far to identify a cell cycle related biomarker suggests that CDK4/6 inhibitors may be acting in more complex ways than solely enforcing cytostatic growth arrest. Recent investigations from several groups and the work I present in this thesis provide alternative mechanistic explanations for the clinical activity of CDK4/6 inhibitors.

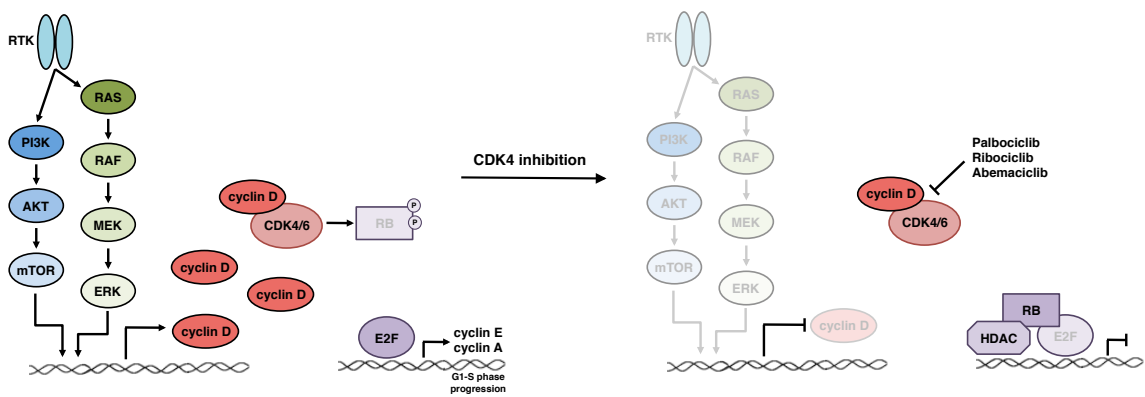


Figure 1.1. Cytostatic growth arrest after CDK4/6 inhibition

When combined with signaling pathway inhibitors, a more durable cell cycle exit or cytostasis can be achieved by directly and indirectly repressing the accumulation of the D-type cyclins and blocking the activity of CDK4/6.

CDK4/6 in the tumor microenvironment

Our understanding of the relationship between cancer cells and the supporting cells that create a tumor microenvironment has significantly advanced during the last 10 years. The extraordinarily complex microenvironment is not only supportive for tumor growth but also can drive the transition of slow growing, indolent tumors into a more aggressive state.

The importance of CDK4 activity within the microenvironment was first demonstrated by crossing an RCAS-PDGF/nestin-TvA mouse model of oligodendroglioma into a CDK4 deficient background [60]. CDK4 is required for the proliferation of the tumor cells; however, reconstituting incipient CDK4 deficient tumor cells with CDK4 expression vectors is not sufficient for tumors to progress to a more aggressive state when the rest of the animal is CDK4 deficient. The lack of progression in this model is associated with a defect in the maturation of tumor-associated microglia, which remain in a sentinel mode in the absence of CDK4. Thus, CDK4 is required for both the proliferation of tumor cells and for the maturation of the tumor microenvironment, and both functions are necessary for the progression of disease in this model.

Recently, in a variety of breast cancer models, including patient-derived xenografts and an MMTV-HER2 mouse, it was demonstrated that both abemaciclib and palbociclib induce growth arrest and up-regulation of antigen processing and presentation in tumor cells [61]. Consistent with this, the number of CD3⁺ cells recruited into the tumor mass increases after treatment, allowing for the stimulation of cytotoxic T-cell lymphocytes. Additionally, CDK4 is necessary for the development of CD4⁺FOXP3⁺ regulatory T-cells that can suppress cytotoxic T-cell responses. In both tumor bearing and non-tumor bearing animals, CDK4 deficiency is associated with a reduced number of infiltrating and circulating CD4⁺FOXP3⁺ regulatory T-cells with minimal impact on other T-cell subsets [61, 62]. Thus, by enhancing the antigenicity of the tumor cell and suppressing the negative regulatory cells, one can achieve a substantial effect on tumor growth by using CDK4/6 inhibitors (**Figure 1.2**).

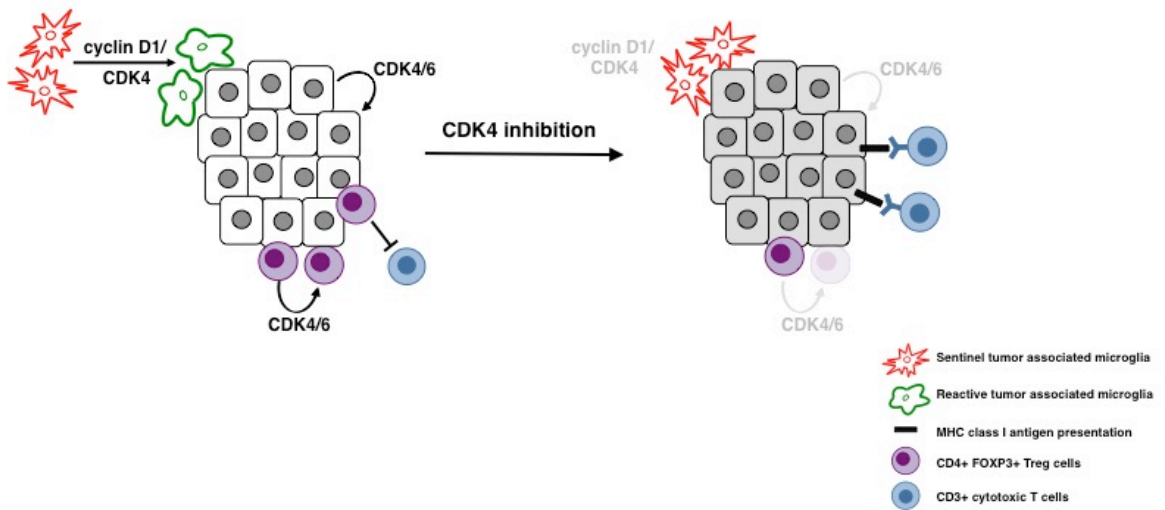


Figure 1.2. CDK4/6 inhibitor induced immunologic changes

CDK4/6 inhibitors can directly affect the proliferation or maturation of cells resident in the tumor microenvironment and enhance the immunogenicity of tumor cells.

The impact of CDK4/6 inhibitors on cellular metabolism

It has long been recognized that cell division is coordinated with metabolic state. Several non-Rb targets for CDK4/6 have been identified in the metabolic machinery. For example, phosphorylation of AMPK α 2 by CDK4 is associated with increased glycolysis and decreased fatty acid oxidation in mouse embryonic fibroblasts [63]. In contrast, CDK4 phosphorylation of GCN5 can lead to acetylation of PGC-1 α and decreased glucose metabolism in hepatic cells [64].

There is some evidence that changes in metabolic pathways may underlie the success of CDK4/6 inhibition *in vitro* (**Figure 1.3**). Inhibition of CDK4/6 with any of the three drugs in pancreatic ductal adenocarcinoma cell lines alters glycolytic and oxidative metabolism leading to an increase in reactive oxygen species (ROS) in an Rb-dependent manner [65]. Combining CDK4/6 inhibition with an mTOR inhibitor, a BCL2 inhibitor, or reducing reactive oxygen species scavengers drives these cells into apoptosis, whereas treatment with single agents alone is not sufficient.

In T-cell acute lymphoblastic leukemia, inhibition of CDK6 or genetic repression of cyclin D3 induces apoptosis [24, 66, 67]. These cells express low levels of cyclin D1, cyclin D2, and CDK4, and the proliferative decision is dependent upon cyclin D3 and CDK6 [68, 69]. The cyclin D3/CDK6 kinase complex can phosphorylate 6-phosphofructokinase and pyruvate kinase M2 [69]. This has the effect of pushing glycolytic intermediates into the pentose phosphate and serine pathways, and inhibition of CDK6 (through treatment with palbociclib, ribociclib, or knockdown of CDK6) depletes the antioxidants NADPH and glutathione, increasing the concentration of ROS and triggering apoptosis.

While both of these mechanisms share the end result of increased glycolysis, the consequences are not uniform. It is likely that changes in metabolism after CDK4/6 inhibition will be context-specific and may be dependent on the oncogenic drivers that set up unique metabolic pathways and concurrent vulnerabilities.

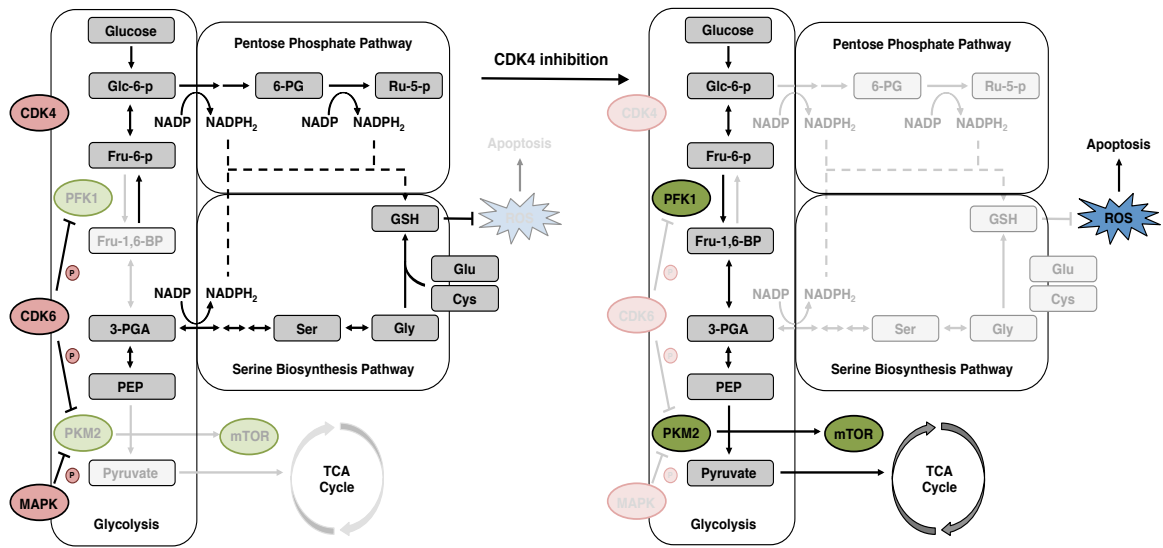


Figure 1.3. Metabolic consequences of CDK4/6 inhibition

CDK4/6 inhibition can alter the metabolic state of tumor cells, leading to an increase in reactive oxygen species and apoptosis.

The outcome of CDK4/6 inhibition can be quiescence or senescence

When cells exit the cell cycle from G₁ they can quiesce, senesce, or apoptose. Several groups have looked at the terminal fate of cells treated with CDK4/6 inhibitors *in vitro*. Depending on the cell type and the transforming event, many Rb-positive cells undergo quiescence or senescence (**Figure 1.4**) [24, 25, 57, 66, 70, 71]. Much of the work characterizing cell fate after CDK4/6 inhibition was performed in mouse models where each tumor type has only one outcome (i.e. quiescence *or* senescence). The underlying differences in driver mutations and tissue type specificity have made it difficult to understand what contributes to the choice between these different cell states.

Unlike apoptotic cells, quiescent and senescent cells remain alive and metabolically active. Quiescence is defined as a state of growth arrest that is readily reversible, whereas senescence is a more permanent form of growth arrest, and cells cannot return to the cell cycle once the inducing signal is removed. These two states are similar in that they both display a loss of BrdU incorporation and reductions in cyclin A and phosphorylated Rb (all markers of cell cycle progression). Senescence is further identified by a number of markers (see *Defining Senescence*), but quiescent cells are more difficult to identify, in part because they do not have many changes in morphological characteristics compared to their cycling counterparts [72]. While some studies use acridine orange staining to identify quiescent populations based on a lowered RNA content [73], it is clear that quiescent cells, like senescent cells, have distinct expression changes, including increased expression of several genes [74]. Unlike quiescent cells, senescent cells will not return to the cell cycle following removal of the inducing signal and are generally refractory to other proliferation-inducing signals [75]. Given the differences in the permanence of the cell cycle arrest, it has been proposed that senescence is a favorable clinical outcome compared to quiescence, though this has never been directly tested. Therefore, one mechanism that could underlie differences in response to CDK4/6 inhibition *in vivo* is the outcome of growth arrest, *vis a vis* quiescence or senescence.

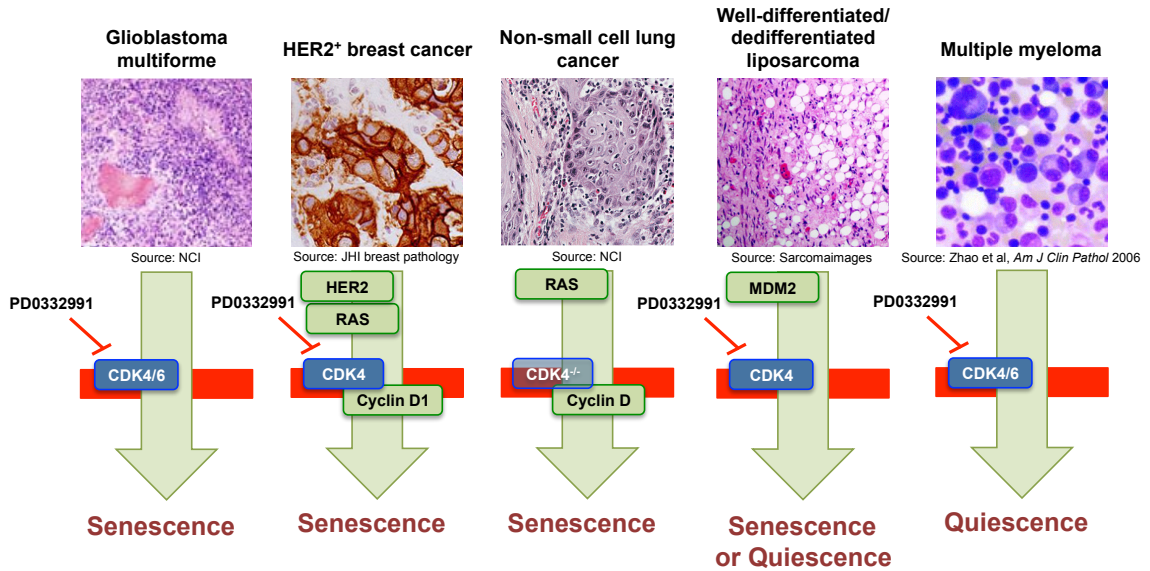


Figure 1.4. Possible outcomes of cell cycle exit

Multiple studies have shown that CDK4 inhibition can drive exit from the cell cycle into senescence or quiescence depending on tumor type. Of note, well-differentiated/dedifferentiated liposarcoma was the first disease where it was shown that this fate decision is not just cell type dependent as some cell lines derived from the same tumor type senesce while others quiesce.

Cellular Senescence

Defining senescence

Senescence was first described by Leonard Hayflick in the 1960s after he observed a tissue culture phenomenon where non-immortalized and non-transformed cells stopped dividing after a finite period of time [76]. Senescence is now appreciated as a critical *in vivo* phenomenon with consequences in development [77, 78], aging [79] and disease [75, 80] (**Figure 1.5**). Senescent cells remain transcriptionally and metabolically active and are impervious to the cell-cycle promoting effects of extracellular growth signals. However, studies on the inducers and consequences of senescence are limited by a lack of markers that can be used to identify a senescent cell *in vivo*, and the definition of a senescent cell is often controversial [81-84]. Thus, to define a cell as senescent, investigators typically demand that it accumulates two or more specific assayable characteristics. These include the accumulation of senescence-associated beta-galactosidase (SA- β -Gal), changes in chromatin including the formation of senescence-associated heterochromatic foci (SAHF), the accumulation of the p16^{Ink4a} CDK inhibitor, an increase in DNA damage foci and reactive oxygen species, and retrotransposon activation. However, none of these markers are unique to senescent cells and not all senescent cells express each of these markers. Additionally, no panel of markers has been successfully utilized *in vivo* in order to identify and study populations of senescent cells [84].

It has become widely accepted that the strictest definition of senescence, and the way in which a senescent cell can be functionally distinguished from other non-cycling cells, is: (1) they fail to return to the cell cycle when the signal that induced their exit is removed, (2) they secrete a collection of cytokines, proteases and growth factors that can lead to inflammation known collectively as the senescence-associated secretory program (SASP) [85], and (3) they are relatively more resistant to apoptotic stimuli [86, 87]. However, these hallmarks are also fraught with issues when it comes to using them to identify senescent cells *in vitro* and *in vivo*. For instance, when surveying tissues, one cannot determine if a cell will return to the cell cycle, and

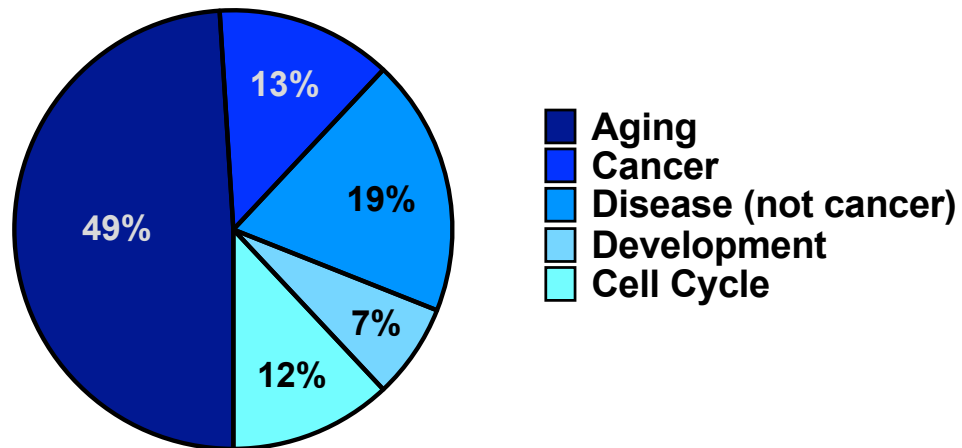


Figure 1.5. Keywords associated with publications pertaining to senescence

Scopus was queried in December 2017 for publications with the key word ‘senescence’ and either ‘aging’, ‘cancer’, ‘disease’, ‘development’, or ‘cell cycle’. The number of articles with matching keywords is shown as a percent of total articles in the query. The ‘disease’ query specifically excluded results that also contained ‘cancer’. Results included cardiovascular, metabolic, and cognitive diseases.

the precise genetic and molecular signature of the inflammatory program is typically cell type and signal specific [88-90].

Pathways into senescence

Many physiologic triggers of senescence have been identified in both primary non-transformed cells and cancer-derived transformed cell lines (**Figure 1.6**). In non-transformed cells these include telomere attrition [91, 92], irreparable DNA damage or oxidative stress [93, 94], and the expression of oncogenes that drive inappropriate proliferation [95]. Additionally, senescence can be induced in transformed cancer cells by stressors that drive either a G₁ or G₂ cell cycle arrest, including irreparable DNA damage [96] or CDK4 inhibition [57, 71, 97].

Each of these stimuli is propagated along molecular pathways that drive senescence. Many of these pathways involve proteins that also regulate the cell cycle and DNA damage response, including p53/p21, p16/Rb, and ATM/ATR (**Figure 1.6**) [98]. The diverse cellular functions of these pathways have made it difficult to separate their involvement in senescence from their roles in cell cycle exit. Such overlap also complicates studies whose aim is to understand why a cell would exit into senescence instead of one of the other possible G₀-G₁ fates, as manipulating their expression will toggle response between senescence and continued proliferation rather than another arrested state.

The decision between senescence and apoptosis may be based in part on the amount and duration of stress exposure. For example, treatment with low concentrations of doxorubicin will induce senescence, while treatment with high concentrations will drive apoptosis [99, 100]. p53 dynamics might underlie some of this difference. Cells that induce p53 accumulation faster or see p53 in a sustained fashion will apoptose, whereas cells that see p53 in a pulsatile fashion fail to apoptose despite reaching similar total levels of p53 expression [101-103]. Nevertheless, the amount of the signal is not necessarily sufficient as reactivation of p53 to similar levels can drive senescence or apoptosis *in vivo* depending on tumor type [88, 104]. In this case, differences in

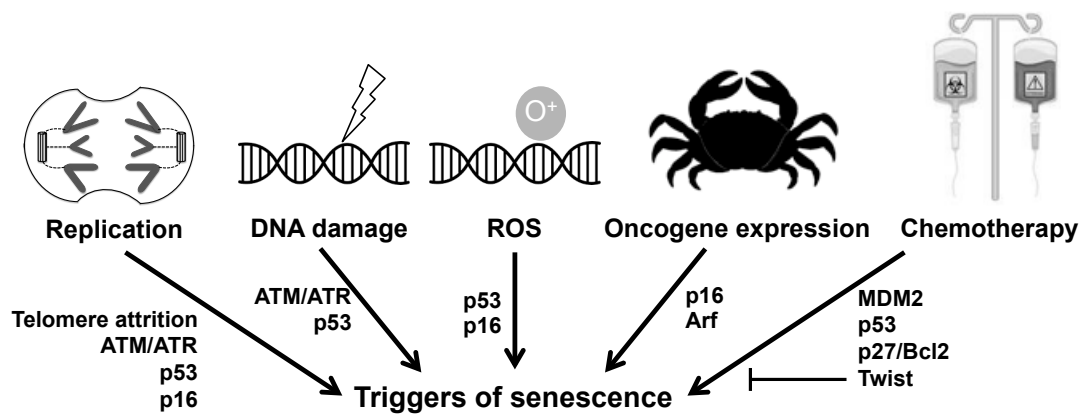


Figure 1.6. Triggers of senescence

Depicted are stimuli that can prompt a cell to enter into senescence and the best established molecular drivers of each.

outcome may be steered by promoter availability/selectivity of p53, or the tissue specific presence of additional p53-interacting proteins [105]. Alternatively, it is worth considering that some environments are permissive for one outcome and not the other. For example, the expression of BCL-2 or inhibition of caspases can cause a switch from apoptosis to senescence in response to DNA damage [100, 106].

In the case of CDK4/6 inhibitors, studies of p53 and cellular response to stress can provide a paradigm for thinking about differences in cell fates, but are not directly applicable as the senescence pathway is both p16 and p53 independent [57, 71, 97]. In my thesis work I hypothesized that one way to tease apart the decision between quiescence and senescence is to use cell lines that are genetically similar but have different outcomes in response to CDK4/6 inhibition, preferably in a disease where there is patient material available to test if these mechanisms are clinically relevant.

Thesis Objectives

Prior work in the Koff lab identified that a subset of well-differentiated and dedifferentiated liposarcoma (WD/DDLS) cell lines undergo senescence after CDK4/6 inhibition, while the remaining cell lines undergo quiescence. Furthermore, senescence is driven by a reduction in MDM2 protein levels. Therefore, I proposed that these cell lines provided an opportunity to determine what underlies the decision to undergo senescence or quiescence.

In chapter three of this thesis, I identify the molecular mechanisms that control MDM2 regulation, including dissociation of the deubiquitinase HAUSP, localization of the PDZ and LIM domain containing protein PDLIM7, and expression of the type II cadherin CDH18. Furthermore, my discovery that CDH18 expression correlates with response to palbociclib treatment in patients with WD/DDLS establishes that this pathway is a clinically relevant mechanism for CDK4/6 inhibitor response.

In chapter four, I show that quiescence and senescence are not an either/or decision as was first thought, but rather a sequential pathway where quiescent cells decide whether or not to progress into senescence. I have termed this transition senescence after growth arrest or SAGA. Furthermore, I discuss how the conceptual breakthrough of SAGA allowed me to develop a cellular model system in which phenotypic changes can be evaluated as cells enter into senescence in a synchronous manner.

Finally, in chapter five, I demonstrate how this system can be used to evaluate the transcriptional changes that occur as cells progress through SAGA and I identify elements of the senescence-associated secretory program that are necessary for irreversible growth arrest. Collectively, my research maps a new biological transition and yields unprecedented insight into how cells enter into senescence after growth arrest.

CHAPTER 2: MATERIALS AND METHODS

Cell lines

The well-differentiated and dedifferentiated liposarcoma (WD/DDLS) cell lines used in this thesis were generated by Samuel Singer's lab and have previously been described [57, 107]. The non-small cell lung cancer (NSCLC) cell lines used in these studies include H1975 (ATCC CRL-5908) and H358 (ATCC CRL-5807). All the cell lines were characterized for their response to CDK4 inhibition [57, 108]. All cell lines were maintained in complete media containing Dulbecco's Modified Eagle's medium with high glucose (4,500 mg/L) supplemented with 10% heat inactivated fetal bovine serum (unless otherwise indicated) and 2 mM L-glutamine.

Lentivirus constructs

Lentivirus vectors were generated in HEK293T cells by triple transfection with the vector of interest, psPAX2, and pMD2.G [57]. Infected cells were selected using puromycin (1 µg/mL) or blasticidin (3 µg/mL) as appropriate. Short hairpin RNAs (shRNA) were delivered in the pLKO.1 vector (Open Biosystems). shRNA sequences are contained in **Table 2.1**.

Real-time quantitative PCR

RNA was extracted from cells using the QIAGEN RNeasy kit per manufacturer's instructions. Complementary DNA (cDNA) was synthesized from 1 µg of each RNA sample using the One *Taq* RT-PCR Kit and oligo-dT primers (New England BioLabs). cDNA was diluted 1:5 and 1 µL was used per reaction for real-time quantitative PCR (RT-qPCR). RT-qPCR was performed by using 400 nM of each forward and reverse primer and SYBR Green PCR Master Mix (Life Technologies). RT-qPCR was performed on Viia 7 Real-Time PCR System (Thermo Scientific). Primer sequences are contained in **Table 2.2**.

Gene	Gene ID	Clone ID	Sequence
MDM2	4193	TRCN0000003380	CTCAGCCATCAACTTCTAGTA
HAUSP	7874	TRCN0000004057	CCAGCTAAGTATCAAAGGAAA
		TRCN0000010845	CGTGGTGTCAAGGTGACTAA
PDLIM7	9260	TRCN0000161061	GCGAGACTATGAGAAGATGTT
		TRCN0000166638	CGTCTGTGCGATATGTCAGAT
CREBBP	1387	TRCN0000006485	CCCATAACTTTGTGATGTTT
		TRCN0000006486	GCTATCAGAAATAGGTATCATT
P300	2033	TRCN0000039884	CCAGCCTCAAAC TACAATAAA
		TRCN0000039886	CCC GG TGA ACTCTCCTATAAT
PRKCD	5580	TRCN0000195598	CGGCATGAATGTGCACCATAA
		TRCN0000195408	CAGAGCCTGTTGGGATATATC
NEDD4-1	4734	TRCN0000007550	GCCTTCTCTGCTGCATAT
		TRCN0000007554	CGGTTGGAGAATGTAGCAATA
ANGPTL4	51129	TRCN0000155024	GAGAGGCAGAGTGGACTATTT
		TRCN0000150798	GCAGAGTGGACTATTTGAAAT
IGFBP3	3486	TRCN0000072509	CCTCCATTCAAAGATAATCAT
		TRCN0000072511	CCAGCGCTACAAGTTGACTA
IGFBP7	3490	TRCN0000080109	CCTCATCTGGAAACAAGTAAA
		TRCN0000077944	GCTGGTATCTCCTCTAAGTAA
PLAT	5327	TRCN0000050913	CCGCTGCACATCACAACATTT
		TRCN0000050917	GCTGGGAAGTGTGTGAAATA
CDH1	999	TRCN0000237844	ACACCCGGGACAACGTTTATT
		TRCN0000237840	ATACCAGAACCTCGAACTATA
		TRCN0000237841	AGATTGCACCGGTCGACAAAG
CDH2	1000	TRCN00000312701	GTGCAACAGTATACGTTAATA
		TRCN0000053978	CCAGTGACTATTAAGAGAAAT
		TRCN0000327707	CCAGTGACTATTAAGAGAAAT
CDH3	1001	TRCN0000054018	CCCAGATGAAATCGGCAACTT
		TRCN0000054021	CCTACCAGGTACTTCTGTGAT
		TRCN0000054022	CAGCTCTGTTTAGCACTGATA
CDH4	1002	TRCN0000054059	CGACCTGTACATCTACGTCAT
		TRCN0000054060	CACGTCCATCATCAAAGTCAA
		TRCN0000054062	CCAGATCTATCTCATTGACAT
CDH5	1003	TRCN0000054089	CCTCACGGATAATCAGGATAA
		TRCN0000054090	CGTGGATTACGACTTCCTTAA
		TRCN0000054091	CCGCAATAGACAAGGACATAA
CDH11	1009	TRCN0000054335	GCGCCAAGTTAGTGTACAGTA
		TRCN0000054336	CCACTTCCAACCAGCCAATT
		TRCN0000094829	GCCAGCTTAAACCATACAAT
		TRCN0000054334	CCGTGAGAACATCATTACTTA
CDH12	1010	TRCN0000054333	GCAGATTTGTATGGTTCCAAA
		TRCN0000055505	GCTGGCAACAATTCTCCTTT
		TRCN0000055506	GCAGGCAGCAAGATTGTATT
		TRCN0000055507	GCAGACATGTTGGCGAAGAA
CDH15	1013	TRCN0000055568	GCACTTCATCAATGATGGCTT
		TRCN0000055569	CCTTCGAGACAATGTCCTCAA
		TRCN0000055571	CTGTGAACACTACGAACTCAA
CDH16	1014	TRCN0000055616	CTCTGCAAGAACCTCAGTTAT
		TRCN0000055615	CCTGGTGATCCACTTCCTAAA
		TRCN0000055614	CCTGGTAGCAATAGGAATCTT
		TRCN0000055617	CCCTTTATACCTGACCAAGTT
CDH18	1016	TRCN0000055704	GCCAGGGAATATGATATTATT
		TRCN0000055705	CCTGCCTGTAAATCCAAACTT
		TRCN0000055703	GCTGGGACTATATTTATCATT
		TRCN0000055706	CGACACAATCAGACCAGGATT

Table 2.1. shRNA sequences

Gene	Forward Primer	Reverse Primer
HAUSP	CCCTCCGTGTTTTGTGCGA	AGACCATGACGTGGAATCAGA
PDLIM7	CAGAGCCGCACCTCCATTG	TGGTGACACACGGGAGTCT
CREBBP	CCTGCCACGTACAGACTG	GGCCAGAGTTACTATTGAGGAGG
P300	GCTTCAGACAAGTCTTGGCAT	ACTACCAGATCGCAGCAATTC
PRKCD	GTGCAGAAGAAGCCGACCAT	CCCAGATTAGCACAATCTGGA
NEDD4-1	TCCAATGATCTAGGGCCTTTACC	TCCAACCGAGGATCTTCCCAT
ANG	CTGGGCGTTTTGTGTTGGTC	GGTTTGGCATCATAGTGTGG
ANGPTL4	GGCTCAGTGGACTTCAACCG	CCGTGATGCTATGCACCTTCT
BMP6	TGTTGGACACCCGTGTAGTAT	AACCCACAGATTGCTAGTGGC
CCL20	TGCTGTACCAAGAGTTGCTC	CGCACACAGACAACCTTTTCTTT
CSF1	TGGCGAGCAGGAGTATCAC	AGGTCTCCATCTGACTGTCAAT
CSF2	TCCTGAACCTGAGTAGAGACAC	TGCTGCTTGTAGTGGCTGG
CXCL1	AGGGAATTCACCCCAAGAAC	TGTTCAGCATCTTTTCGATGA
CXCL9	CCAGTAGTGAGAAAGGGTCGC	AGGGCTGGGGCAAATGT
CXCL10	GTGGCATTCAAGGAGTACCTC	TGATGGCCTTCGATTCTGGATT
CXCL11	GACGCTGTCTTTGCATAGGC	GGATTTAGGCATCGTTGTCTTT
IGFBP3	AGAGCACAGATACCCAGAACT	GGTGATTCAGTGTGTCTTCCATT
IGFBP5	ACCTGAGATGAGACAGGAGTC	GTAGAATCCCTTTCGGTCACAA
IGFBP7	CGAGCAAGGTCTTCCATAGT	GGTGTGGGATTCGATGAC
IL1A	AGATGCCTGAGATACCCAAAACC	CCAAGCACCCAGTAGTCT
IL1B	TTTGACACATGGGATAACGAGG	TTTTTGTGTGAGTCCCGGAG
IL6	ACTCACCTCTTCAGAACGAATG	CCATCTTGGAAAGTTACAGTTG
IL7R	CTCCAACCGCAGCAATGTAT	AGATGACCAACAGAGCGACAG
IL8	ACTGAGAGTGATTGAGAGTGGAC	AACCTCTGCACCCAGTTTTC
MMP1	AAAATTACACGCCAGATTTGCC	GGTGTGACATTACTCCAGAGTTG
MMP3	CGGTTCGCCTGTCTCAAG	CGCCAAAAGTGCCTGTCTT
PLAT	AGCGAGCCAAGGTGTTCAA	CTTCCAGCAAATCCTTCGGG
SERPINE1	AGTGGACTTTTCAGAGGTGGA	GCCGTTGAAGTAGAGGGCATT
SERPING1	CTGGCTGGGGATAGAGCCT	GAGATAACTGTTGTGCGACCT
TIMP1	ACCACCTTATACCAGCGTTATGA	GGTGTAGACGAACCGGATGTC
TNSFR11B	CACAAATGCAGTGTCTTTGGTC	TCTGCGTTTACTTTGGTGCCA
TYRO3	CGGTAGAAGGTGTGCCATTTT	CGATCTTCGTAGTTCCTCTCCAC
VEGFA	AGGGCAGAATCATCACGAAGT	AGGGTCTCGATTGGATGGCA
β -Actin	CATGTACGTTGCTATCCAGGC	CTCCTTAATGTACGCACGAT

Table 2.2. Primer sequences for RT-qPCR analysis

Immunoblots

Cells were lysed with a buffer containing 50 mM Tris-HCl, pH 7.4, 250 mM NaCl, 5 mM EDTA, 0.5% NP40, 2 mM PMSF, and protease inhibitors. Depending on the antibody used, forty to eighty micrograms of protein were resolved by SDS-PAGE and transferred to PVDF membranes. Membranes were incubated overnight with primary antibodies.

The antibodies used for immunoblotting were MDM2 (Santa Cruz Biotechnology SMP14) 1:500, CDK4 (Santa Cruz Biotechnology C-22) 1:1000, PDLIM7 (Santa Cruz Biotechnology H-110) 1:2000, CDH18 (Abnova 6F7) 1:500, Tubulin (Santa Cruz Biotechnology C-11) 1:2000, and FLAG (Sigma M2) 1:1000. Loading and protein levels were quantified by densitometry analysis using ImageJ software.

Immunoprecipitation

Immunoprecipitation was performed by incubating 1 mg of protein lysate with 15 μ L MDM2 SMP14 antibody or a mouse IgG control antibody overnight rotating at 4°C. Immune complexes were captured on 20 μ L of protein G dynabeads (Thermo Fisher 1003D) by rotating for 20 minutes at room temperature and subsequently eluted with 20 μ L of 2X sample buffer.

In order to facilitate identification of PDLIM7 on an immunoblot after immunoprecipitation, cells were transduced with a lentivirus encoding GFP tagged PDLIM7 in an LT3 vector. Expression was induced by adding 10 μ g/mL doxycycline to the media for two days before cells were harvested.

Senescence Assays

7 days after treatment with 1 μ M PD0332991, unless otherwise noted, cells were plated in to chamber slides. Senescence-associated beta-galactosidase (SA- β -Gal) was assayed using the Senescence β -Galactosidase Staining Kit (Cell Signaling Technologies 9860) according to manufacturer's instructions, and the cell number was measured by Hoechst staining. SA- β -Gal

levels below 20% are generally considered to be background due to the sensitivity of this assay to culture conditions affecting autophagy. Senescence-associated heterochromatic foci (SAHF) and ATRX foci were assayed by fixing cells as described in the immunofluorescence methods section. ATRX foci were quantified as the number of nuclear foci per cell and SAHF were quantified as the percentage of cells with > 5 nuclear HP1 γ foci per cell in the population. Clonogenic growth arrest was assayed by treating cells with 1 μ M PD0332991 for 10 days and then trypsinizing and replating 10,000 cells in complete, drug free media. After 21 days cells were stained with crystal violet. The number of colonies was determined by counting individual colonies that were greater than 2 mm in size.

Immunofluorescence

Cells were plated in 4-well glass chamber slides (Lab-Tek). Cells were fixed for 15 minutes with 4% paraformaldehyde, permeabilized for 5 minutes with 0.1% Triton-X100 v/v in phosphate buffered saline (PBS), incubated for 20 minutes with blocking buffer containing 0.5% v/v Tween-20 and 1% w/v bovine serum albumin in PBS, and incubated overnight with primary antibody diluted in blocking buffer. Dilutions for antibodies were as follows: HP1 γ (EMD Millipore 05-690) 1:5000, ATRX (Santa Cruz Biotechnology sc-15408) 1:2000, pan-Cadherin (BD Biosciences 610181) 1:1000, and PDLIM7 (Santa Cruz Biotechnology sc-98370) 1:2000. Cells were washed three times with PBS then incubated for 1 hour at room temperature with fluorescent secondary antibodies Alexa Fluor Rabbit 488 (Thermo Fisher 11008) and Mouse 546 (Thermo Fisher 11030) diluted at 1:500. Slides were counterstained with Hoechst for nuclear visualization. The Duolink Proximity Ligation Assay (Sigma DUO92101) was performed according to manufacturer's instructions.

CRISPR/Cas9

lentiCas9-Blast and lentiGuide-Puro were a gift from Feng Zhang (Addgene 52962 and 52963). The following guide sequences targeting CDH18 were designed using Benchling software: CDH18 KO1, 5'- GCC TGA GTC TGG GCT TTC CG -3'; CDH18 KO2, 5'- CTA CCT ATG GAA ACA GCG CT -3'. Guides were tested for successful genomic editing by the T7 endonuclease mismatch assay as described previously [109]. Guides were transduced into LS8817 cells and selected in puromycin 1 µg/mL for 6 weeks. Clones that demonstrated efficient cutting were sequenced and tested for the loss of CDH18 protein as measured by immunoblot. Cells were maintained in culture for up to 8 weeks after sequencing while subsequent experiments were carried out.

Immunohistochemistry

Formalin fixed paraffin embedded blocks were sectioned at 4 micron thickness. The histological status (well-differentiated or dedifferentiated) of patient samples was identified by hematoxylin and eosin by Dr. Cristina Antonescu. Immunohistochemistry detection with CDH18 antibody on a parallel section was performed at the Molecular Cytology Core Facility of Memorial Sloan Kettering Cancer Center using the Discovery XT processor (Ventana Medical Systems). Tissue sections were blocked first for 30 minutes in Mouse Ig blocking reagent (Vector Labs MKB-2213) in PBS. A mouse monoclonal antibody to CDH18 (Abnova H00001016-M01) was used at a 3 mg/mL concentration and incubated for 4 hours, followed by 60 minute incubation with biotinylated anti-mouse IgG (Vector Labs BMK-2225) at a 5.75 mg/mL concentration. Blocker D, Streptavidin-HRP and DAB detection kit (Ventana Medical Systems 760-124) were used according to the manufacturer instructions. Tumor cells were identified within the sample based on their nuclear morphology. Samples where greater than 80% of the tumor cells throughout contained cytoplasmic CDH18 staining were deemed positive.

Patient Sample Usage

The design and approvals of clinical trials with palbociclib have been previously described [55, 56]. Surgical resections were obtained under IRB 10-094.

Statistical analysis

For the cytological and immunoblot statistics, 2 tailed t-tests were performed using Prism software and p-values are reported. Data is presented as a mean of biological replicates with error bars derived from the standard deviation unless otherwise stated. Based on expected values of CDK4 inhibitor-induced senescence from our previous work and others [57, 71, 108] and post-hoc calculations, all studies had sufficient sample sizes for an alpha level of 0.05 and a power of greater than 80%.

Disease progression and death were the endpoints of the clinical study. Disease progression was defined as the time from the start of treatment to the occurrence of disease progression. Death was defined as the time from the start of treatment to either the occurrence of death due to any cause or the date of last follow-up. The clinicopathologic variables examined were CDH18 staining (positive vs. negative), treatment dosage level (125 mg vs. 200 mg), disease subtype (well-differentiated vs. dedifferentiated), and prior therapy (yes vs. no). The probabilities of progression and death were each estimated using the Kaplan-Meier method. The associations of these outcomes with the clinicopathologic variables were examined using the log-rank test for categorical variables. P-values ≤ 0.05 were considered significant. All analyses were performed using R version 3.2.0 (cran.r-project.org).

RNA sequencing

RNA quality was checked on a BioAnalyzer to ensure a minimum RNA Integrity Value of 7. Libraries were generated using 500 ng of input RNA per sample according to the manufacturer's instructions for TruSeq mRNA Library Prep Kit V2 (Illumina) with 8 cycles of PCR. Libraries

were pooled and run on an Illumina HiSeq 2500 high output to obtain 40 million paired-end 125 nucleotide-length reads. The RNA-seq reads were aligned to the human reference sequence hg19 with STAR software version_2.4.0c [110]. The raw counts were then subjected to the Bioconductor package DESeq2 to call for differential expression between the groups of samples. Protocol found below. All analyses were performed using R version 3.2.0 (cran.r-project.org).

1. Construct a **Count Matrix** in Microsoft Excel with gene names (ENTREZ ID) in rows of Column 1 and time points or conditions in row 1 for each column.
 - a. Save the file as a comma delineated file with a .csv extension and add a prefix of “CountMatrix” followed by a description of the experiment.
 - b. Open the .csv file in a text editor such as Notepad.
 - c. Delete the comma in front of the first column.
 - d. Save the file.

	R3_Control	R3_Doxy	R3_Doxy-PD	R3_Day03	R3_Day04	R3_Day05
ENSG00000156508	1070518	697916	659906	821307	918874	716510
ENSG00000135506	902206	827898	699026	1008181	953006	935224
ENSG00000115414	851660	347654	341395	679676	756732	1137693
ENSG00000169429	809421	2082516	1783769	292071	413795	24705
ENSG00000210082	787966	2069977	1482771	577240	566796	657897
ENSG00000198804	677385	138411	60263	827209	719795	1025131
ENSG00000120708	547096	250139	130566	441669	420713	813508
ENSG00000166598	506433	249201	333441	287124	290680	317917
ENSG00000150093	470467	286194	176903	391598	418130	487737
ENSG00000085662	450293	155169	123404	314374	266118	96011

2. Construct a **Sample Table** in Microsoft Excel such that column 1 contains sample ID, column 2 contains the names of treatments or time points, and column 3 contains replicate ID (1, 2, 3 etc.).
 - a. Cell A1 should be blank, A2 should say “**time**” and A3 should say “**replicate**”
 - b. Save the file as a comma delineated file with a .csv extension and add a prefix of “ColData” followed by a matching description of the experiment from Step 1A.
 - c. Open the .csv file in a text editor such as Notepad.
 - i. This will
 - d. Delete the comma in front of the first column.
 - e. Save the file.

	time	replicate
R3_Control	Untreated	R3
R3_Doxy	Dox	R3
R3_Doxy-PD	DoxPD_00	R3
R3_Day03	DoxPD_03	R3
R3_Day04	DoxPD_04	R3
R3_Day05	DoxPD_05	R3

3. **Modify the red text in the script of Step 5 to match the Count Matrix and Sample Table file names from Steps 1A and 2A.**
 - a. Alternatively, name files specifically CountMatrixYOURFILENAME.csv and ColDataYOURFILENAME.csv.
4. Open **R studio**.
 - a. Lines of scripts preceded by a “#”, shown below in green, are ignored by R and are used to explain the function of code, shown in blue.

5. **Copy and paste** the following script through the **STOP** point into the R console:

```
# Process a SummarizedExperiment and output heatmap and PCA.
# By Mary E. Klein, modified from https://www.bioconductor.org/help/workflows/rnaseqGene/.
# Load packages required for data processing.
source("http://bioconductor.org/workflows.R")
workflowInstall("rnaseqGene")
library("airway")
library("DESeq2")

# Import data. NOTE: change "YOURFILENAME" to match corresponding file names.

CountMatrix <- read.csv("CountMatrixYOURFILENAME.csv")
SampleTable <- read.csv("ColDataYOURFILENAME.csv")

# Assign table information to a DESeqDataSet.

colnames(CountMatrix) <- NULL

ddsMat <- DESeqDataSetFromMatrix(countData = CountMatrix,colData = SampleTable,design = ~ time +
replicate)

dds <- ddsMat[ rowSums(counts(ddsMat)) > 1, ]

# Stabilize variance across the mean by regularized-logarithm transformation.

rld <- rlog(dds, blind=FALSE)

# Determine parameters of the data and generate a scatter plot of the sequencing depth.

par( mfrow = c( 1, 2 ) )
dds <- estimateSizeFactors(dds)
plot(log2(counts(dds, normalized=TRUE)[,1:2] + 1), pch=16, cex=0.3)
plot(assay(rld)[,1:2], pch=16, cex=0.3)

# Calculate Euclidean distances between samples.

sampleDists <- dist( t( assay(rld) ) )

# Visualize distances between samples by heatmap.

library("pheatmap")
library("RColorBrewer")
sampleDistMatrix <- as.matrix( sampleDists )
rownames(sampleDistMatrix) <- paste( rld$time, rld$replicate, sep="R" )
colnames(sampleDistMatrix) <- NULL
colors <- colorRampPalette( rev(brewer.pal(9, "Blues")) )(255)
pheatmap(sampleDistMatrix,clustering_distance_rows=sampleDists,clustering_distance_cols=sampleDists,
col=colors)

# Generate a Principle Component Analysis plot.

plotPCA(rld, intgroup = c("time", "replicate"))
(pcaData <- plotPCA(rld, intgroup = c( "time", "replicate"), returnData=TRUE))
percentVar <- round(100 * attr(pcaData, "percentVar"))

library("ggplot2")
ggplot(pcaData, aes(PC1, PC2, color=time, shape=replicate)) + geom_point(size=3) +
  xlab(paste0("PC1: ",percentVar[1],"% variance")) +
```

```
ylab(paste0("PC2: ",percentVar[2],"% variance")) +
coord_fixed()
```

```
# Begin a differential expression pipeline on raw counts.
```

```
dds <- DESeq(dds)
```

```
# -----STOP-----.
```

6. After running the above script through the STOP after the differential expression DESeq(dds) calculation, the following script can be run iteratively to specifically compare two samples within a sample set. Change the values in **red** to match sample names defined in the **Sample Table** file generated at Step 2.

```
# Output the log2 fold changes and p-values between specific treatments specified in "time" columns then
output summary data of the comparison.
```

```
# Note: Change values in red to match desired sample comparisons.
```

```
res <- results(dds, contrast=c("time", "Untreated", "Dox"))
summary(res)
```

```
# Assign ENSEMBL Gene symbols to match the ENTREZID number of the RNA-seq data.
```

```
library("genefilter")
library("AnnotationDbi")
library("org.Hs.eg.db")
res$symbol <- mapIds(org.Hs.eg.db,
                    keys=row.names(res),
                    column="SYMBOL",
                    keytype="ENSEMBL",
                    multiVals="first")
res$entrez <- mapIds(org.Hs.eg.db,
                    keys=row.names(res),
                    column="ENTREZID",
                    keytype="ENSEMBL",
                    multiVals="first")
```

```
# Sort the table by adjusted p-values
```

```
resOrdered <- res[order(res$padj),]
```

```
resOrderedDF <- as.data.frame(resOrdered)
```

```
# Output a results file named for the compared samples.
```

```
write.csv(resOrderedDF, file="results_ Untreated _vs_ Dox.csv")
```

```
# -----STOP-----.
```

7. Specific log₂() values comparing the two samples are stored in a .csv file as named in the last line of code. Change the values in red in Step 6 to the next samples to be compared then repeat Step 6.
8. Repeat Steps 6 and 7 until all comparisons have been made.

Heatmap generation and gene set enrichment analysis

Heatmaps were generated using gplots software and hierarchical cluster analysis was performed by R's hclust function. Protocol found below. Gene set enrichment analysis was performed using publically available software from the Broad Institute [111, 112]. Pathways with a false discovery rate of <0.05 were considered significant.

1. Construct a **Matrix** in Microsoft Excel with gene names of interest in rows of Column 1 and time points or conditions in row 1 for each column with the fold changes below.
 - a. Save the file as a comma delineated file with a .csv extension
 - b. Open the .csv file in a text editor such as Notepad.
 - c. Delete the comma in front of the first column.
 - d. Save the file.
2. Open **R studio**.
 - a. Lines of scripts preceded by a "#", shown below in green, are ignored by R and are used to explain the function of code, shown in blue.
3. **Copy and paste** the following script through the **STOP** point into the R console:

```
# Load required packages
install.packages("gplots")
library(gplots)

# Load data and transform data into a matrix
data <- read.csv(file = "YOURFILENAME.csv", header = TRUE, row.names = 1)
data_matrix <- data.matrix(data)

# Create the basic heatmap
heatmap.2(as.matrix(data_matrix), col=redgreen(75), Rowv= TRUE, Colv=FALSE, scale="row", key=T,
keysize=1.5,density.info="none", trace="none",cexCol=0.9, cexRow=.2)

# Rowv/Colv asks if you want to cluster each variable. If yes=TRUE, if no=FALSE
# Scale is the algorithm R uses to color the information. If you want it to select a middle point for each gene
separately you use "row"
# Key size controls how large the color key is
# Trace is a graphical representation of the color intensity. You can have none, both, row, or column
# cexCol/Row is the type face size
# col is the colors you're using. By telling it redgreen 75 you're setting the colors red and green and 75
shades to deliniate all the numerical changes. For all the R color options go to
http://www.stat.columbia.edu/~tzheng/files/Rcolor.pdf

myCol <- colorRampPalette(c("green", "white", "red"))

# Replot your heatmap and save it

heatmap.2(as.matrix(data_matrix), col = myCol, Rowv= TRUE, Colv=FALSE, scale="row", key=T,
keysize=1.5,density.info="none", trace="none",cexCol=0.9, cexRow=.9)

# -----STOP-----
```

CHAPTER 3: PDLIM7 AND CDH18 DEPENDENT REGULATION OF MDM2 IS A CLINICALLY RELEVANT MECHANISM OF ACTION FOR CDK4 INHIBITORS

Introduction

Well-differentiated and dedifferentiated liposarcoma

Well-differentiated and dedifferentiated liposarcomas (WD/DDLS) are characterized by an amplification of the 12q13-15 region, which includes both *CDK4* and *MDM2* [113]. Patients with amplification of *MDM2*, but not *CDK4*, tend to have better prognosis (<10% of patients) [114]. Clinical progression of disease occurs when well-differentiated tumors (WDLS) dedifferentiate into their more aggressive counterpart (DDL); however, what drives this progression is often unclear. WD/DDLS is a relatively radio- and chemo-resistant disease, leaving few options for patient care besides surgical resection [115]. Indeed, the established benchmark of a successful single agent chemotherapy in WD/DDLS is one that exceeds a mere 12 week progression free survival in 40% of patients [116]. Although there is a low rate of metastasis, DDL is a fast growing and aggressive disease with high rates of local recurrence, resulting in poor overall survival for this subtype of liposarcoma compared to other sarcomas [117].

CDK4/6 inhibitors were examined as a possible treatment for WD/DDLS at Memorial Sloan Kettering. Two phase II clinical trials were completed using palbociclib (also known as PD0332991). In these trials, progression free survival (PFS) at 12 weeks was approximately 60% with a median PFS of 18 weeks [55, 56]. However, the range of patient response was broad. 40.4% of patients progressed in ≤ 12 weeks, 37.1% of patients had stable disease for 12-36 weeks, and 22.5% of patients maintained stable disease for ≥ 36 weeks based on RECIST criteria. While these results are considered promising, it begs the question of why a third of patients do not respond and why a small number of patients have strong, durable responses. Therefore, we became interested in the ability of tumors to respond to CDK4/6 inhibition, what this response entails molecularly, and why some patients have no clinical benefit.

WD/DDLS cell lines undergo quiescence or senescence after CDK4 inhibition

Previous members of the lab obtained a panel of WD/DDLS cell lines that were derived from patients, but not from patients treated with CDK4/6 inhibitors. Each of these cell lines has amplifications of *MDM2* and *CDK4* along with a heterogeneous assortment of other copy number alterations. When these cells are treated with the CDK4/6 inhibitor PD0332991 for 7 days, a subset of the cell lines undergo quiescence and the others undergo senescence [57]. There is neither a change in apoptosis, nor a change in differentiation status after treatment. Similar results are observed with other treatments including the alternative CDK4/6 inhibitors ribociclib and abemaciclib, knockdown of CDK4 by shRNA, and constitutive expression of a non-phosphorylatable variant of Rb. Collectively, this suggests that the decision to exit the cell cycle into a senescent or quiescent state is dependent on the action of CDK4 on Rb.

Quiescence is defined by an accumulation of cells in the G_0/G_1 phase, lowered BrdU incorporation, and reduced Rb phosphorylation. Furthermore, quiescent cells will return to the cell cycle when drug is removed. We refer to cell lines that will undergo quiescence as non-responders. On the other hand, senescent cells also have lowered BrdU incorporation and reduced Rb phosphorylation, but they distinctly have an increased amount of senescence-associated beta-galactosidase (SA- β -Gal), increased numbers of HP1 γ foci (a marker of the formation of senescence-associated heterochromatic foci or SAHF), and an increase in the number of ATRX foci per cell nucleus [57, 108]. Furthermore, senescent cells undergo an irreversible cell cycle arrest and will not return to the cycle once the drug is removed. We refer to cell lines that undergo senescence as responders.

Changes in MDM2 expression underlie the decision between quiescence and senescence

When comparing differences in cells that undergo quiescence from those that are senescent following CDK4/6 inhibition, it was noted that senescent cells have reduced levels of MDM2 protein whereas quiescent cells do not [57]. Enforced MDM2 expression prevents CDK4

inhibitor-induced senescence, and knocking down MDM2 in cycling cells is sufficient to induce senescence. This information suggests that reduced levels of MDM2 are causally linked to the outcome of CDK4/6 inhibition. Importantly, the causal link is not restricted to cell lines where MDM2 is amplified. Subsets of breast cancer, glioma, non-small cell lung cancer, and prostate cancer cell lines do not have amplification of *MDM2* but can undergo either senescence or quiescence, and the cell fate outcome is often correlated with the change in MDM2 levels after CDK4 inhibition [57, 108] (Klein, unpublished data).

Changes in MDM2 expression associate with WD/DDLS patient outcome

Unfortunately, the ability to identify senescent cells in patient samples is hampered by the absence of senescence specific markers [79]. In a previous pilot study, we obtained seven pre- and post-treatment biopsies from the phase II clinical trials and analyzed MDM2 protein levels in these samples as a surrogate marker. Rb levels were reduced in post-treatment biopsies from all patients. MDM2 protein levels were reduced in four post-treatment samples from patients who performed well on trial (>24 weeks) and were unaffected or increased in three post-treatment samples from patients who performed poorly (<12 weeks) [57]. While this was a small study, it supports the possibility that senescence may be a clinically relevant mechanism of action. However, the response of MDM2 is assayed after treatment and cannot serve as a predictive biomarker. Thus, I set out to understand how regulation of MDM2 occurs in cells that undergo either CDK4 inhibitor-induced quiescence or senescence with the hypothesis that a more thorough understanding of this mechanism would reveal a pre-treatment indicator of patient response.

Known regulators of MDM2

MDM2 is an oncogene whose overexpression can induce the transformation of cultured cells [118]. Structurally, it contains an N-terminal p53-binding domain, a central acidic domain

and zinc finger, and a C-terminal ring finger that is responsible for its E3-ligase activity [119-122]. MDM2 has several substrates, a major one being p53 [119, 123]. MDM2 and p53 form a tight feedback loop, and likely because of the importance of maintaining appropriate p53 levels in the cell, MDM2 is itself tightly regulated [124].

MDM2 has been shown to be regulated transcriptionally, post-transcriptionally, and post-translationally [125, 126]. Two promoters control MDM2 expression: one is dependent on p53 activity and one is p53 independent [127]. Additionally, there are several microRNAs that can target MDM2 transcripts and repress translation [126]. MDM2 protein activity and availability can further be controlled by nucleo-cytoplasmic shuttling [128]. There are also a large number of post-translational modifications that contribute to alterations in MDM2 activity and stability [125, 129]. Finally, as an E3 ligase MDM2 can ubiquitinate not only other substrates but also can be regulated by auto-ubiquitination, or it can be *trans*-ubiquitinated by multiple E3 ligases (**Figure 3.1**) [130-135]. The complex regulation of MDM2 allows for the integration of many signaling pathways, including DNA damage, oncogenic activation, and chronic stress.

Results

MDM2 turnover is increased in cells that undergo senescence

Previous work showed that while MDM2 RNA levels were repressed slightly after CDK4 inhibition, this occurred in all cell lines whether they underwent senescence or quiescence after drug treatment [57]. On the other hand, I found MDM2 protein turnover was different in responder and non-responder cell lines after CDK4 inhibition. MDM2 protein turnover was accelerated after treatment with PD0332991 in the responder cell line LS8817 but not in the non-responder cell line LS8107 (**Figure 3.2**). Additionally, MDM2 protein accumulated upon addition of the proteasome inhibitor MG132 in PD0332991-treated responder cell lines, suggesting that the loss of MDM2 was at least partially due to increased proteasome-dependent turnover (**Figure 3.3**).

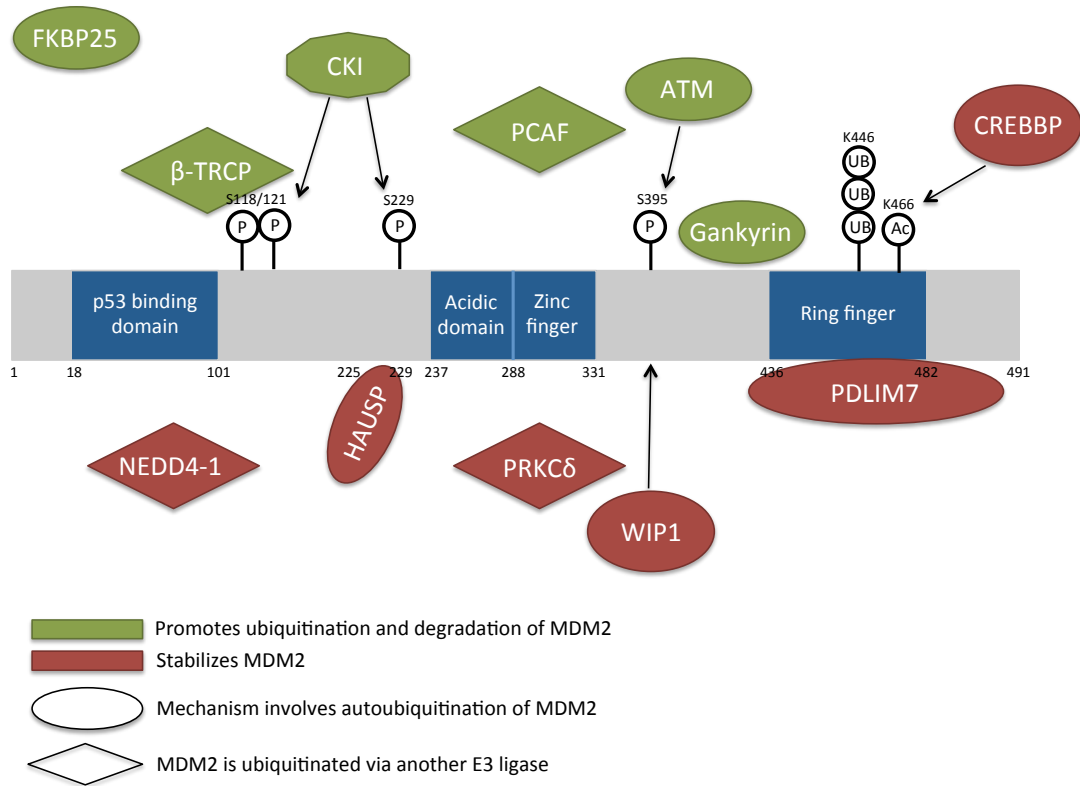


Figure 3.1. Known mechanisms that can affect MDM2 ubiquitin dependent turnover

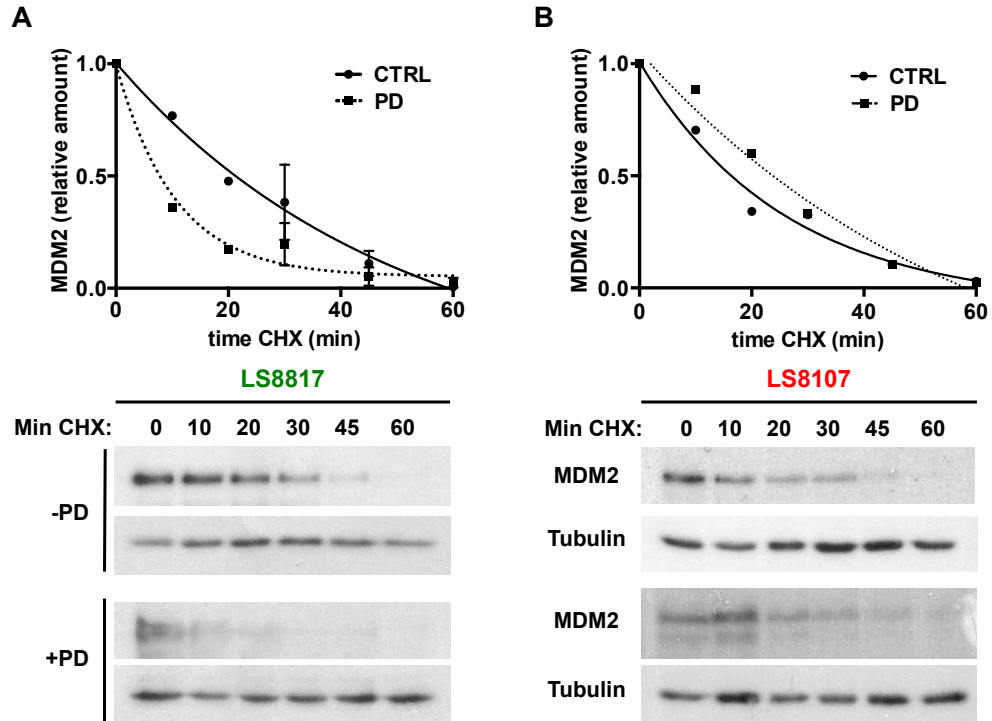


Figure 3.2. PD0332991 induces accelerated MDM2 turnover in LS8817 cells

LS8817 and LS8107 cells were treated with 1 μ M PD0332991 (PD) for two days and then exposed to 75 μ g/mL cyclohexamide (CHX) for the time (minutes) indicated. MDM2 and tubulin were measured by immunoblot. A representative image is shown below and the relative amounts were quantified from two independent experiments (mean \pm standard deviation) above.

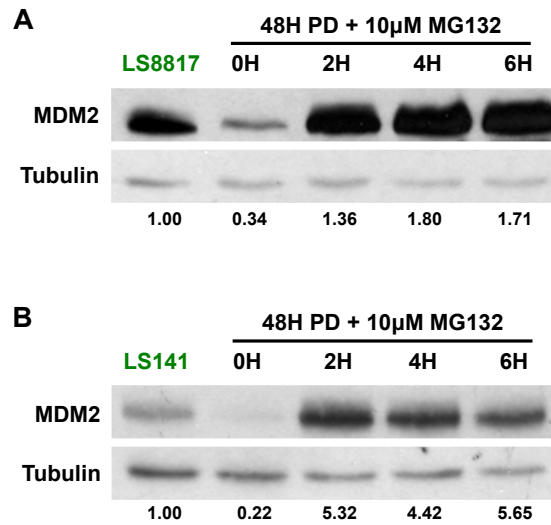


Figure 3.3. MG132 causes accumulation of MDM2 protein in responder cells treated with PD0332991

LS8817 and LS141 cells were treated with 1 μ M PD0332991 (PD) for two days and then treated with 10 μ M MG132 for the time (hours) indicated. MDM2 protein levels were measured using immunoblot. Tubulin served as a loading control. The relative amount (MDM2/tubulin) is quantified below each lane.

To determine if auto- or *trans*-ubiquitination was required for MDM2 turnover after CDK4 inhibition, I transduced LS8817 cells with lentiviral vectors expressing FLAG-tagged MDM2 with either the wild-type MDM2 coding sequence (FMDM2^{WT}) or a mutation in the E3 ligase domain (FMDM2^{C464A}). FMDM2^{C464A} can be *trans*-ubiquitinated but cannot be auto-ubiquitinated [130, 132]. FMDM2^{WT} could be turned over after CDK4 inhibition, but FMDM2^{C464A} was stable after PD0332991 treatment, leading to the conclusion that CDK4 inhibitor-enhanced MDM2 turnover was dependent on auto-ubiquitination (**Figure 3.4**).

HAUSP dissociates from MDM2 as cells exit the cell cycle

A major requirement of MDM2 auto-ubiquitination dependent turnover is the dissociation of the deubiquitinase HAUSP. Interaction of MDM2 with HAUSP inhibits turnover of MDM2 but allows its E3 ligase activity towards other substrates [136, 137]. Thus, I probed if an interaction of MDM2 and HAUSP was affected differently by CDK4 inhibition in responder and non-responder cells. I found that MDM2 and HAUSP associated in both cycling responder and cycling non-responder cells, and that this complex was dissociated in all cell lines treated with CDK4 inhibitors (**Figure 3.5, A**). Loss of binding to MDM2 is not due to a reduction in HAUSP protein after PD0332991 addition (**Figure 3.5, B**). Thus, a failure to dissociate HAUSP could not account for MDM2 stability in quiescent non-responder cells.

To determine if the decreased interaction between MDM2 and HAUSP was sufficient to induce MDM2 protein loss and senescence, I obtained two independent shRNA hairpins against HAUSP. Knockdown of HAUSP alone in responder cell lines was sufficient to induce the accumulation of SA- β -Gal and SAHF positive cells, as well as reduce MDM2 protein levels (**Figure 3.6**). Interestingly, knockdown of HAUSP alone in non-responder cell lines was insufficient to induce the accumulation of senescence markers or drive the loss of MDM2 protein (**Figure 3.6**). This data led to the hypothesis that another factor was preventing MDM2 turnover in quiescent non-responder cells.

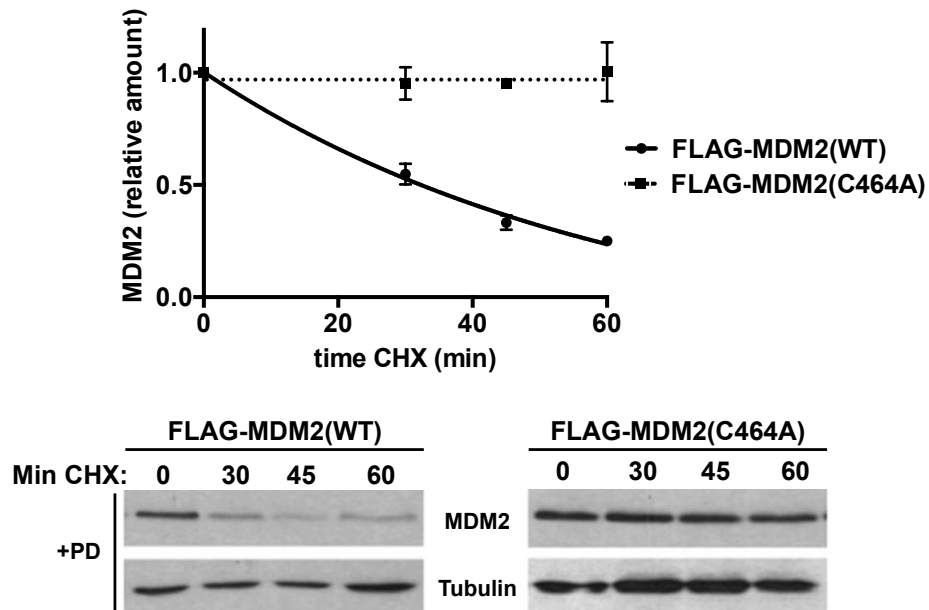


Figure 3.4. Mutating the E3 ligase domain of MDM2 prevents PD0332991 induced turnover
 LS8817 cells were transduced with a lentiviral vector containing either a FLAG-tagged MDM2 that was wild-type or FLAG-tagged MDM2 that was mutated at the C464 residue (cysteine→alanine). After selection, cells were treated with 1 μ M PD0332991 (PD) for two days and then exposed to 75 μ g/mL cyclohexamide (CHX) for the time (minutes) indicated. MDM2 and tubulin were measured by immunoblot. A representative image is shown below and the relative amounts were quantified from two independent experiments (mean \pm standard deviation) above.

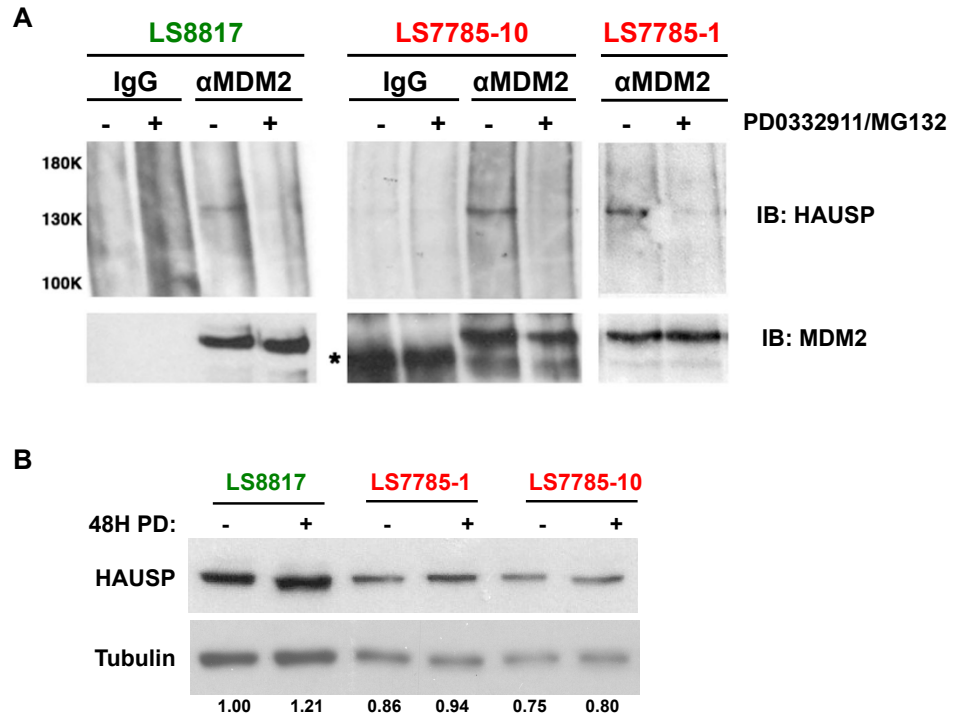


Figure 3.5. HAUSP dissociates from MDM2 after treatment with PD0332991

(A) LS8817, LS7785-10, and LS7785-1 cells were treated with 1 μ M PD0332991 (PD) for 2 days and 5 μ M MG132 was added for 2 hours prior to protein extraction. MDM2 was immunoprecipitated and HAUSP immunoblotted. IgG served as a control. (B) HAUSP protein levels were detected using immunoblot. Tubulin served as a loading control. The relative amount (HAUSP/tubulin) is quantified below each lane.

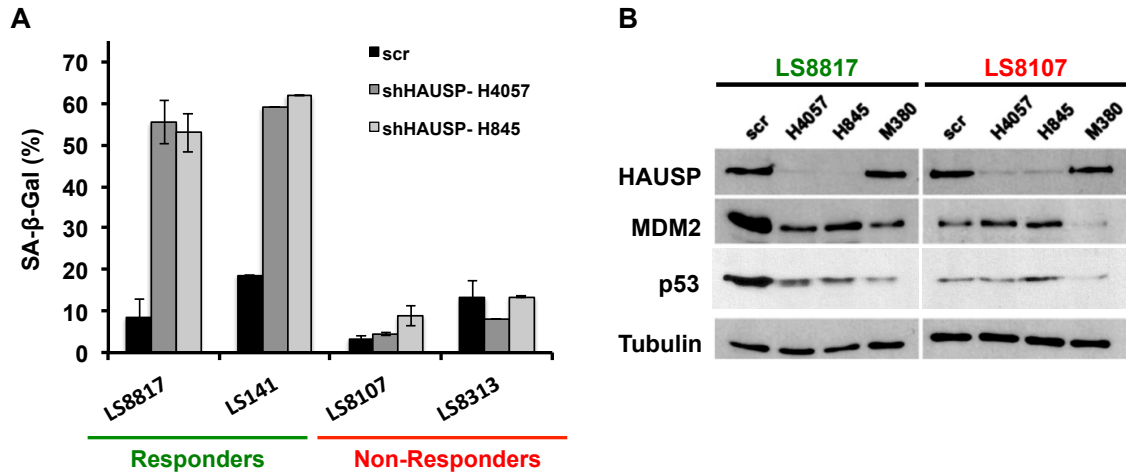


Figure 3.6. PDLIM7 knockdown allows PD0332991 to induce MDM2 down regulation and accumulation of SA-β-Gal in responder cell lines

The responder cell lines LS8817 and LS141 and non-responder cell lines LS8107 and LS8313 were transduced with two different HAUSP knockdown lentiviral vectors (H4057 or H845) or a non-specific vector (scr) and selected in puromycin for 10 days. (A) The number of cells staining for SA-β-Gal were quantified. The mean and standard deviation (n=2) is plotted. (B) HAUSP, MDM2, and p53 protein levels were measured using immunoblot. For comparison, the effect of an MDM2 knockdown lentiviral vector (M380) is shown. Tubulin served as a loading control.

PDLIM7 knockdown allows PD0332991 to induce senescence in non-responder cells

To gain insight into how MDM2 turnover was prevented in CDK4 inhibitor-induced quiescent cells, I carried out an shRNA knockdown screen in the non-responder cell line LS8107 to individually reduce the expression of five gene products previously reported to regulate MDM2 ubiquitination [125] (**Figure 3.7, A**). Of these, only shRNA targeting *PDLIM7* enabled the accumulation of SA- β -Gal after addition of PD0332991 (**Figure 3.7, B**). Knockdown of *PDLIM7* followed by addition of PD0332991 also promoted the accumulation of SA- β -Gal in another non-responder cell line, LS8313 (**Figure 3.8**). Enforced expression of his-biotin tagged *PDLIM7*, in which the coding nucleic acid sequence was silently mutated to prevent interaction with the shRNA, prevented this accumulation (**Figure 3.8**).

To confirm that reducing *PDLIM7* altered the outcome of PD0332991 induced cell cycle exit, I expanded my analysis to other markers of senescence. Seven days after the addition of PD0332991 to cell lines expressing one of two different shRNAs targeting *PDLIM7*, LS8107^{shP061} or LS8107^{shP638}, the accumulation of SA- β -Gal, HP1 γ foci, and ATRX foci was increased compared to a cell line expressing a scrambled shRNA, LS8107^{scr} (**Figure 3.9**). MDM2 levels decreased in LS8107^{shP061} and LS8107^{shP638} cells after PD0332991 treatment, but not in LS8107^{scr} cells (**Figure 3.10, A**). Furthermore, reduced levels of MDM2 were associated with the accelerated turnover of MDM2 in LS8107^{shP638} cells (**Figure 3.10, B**). Thus, reducing *PDLIM7* expression alters the outcome of CDK4 inhibitor-induced cell cycle exit to senescence.

Co-knockdown of PDLIM7 and HAUSP is sufficient to induce senescence in LS8107 cells

To test if the HAUSP and *PDLIM7* mechanisms of MDM2 regulation cooperate to induce senescence, I first knocked down *PDLIM7* in LS8107 cells. After selection, I transduced LS8107^{shP638} cells with a second vector encoding an shRNA targeting HAUSP and assayed senescence. Treatment with PD0332991, knockdown of *PDLIM7* alone, or knockdown of HAUSP alone was not sufficient to induce an increase in SA- β -Gal or ATRX foci per cell.

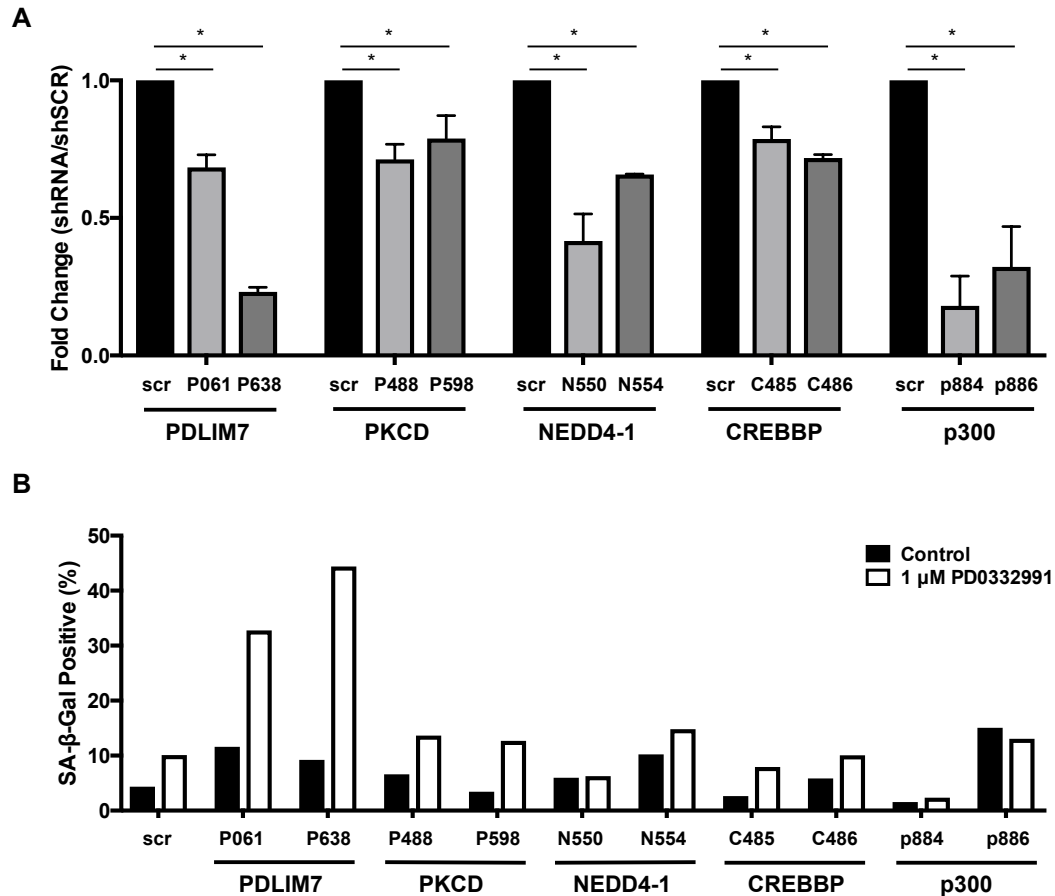


Figure 3.7. shRNA knockdown screen targeting known regulators of MDM2

The non-responder cell line LS8107 was transduced with lentiviruses expressing shRNA targeting either the indicated gene product or containing a non-specific sequence (scr), and selected in puromycin for five days. (A) Cells were harvested, RNA extracted, and RT-qPCR performed to measure mRNA expression of the individual targets and quantified relative to the expression level in the LS8107 cells transduced with the scr sequence. β -actin was used as a normalization control. The mean and standard deviation of three technical replicates is plotted. (B) Cells in panel A were treated with 1 μ M PD0332991 (PD) for seven days and the number of cells staining for SA- β -Gal quantified.

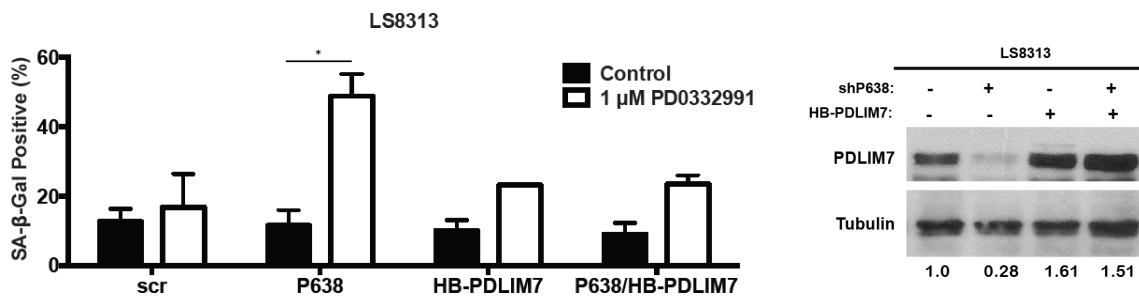


Figure 3.8. PDLIM7 knockdown allows PD0332991 to induce accumulation of SA-β-Gal in non-responder LS8313 cells and can be rescued by expression of a wobble mutant PDLIM7
 The non-responder cell line LS8313 was transduced with a PDLIM7 knockdown lentiviral vector (shP638) or a non-specific vector (scr). Cells were then transduced with a his-biotin tagged PDLIM7 wobble expression vector, wherein the sequence was mutated to prevent recognition by the shRNA without affecting coding sequence. After selection for 5 days, cells were treated with 1 μM PD0332991 (PD) for 7 days and the number of cells staining for SA-β-Gal were quantified. The mean and standard deviation (n=2) is plotted. PDLIM7 protein levels were measured using immunoblot. Tubulin served as a loading control. The mean relative amount (PDLIM7/tubulin) is quantified below each lane.

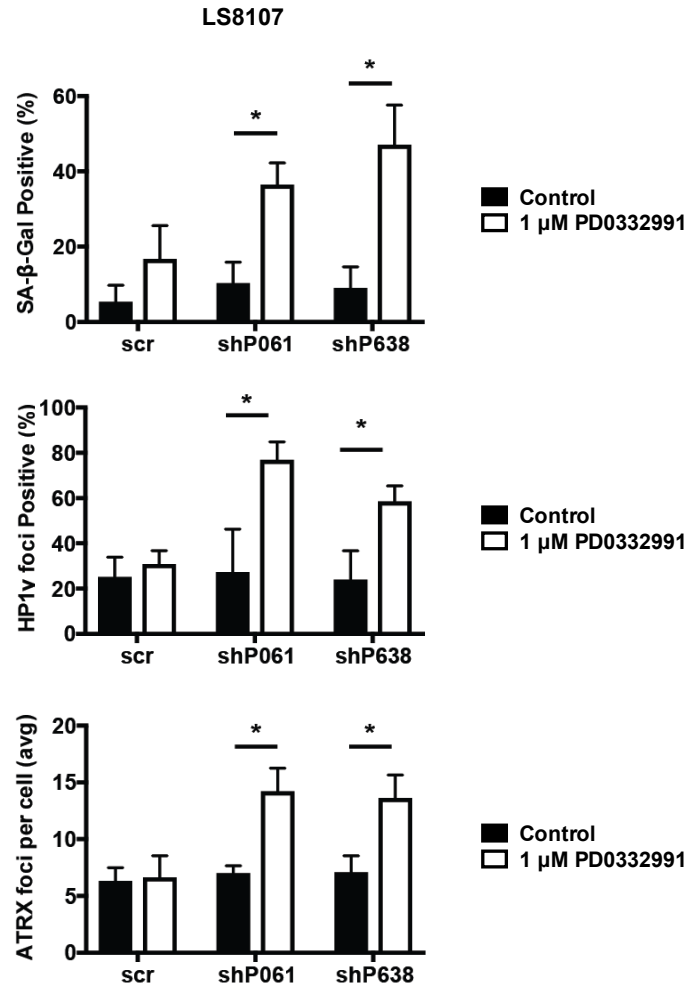


Figure 3.9. PDLIM7 knockdown allows PD0332991 to induce senescence in LS8107 cells

LS8107 cells were transduced with two different PDLIM7 knockdown lentiviral vectors (shP061 or shP638) or a non-specific vector (scr) and treated with 1 μM PD0332991 for seven days. The number of cells staining for SA-β-Gal, HP1γ foci, and the number of ATRX foci per cell were quantified. The mean and standard deviation of four independent experiments is plotted.

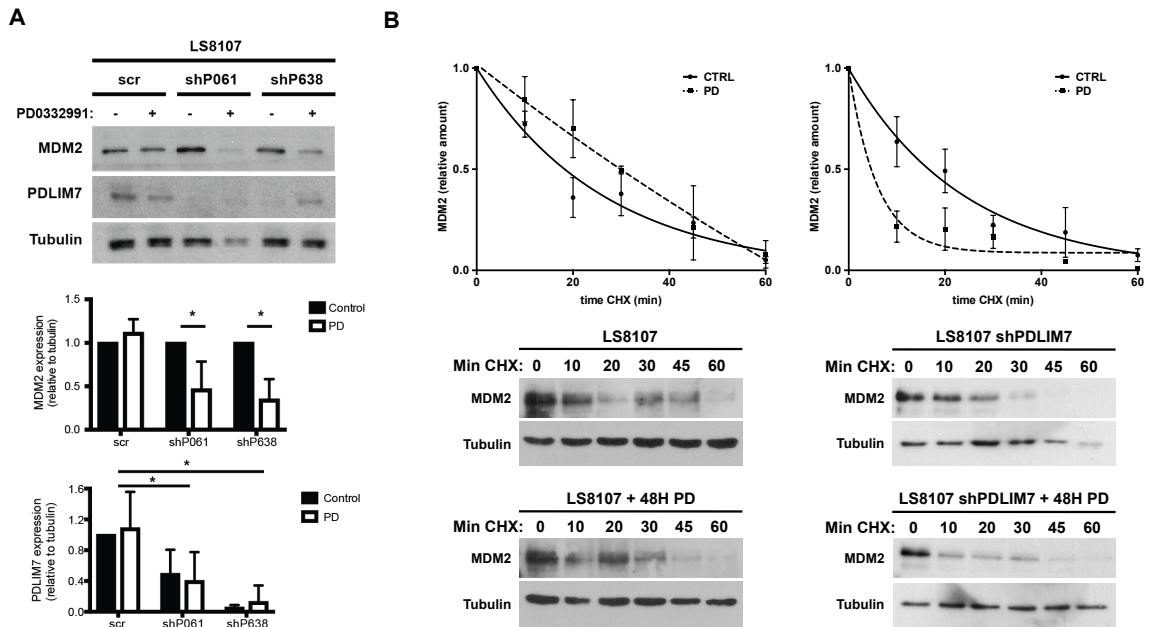


Figure 3.10. PDLIM7 knockdown allows PD0332991 to induce MDM2 down-regulation in LS8107 cells

(A) LS8107 cells were transduced with two different PDLIM7 knockdown lentiviral vectors (shP61 or shP638) or a non-specific vector (scr) and treated with 1 μ M PD0332991 (PD) for seven days. MDM2 and PDLIM7 protein levels were detected using immunoblot. Tubulin served as a loading control. *Top*, a representative image is shown. *Bottom*, expression was quantified using densitometry and the mean and standard deviation of four independent experiments is shown. (B) LS8107^{scr} and LS8107^{shP638} cells were treated with 1 μ M PD0332991 (PD) for two days and then exposed to 75 μ g/mL cyclohexamide (CHX) for the time (minutes) indicated. MDM2 and tubulin were measured by immunoblot. A representative image is shown below and the relative amounts were quantified from two independent experiments (mean \pm standard deviation) above.

However, co-knockdown of PDLIM7 and HAUSP was sufficient to induce senescence even in the absence of CDK4 inhibition (**Figure 3.11**).

The association of PDLIM7 with MDM2 is cell line and condition dependent

PDLIM7 is a PDZ and LIM domain containing protein that binds directly to MDM2 and inhibits its autoubiquitination, but does not block its E3 ligase activity [133]. To determine if PDLIM7 was physically associated with MDM2 differently in non-responder and responder cell lines, I transduced LS8107 and LS8817 cells with an N-terminally GFP-tagged PDLIM7 and immunoprecipitated MDM2. Tagging PDLIM7 facilitates its identification by immunoblot because the immunoglobulin heavy chain obscures the endogenous protein (**Figure 3.12, A**). An interaction was detected in cycling non-responder LS8107 cells, but not in cycling responder LS8817 cells (**Figure 3.12, B**). To ask if there was a condition where LS8817 cells have an interaction between PDLIM7 and MDM2, I subjected LS8817 cells to serum starvation, which induces cell cycle exit but does not cause a change in MDM2 protein or senescence markers [57, 108]. An interaction was detected between PDLIM7 and MDM2 in serum-starved cells (**Figure 3.12, B**). This suggests that the interaction of PDLIM7 with MDM2 is both cell line and culture condition dependent.

The cytosolic distribution of PDLIM7 is cell line and condition dependent

PDLIM7 was readily detectable in extracts from both LS8107 and LS8817 cells, and the amount was not differentially affected by treatment with PD0332991 (**Figure 3.13, A**). Therefore, I hypothesized that cellular localization of PDLIM7 might be associated with its ability to interact with MDM2. Immunofluorescence microscopy revealed that the localization of PDLIM7 was dynamically controlled. Focal depositions of cytosolic PDLIM7 were detected in cycling LS8817 cells and in LS8817 cells that had undergone senescence following treatment with PD0332991, but not in either cycling or PD0332991 treated quiescent LS8107 cells (**Figure 3.13, B**).

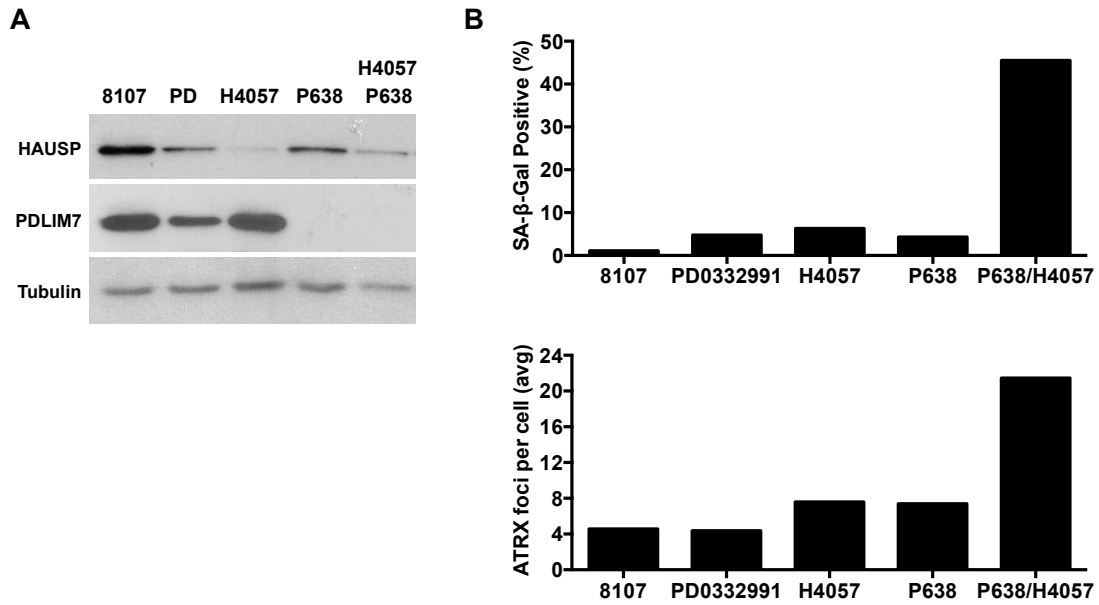


Figure 3.11. PDLIM7 and HAUSP co-knockdown induces accumulation of SA-β-Gal in non-responder LS8107 cells

LS8107 cells were transduced first with a PDLIM7 knockdown lentiviral vector (P638). After selection for 5 days with blastocidin they were transduced with a HAUSP knockdown lentiviral vector (H4057) and selected with puromycin for 5 days. Alternatively, cells were treated with PD0332991 (PD) for 7 days. (A) PDLIM7 and HAUSP protein levels were detected using immunoblot. Tubulin served as a loading control. (B) The number of cells staining for SA-β-Gal and the number of ATRX foci per cell were quantified.

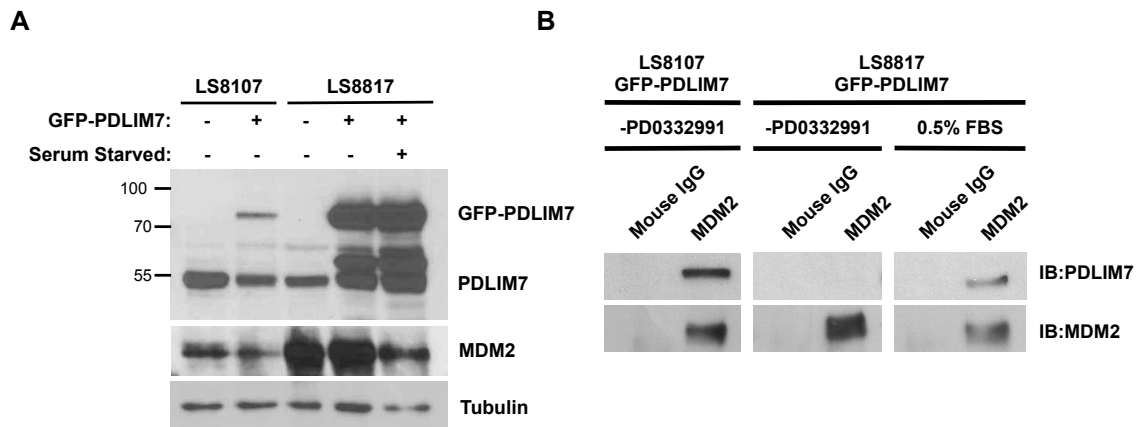


Figure 3.12. The association of PDLIM7 and MDM2 is cell line and condition dependent
 LS8817 and LS8107 cells were transduced with a vector expressing N-terminally tagged GFP-PDLIM7 and selected in puromycin. LS8817 cells were grown in serum-starved conditions with 0.5% serum for 4 days. (A) MDM2 and PDLIM7 protein levels were detected using immunoblot. Tubulin served as a loading control. (B) MDM2 was immunoprecipitated and PDLIM7 immunoblotted (n=3). IgG served as a control. Representative images are shown.

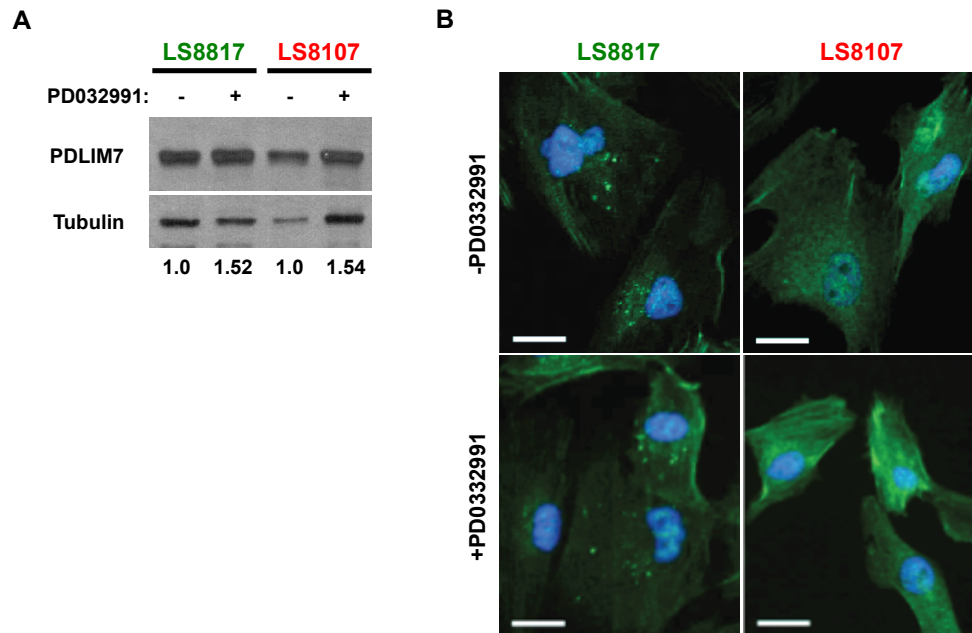


Figure 3.13. PDLIM7 is located in foci in LS8817 cells

The responder cell line LS8817 and non-responder cell line LS8107 were treated with 1 μ M PD0332991 (PD) for 7 days. (A) Cells were harvested for protein and MDM2 and PDLIM7 protein levels were detected using immunoblot. Tubulin served as a loading control. Representative images are shown along with the mean expression value (PDLIM7/tubulin) quantified from four independent experiments below each lane. (B) Cells were fixed, permeabilized, incubated with antibodies against PDLIM7 and fluorescent secondary antibodies, and visualized by immunofluorescence (n=3).

PDZ domain proteins associate with actin and cytoskeletal structures [138-140]. Therefore, I next asked if other structural elements in the cell might have a similar immunofluorescence staining pattern between the two cell lines. There was no focal staining detected with antibodies raised against actin, γ -tubulin, or vimentin in either LS8817 or LS8107 cells. Cytoplasmic foci were detected in LS8817 but not LS8107 cells when incubated with a pan-cadherin antibody (**Figure 3.14**). Additionally, similar cadherin foci were detected in other WD/DDLS, breast, glioma, and NSCLC cell lines that undergo CDK4 inhibitor-induced senescence, but not in a NSCLC cell line that undergoes quiescence (**Figure 3.15**).

Immunofluorescence microscopy with antibodies raised against both PDLIM7 and cadherin showed that foci overlapped in cycling LS8817 cells (**Figure 3.16, A**). Neither PDLIM7 nor cadherin foci were identified in cycling LS8107 cells or serum-starved LS8817 cells. The proximity ligation assay (PLA) can be utilized to confirm the localization of two antibody targets within 40 nanometers of each other [141]. I observed a positive PLA signal in LS8817 cells treated with both antibodies, but not in LS8107 cells treated with both antibodies (**Figure 3.16, B**). I did not observe PLA signal when LS8817 cells were treated with either antibody alone.

PDLIM7 is associated with CDH18 in foci

The surprising appearance of cadherin reactivity in the cytoplasm of a cell prompted me to investigate this further. The peptide immunogen used to generate the pan-cadherin antibody is found throughout the cadherin-C superfamily, which is the conserved cytoplasmic region found in cadherin super family I and II members (**Figure 3.17, A**) [142, 143]. Therefore, to identify the specific cadherin in these foci I knocked down several individual cadherin family members using at least two independent lentiviral shRNA vectors in LS8817 cells and screened for pan-cadherin foci by immunofluorescence microscopy. Only those shRNA targeting CDH18 consistently reduced the number of foci to less than five per cell and increased the number of cells with no foci to approximately 20% (**Figure 3.17, B**).

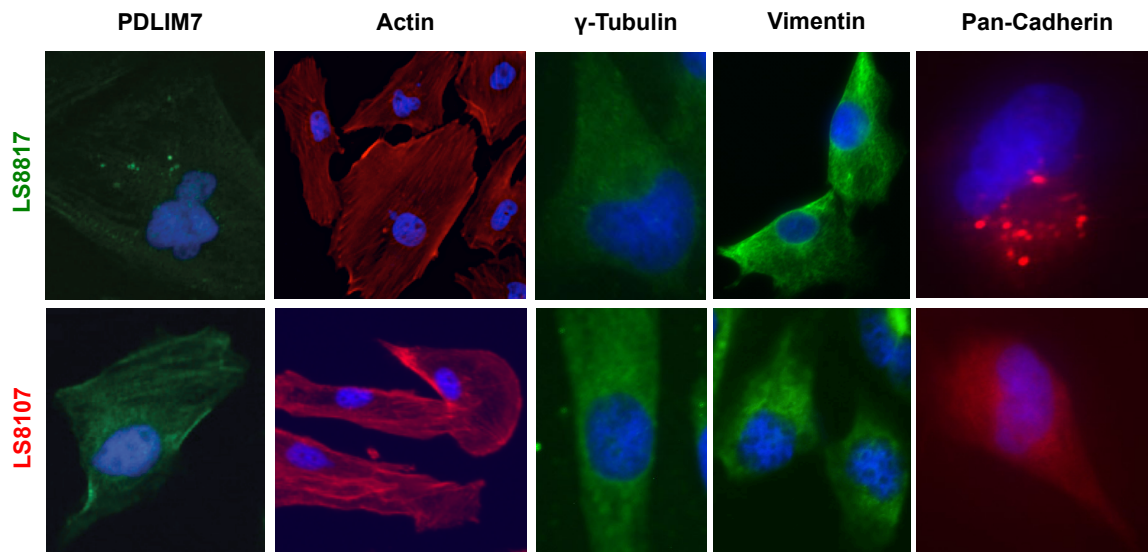


Figure 3.14. Immunofluorescence staining of cytoskeletal elements in LS8817 and LS8107 cells

LS8817 and LS8107 cells were fixed, permeabilized, and independently incubated with antibodies against PDLIM7, actin, γ -tubulin, vimentin and pan-cadherin. Slides were incubated with fluorescent secondary antibodies and visualized using immunofluorescence.

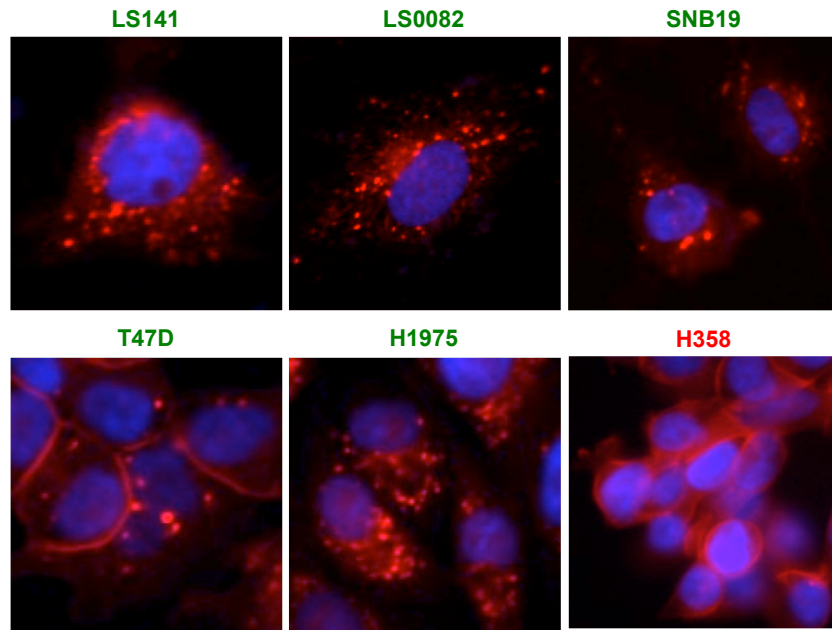


Figure 3.15. Immunofluorescence staining of pan-cadherin in a variety of cell lines

The responder WD/DDLS cell lines LS141 and LS0082, glioma cell line SNB19, breast cancer cell line T47D, NSCLC cell line H1975 and non-responder NSCLC cell line H358 were fixed, permeabilized, and incubated with the pan-cadherin antibody. Slides were incubated with fluorescent secondary antibodies and visualized using immunofluorescence.

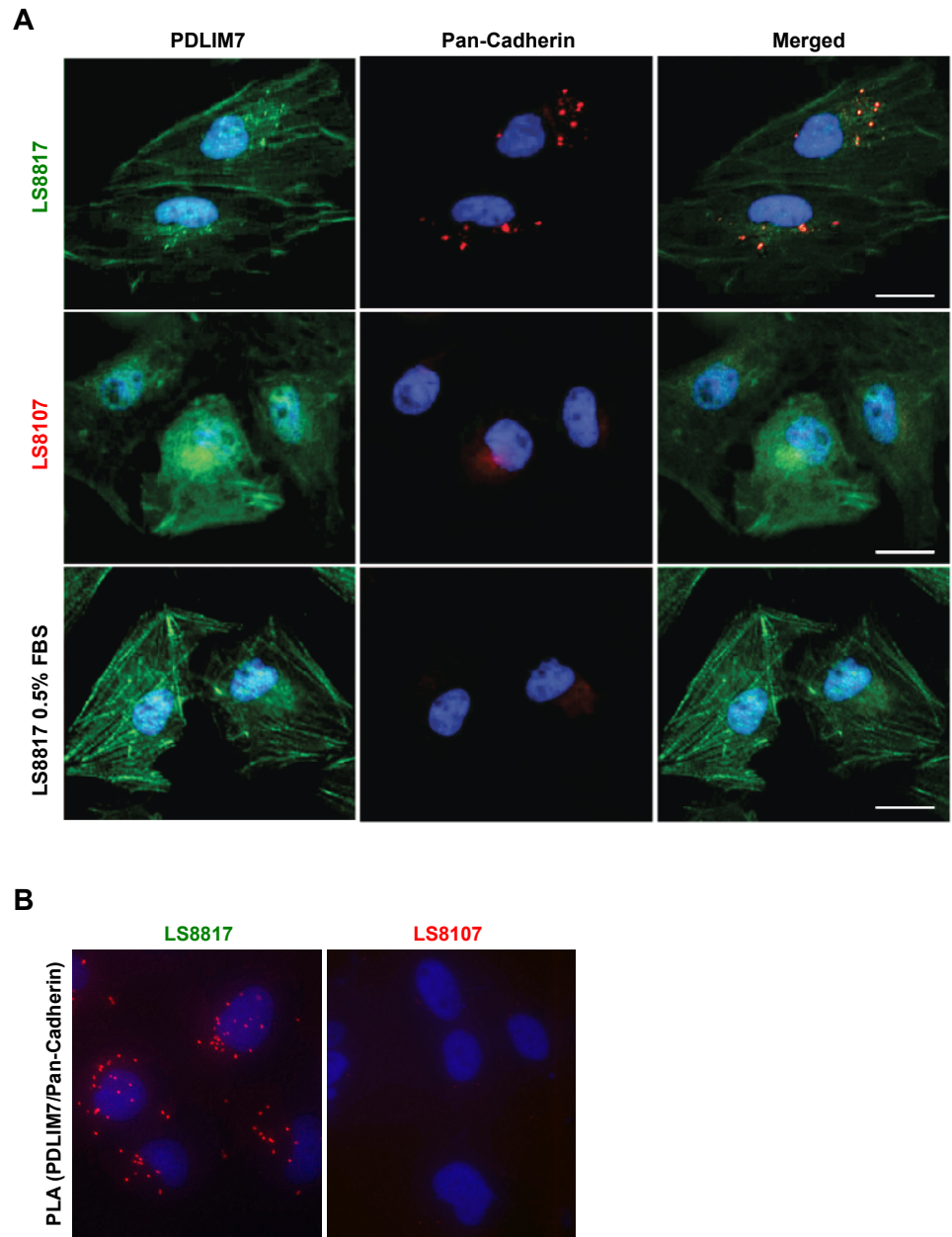
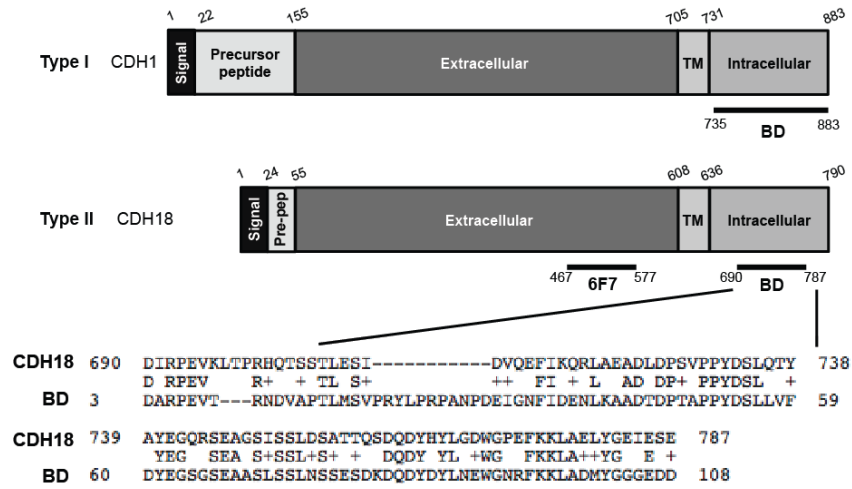


Figure 3.16. PDLIM7 is associated with pan-cadherin foci in a cell line and condition dependent manner

(A) LS8817 and LS8107 cells were treated as shown. Cells were fixed, permeabilized, and incubated with antibodies against PDLIM7 and pan-cadherin. Slides were incubated with fluorescent secondary antibodies and visualized by co-immunofluorescence. (B) LS8817 and LS8107 cells were fixed and incubated with antibodies against PDLIM7 and pan-cadherin followed by antibodies designed for the Sigma Duolink proximity ligation assay. Signal was visualized by immunofluorescence (n=3).

A



B

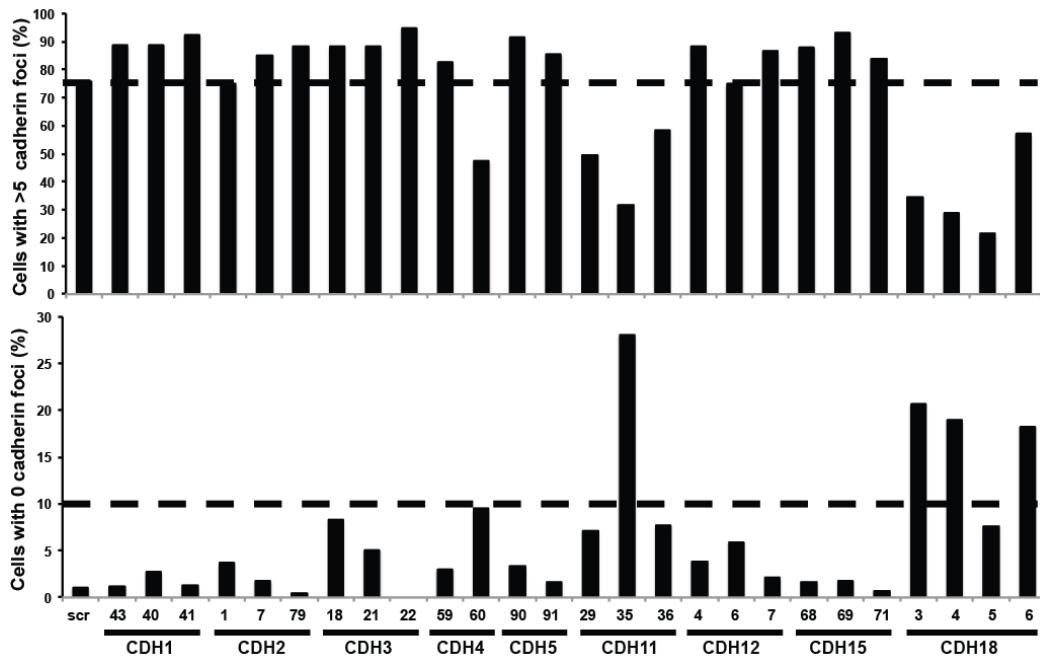


Figure 3.17. Knocking down CDH18 can reduce the appearance of pan-cadherin foci in LS8817 cells

(A) Schematic of a type I cadherin (CDH1) and a type II cadherin (CDH18). Homology to the pan-Cadherin peptide immunogen for BD Biosciences 610181 is shown. (B) LS8817 cells were transduced with independent short hairpins against the cadherin targets indicated and selected in puromycin for 5 days. The cells were fixed, permeabilized, and incubated with an antibody against pan-cadherin. The number of cells containing greater than 5 cadherin foci and 0 cadherin foci were quantified in at least five 20X fields for each knockdown (100-500 cells total).

However, none of the shRNA vectors were able to completely ablate cadherin focal staining. Thus, to test the effect of CDH18 loss on senescence and MDM2 regulation, I worked in collaboration with Scott Dooley and generated two different CDH18 mutant clones of LS8817 cells using CRISPR/Cas9. These independent knockout cell lines, LS8817^{CDH18KO1} and LS8817^{CDH18KO2}, harbor variants in CDH18 exons one and five, respectively. Sanger sequencing confirmed the presence of insertions and deletions that lead to predicted frameshifts (**Figure 3.18, A**). CDH18 protein level was reduced in both clones compared to parental cells (**Figure 3.18, B**).

I next probed the relationship of the PDLIM7 and CDH18 foci. Pan-cadherin staining was unaffected in the PDLIM7 deficient LS8817^{shP638} cells, but PDLIM7 foci were lost in the LS8817^{shP638}, LS8817^{CDH18KO1}, and LS8817^{CDH18KO2} cells (**Figure 3.19, A, B**). Further validating that PDLIM7 is interacting with CDH18 in foci, I detected positive PLA signals using CDH18 and PDLIM7 specific antibodies in LS8817 cells, but not in LS8107 cells, LS8817^{CDH18KO1} cells, or LS8817^{shP638} cells (**Figure 3.19, C**).

Knockout of CDH18 prevents PD0332991 induced MDM2 turnover and senescence

I next asked if CDH18 contributed to CDK4 inhibitor-induced senescence and MDM2 turnover. I treated both LS8817 CDH18 knockout lines with PD0332991 and assayed a number of senescence markers seven days later. These lines were significantly impaired in their ability to undergo CDK4 inhibitor-induced accumulation of SA-β-Gal and HP1γ foci (**Figure 3.20, A**). Furthermore, the LS8817^{CDH18KO1} and LS8817^{CDH18KO2} cells re-entered the cell cycle following removal of PD0332991 (**Figure 3.20, B**). MDM2 levels were not reduced in LS8817^{CDH18KO2} cells following treatment with PD0332991 (**Figure 3.21, A**), nor was the turnover of MDM2 accelerated to the same extent as seen in parental LS8817 cells (**Figure 3.21, B**). Collectively, this suggests that a CDH18 containing complex sequesters PDLIM7 allowing for more rapid turnover of MDM2 and cellular senescence following CDK4 inhibition.

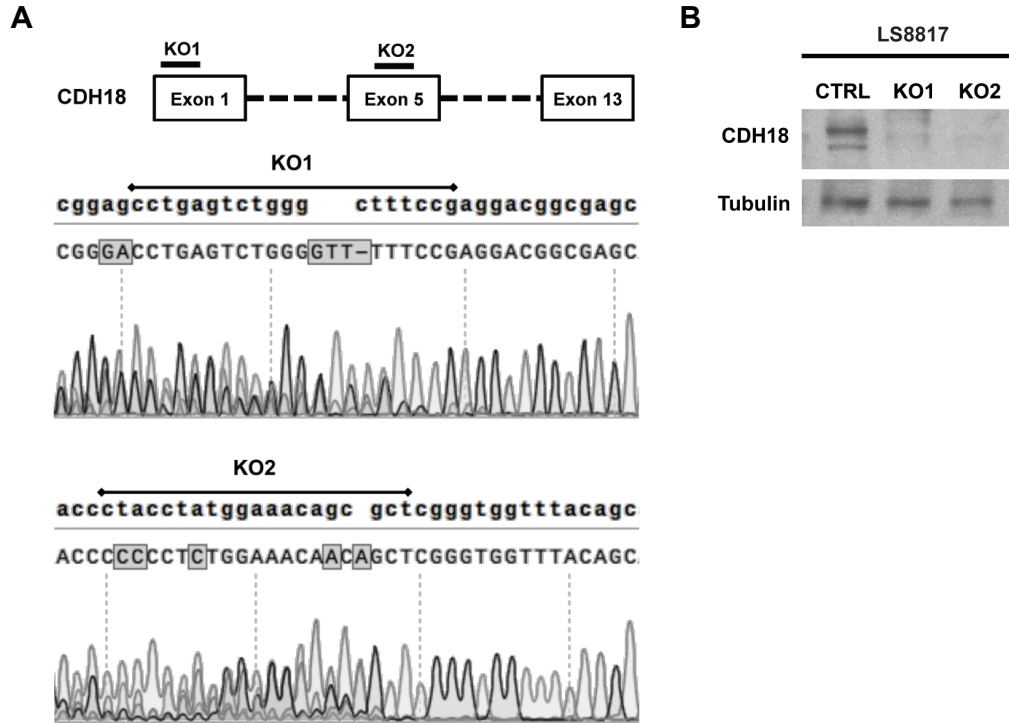


Figure 3.18. Generation of CDH18 knockout cell lines

(A) LS8817 cells were transduced with a vector containing Cas9 and a vector containing a guide RNA against CDH18 (KO1 and KO2). Targeting sequencings are shown. Cutting was confirmed by Sanger sequencing. (B) LS8817 cells transduced with the guide RNAs were harvested for protein. CDH18 protein levels were measured by immunoblot. Tubulin served as a loading control.

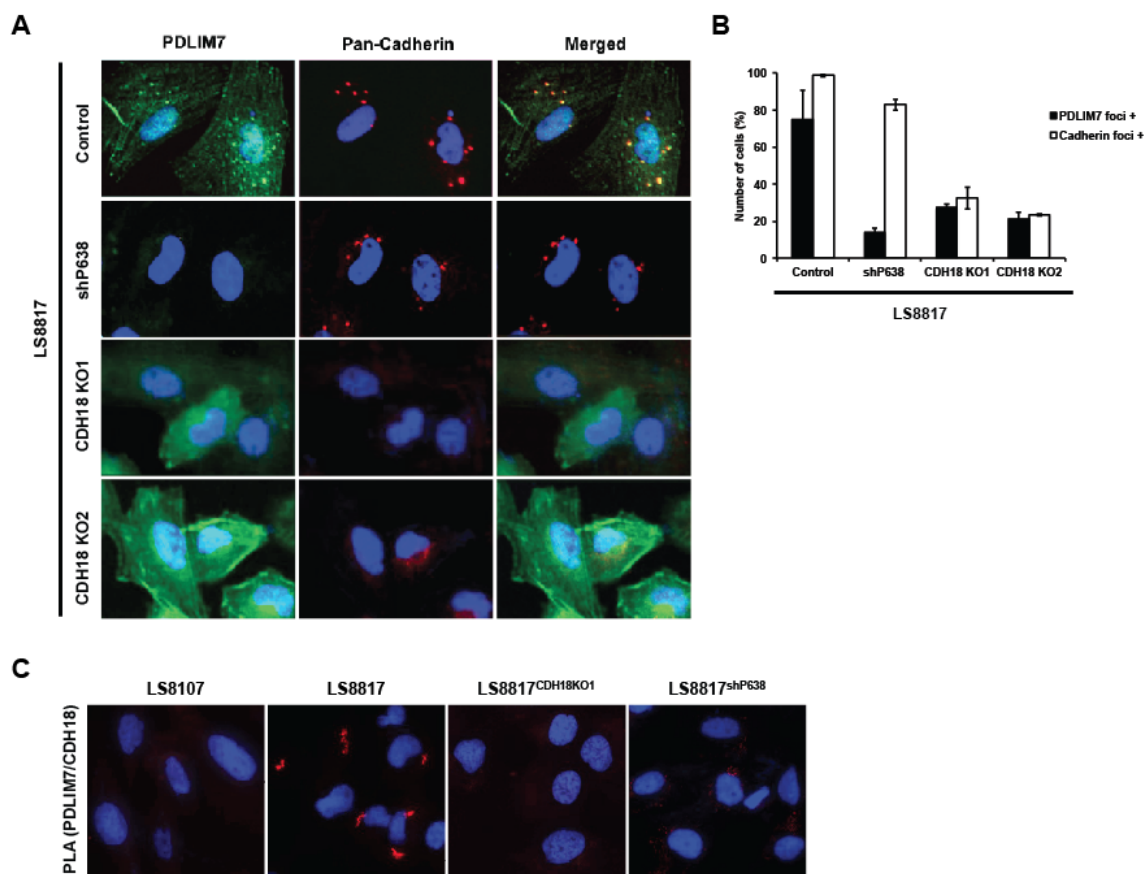


Figure 3.19. PDLIM7 is associated with CDH18 in foci in LS8817 cells

(A) The responder cell line LS8817 was unmanipulated (control), transduced with a PDLIM7 knockdown lentiviral vector (shP638), or a vector containing Cas9 and a vector containing a guide RNA against CDH18 (KO1 and KO2). PDLIM7 and pan-cadherin were visualized by co-immunofluorescence. (B) The number of cells containing PDLIM7 and pan-cadherin foci were quantified (n=2). (C) Non-responder LS8107, responder LS8817, LS8817^{KO1}, and LS8817^{shP638} cells were fixed and incubated with antibodies against PDLIM7 and CDH18 followed by antibodies designed for the Sigma Duolink proximity ligation assay. Signal was visualized by immunofluorescence (n=2).

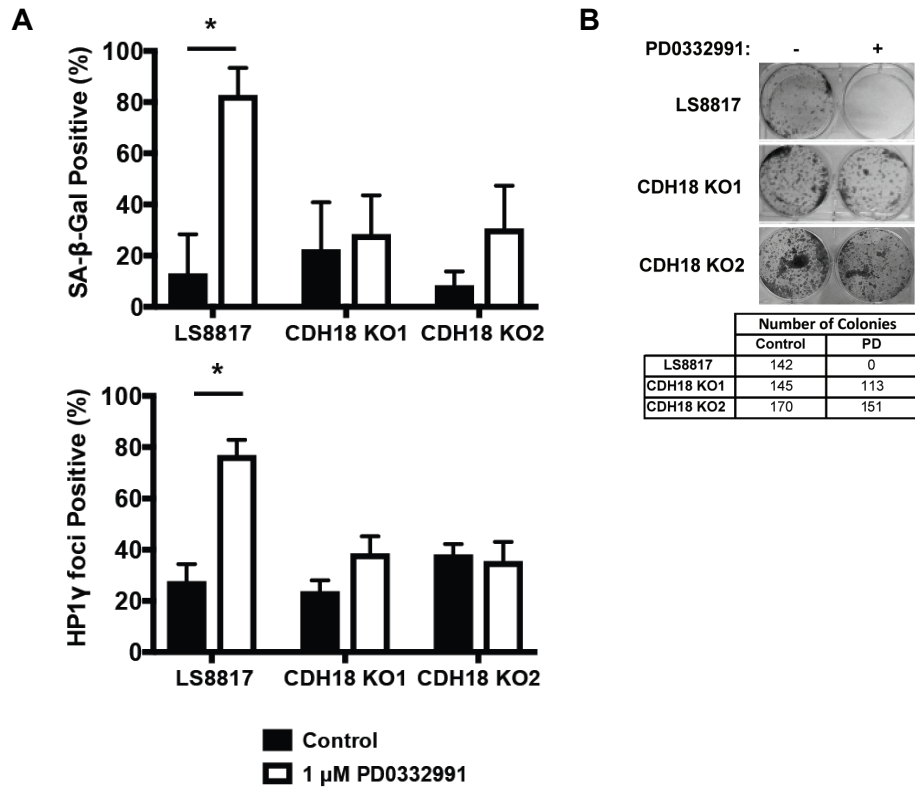


Figure 3.20. Knockout of CDH18 prevents CDK4 inhibitor-induced senescence in LS8817 cells

LS8817 cells and LS8817 cells transduced with the CDH18 knockout guide RNAs (KO1 and KO2) were treated with 1 μM PD0332991 for 7 days. The number of cells (mean ± standard deviation) staining for SA-β-Gal and HP1γ foci were quantified (n=3). (B) LS8817, LS8817 KO1, and LS8817 KO2 cells were treated with 1 μM PD0332991 for 10 days and then plated in drug free media and allowed to grow for 21 days to assess clonogenic growth.

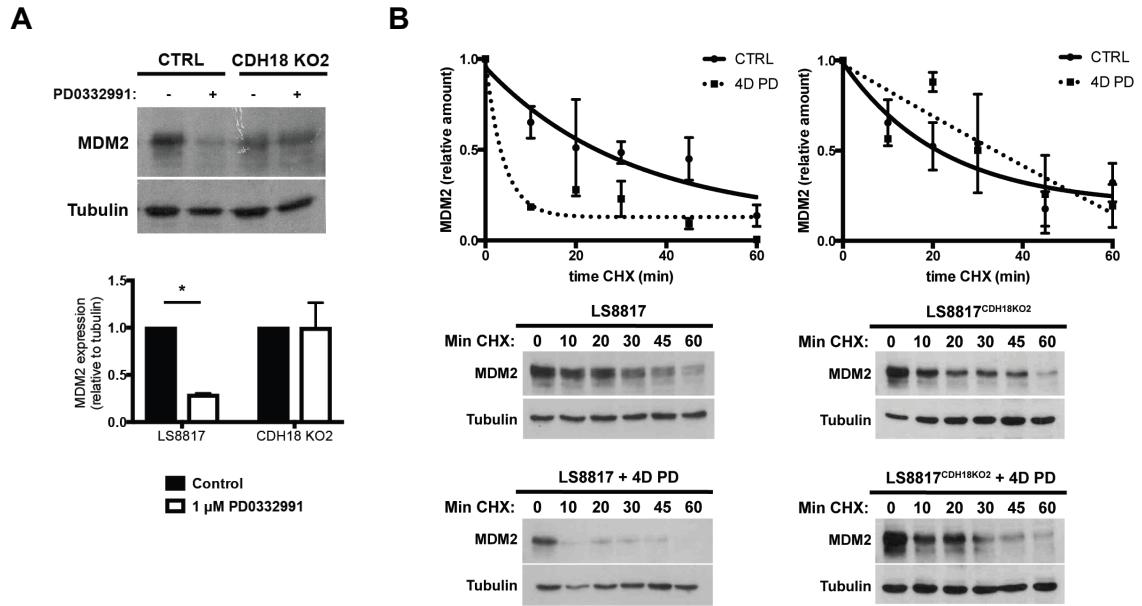


Figure 3.21. Knockout of CDH18 prevents CDK4 inhibitor-induced MDM2 turnover in LS8817 cells

(A) MDM2 protein levels were detected using immunoblot on extracts from LS8817 and LS8817 KO2 cells. Tubulin served as a loading control. Top, a representative image is shown. Bottom, expression was quantified using densitometry and the mean and standard deviation of three independent experiments is plotted. (B) LS8817 and LS8817 KO2 cells were treated with 1 μ M PD0332991 (PD) for 4 days and treated with 75 μ g/mL cyclohexamide (CHX) for the time (minutes) indicated. A representative image is shown below and the relative amounts were quantified from three independent experiments (mean \pm standard deviation) above.

CDH18 is expressed at higher levels in responder cells than non-responder cells

To determine whether differences in CDH18 expression might explain the differential response of cells to CDK4 inhibition, I analyzed CDH18 protein expression in a number of cell lines. CDH18 protein was readily detected in LS8817, LS141, and LS0082 cells, and in the non-small cell lung cancer cell line H1975, all of which senesce following CDK4 inhibition (**Figure 3.22**). Expression of CDH18 was lower in LS8107 and LS8313 cells, and in the non-small cell lung cancer cell line H358, all of which fail to senesce following CDK4 inhibition. All cells expressed PDLIM7, MDM2, and CDK4, albeit at variable levels.

CDH18 expression correlates with extended progression free and overall survival in WD/DDLS patients treated with palbociclib

Since the expression of CDH18 correlated with the outcome of CDK4/6 inhibition in cultured cells, I wondered if CDH18 expression might predict clinical benefit of palbociclib prior to therapy. To test this, I measured CDH18 expression by immunohistochemistry in 49 historical surgical specimens obtained from patients who enrolled in the phase II palbociclib clinical trials, and correlated findings with progression free (PFS) and overall survival (OS) data.

Immunohistochemistry was carried out on formalin fixed paraffin embedded tissue sections obtained from surgical resections performed 100-2100 days prior to palbociclib therapy. Sections ranged from 200 mm² to 600 mm² in size (with an average of 377 mm²). Twenty-eight of these patients received at least one prior systemic therapy sometime between resection surgery and treatment with palbociclib. The median number of therapies received was one (range from one to four). These treatments included gemcitabine, doxil, docetaxel, brivanib, irinotecan, or an MDM2 inhibitor, either alone or in various combinations. Two different dose schedules of palbociclib were used. Thirty-two patients received palbociclib at 125 mg daily for 21 days followed by a rest period of 7 days every 28 days, and seventeen received 200 mg daily for 14 days with a rest period of 7 days every 21 days.

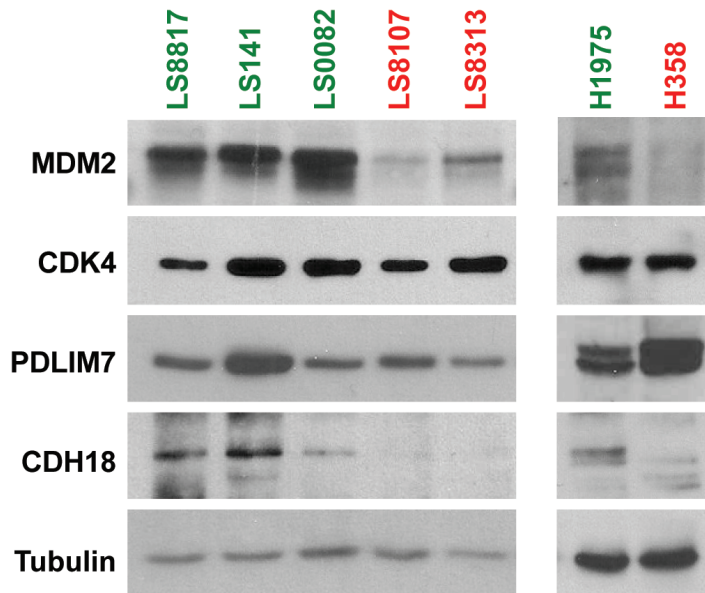


Figure 3.22. CDH18, PDLIM7, MDM2 and CDK4 protein expression levels

Proteins were extracted from asynchronously growing responder WD/DDLS cell lines LS8817, LS141, and LS0082 and the NSCLC cell line H1975 and the non-responder WD/DDLS cell lines LS8107 and LS8313 and the NSCLC cell line H358. Expression levels of the indicated proteins were determined by immunoblot. Tubulin served as a loading control.

The specificity of the antibody used for immunohistochemistry was validated in LS8817^{CDH18KO} cell lines. Blinded pathology review was carried out and reactivity described as positive or negative. Infiltrating inflammatory cells in negative samples served as a positive control for staining, while endothelial cells in blood vessels were a negative control in the positive samples (**Figure 3.23**). Tumors were called CDH18 positive if greater than 80% of the tumor cells in the sample stained positive in the cytoplasm. Five samples were censored from further analysis as positive and negative staining tumor cells were localized into specific domains. Such intratumoral heterogeneity makes the interpretation of expression difficult, but is consistent with the variation reported for genetic markers in liposarcoma [144]. One patient was censored from further analysis because control positive infiltrating inflammatory cells were not located on the slide. Information on the histology of the disease at the time of surgery, dose and scheduling of palbociclib, prior therapies, duration of survival after starting palbociclib, and CDH18 reactivity for the remaining forty-three individual patients analyzed is shown in **Figure 3.24**.

I plotted PFS (**Figures 3.25, A**) and OS (**Figure 3.25, B**) as a function of CDH18 expression. Patients whose tumors had CDH18 expression had better outcomes than those who lacked CDH18 expression (PFS, $p=0.005$; OS, $p=0.0007$). Neither whether patients received therapies between the time of surgery and enrollment on trial nor dosage schedule of palbociclib had a significant affect on either PFS or OS (**Figure 3.26**). However, we noted that all well-differentiated tumors were CDH18 positive (**Table 3.1**). Since well-differentiated liposarcoma often has a better prognosis than dedifferentiated liposarcoma (**Figure 3.26**), we wanted to confirm that this did not skew our analysis. After excluding the well-differentiated samples and only analyzing the 29 dedifferentiated samples, we found there was still a statistically significant better outcome in dedifferentiated patients that were CDH18 positive (PFS, $p=0.05$; OS, $p=0.006$) (**Figure 3.27**).

For all CDH18 positive patients, the median PFS was 17.9 weeks (95% confidence interval, 17 to 25.9 weeks), and the median OS was 42.4 months (95% confidence interval, 38.4

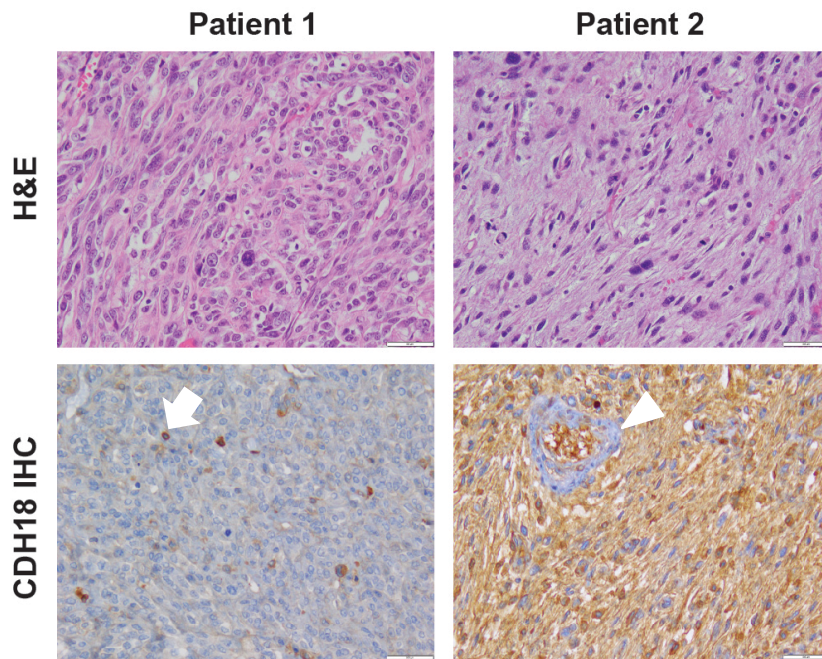


Figure 3.23. CDH18 detection by immunohistochemistry

Patient tumor samples were obtained during surgery and formalin fixed and paraffin embedded. After antigen retrieval, immunohistochemistry was performed using a CDH18 specific antibody. Hematoxylin and eosin (H&E) was used as a counterstain. Samples were blinded during analysis. Representative images are shown from two patients with dedifferentiated histologies, a CDH18 negative tumor (left) and a CDH18 positive tumor (right). Infiltrating inflammatory cells in negative samples served as a positive control for staining (arrow), while endothelial cells in blood vessels were a negative control in the positive samples (arrowhead).

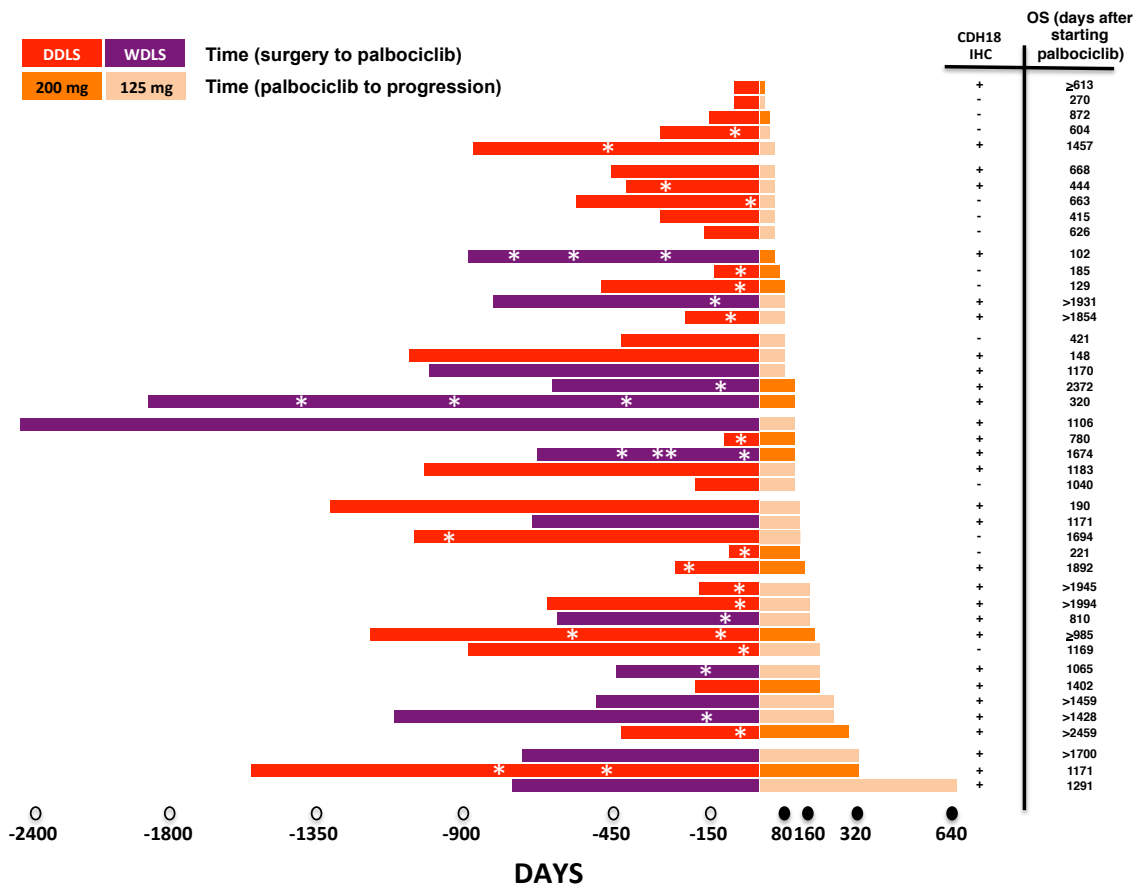


Figure 3.24. CDH18 expression and characteristics of the patient samples used in this study
 Red (dedifferentiated histology) and purple (well-differentiated histology) hues bars represent the time (days) from the most proximal surgical resection to the time the patient began palbociclib. Asterisks denote when patients received therapies between the time of surgical resection and before palbociclib treatment began. Orange hues bars represent the time (days) that the patient was on palbociclib before they progressed as defined in our previous papers [1, 2]. The dosage of palbociclib received is represented by the hue of the bar (light orange, 125 mg protocol; dark orange 200 mg protocol). CDH18 reactivity by immunohistochemistry is indicated to the right. Overall survival (OS) as of December 7, 2017 is indicated to the far right.

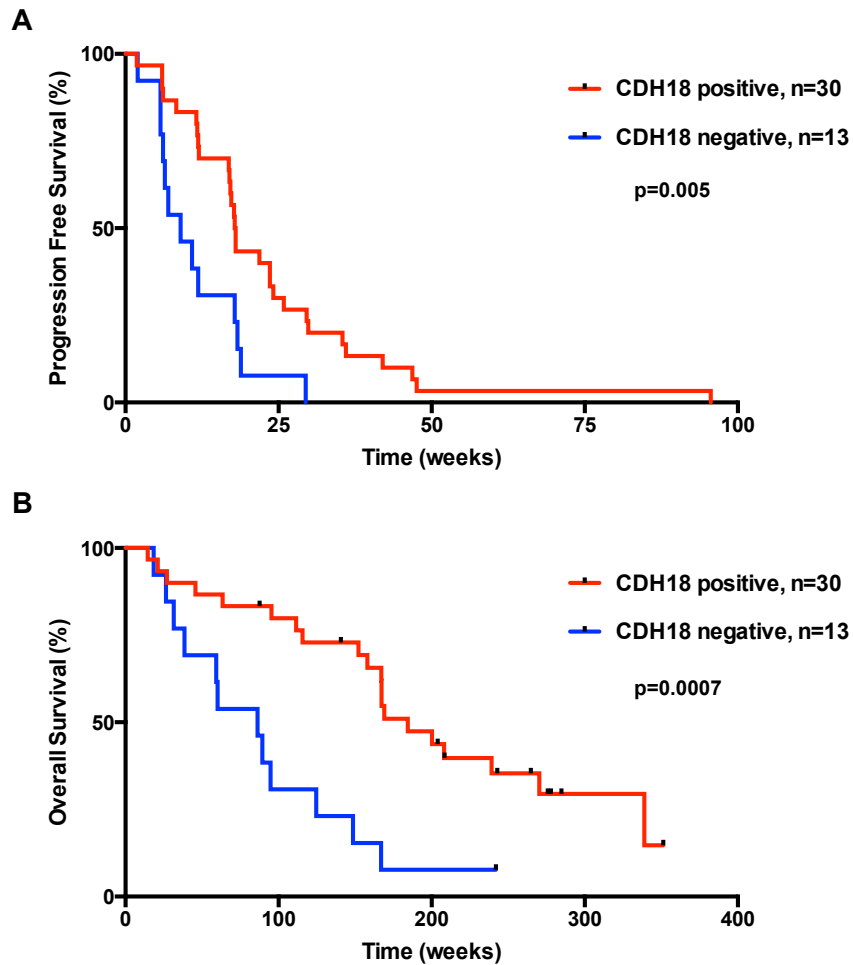


Figure 3.25. CDH18 expression can stratify WD/DDLS patient response to palbociclib monotherapy

(A) Progression free survival was plotted for patients with CDH18 positive and CDH18 negative tumor samples (p=0.005). (B) Overall survival was plotted for patients with CDH18 positive and CDH18 negative tumor samples (p=0.0007).

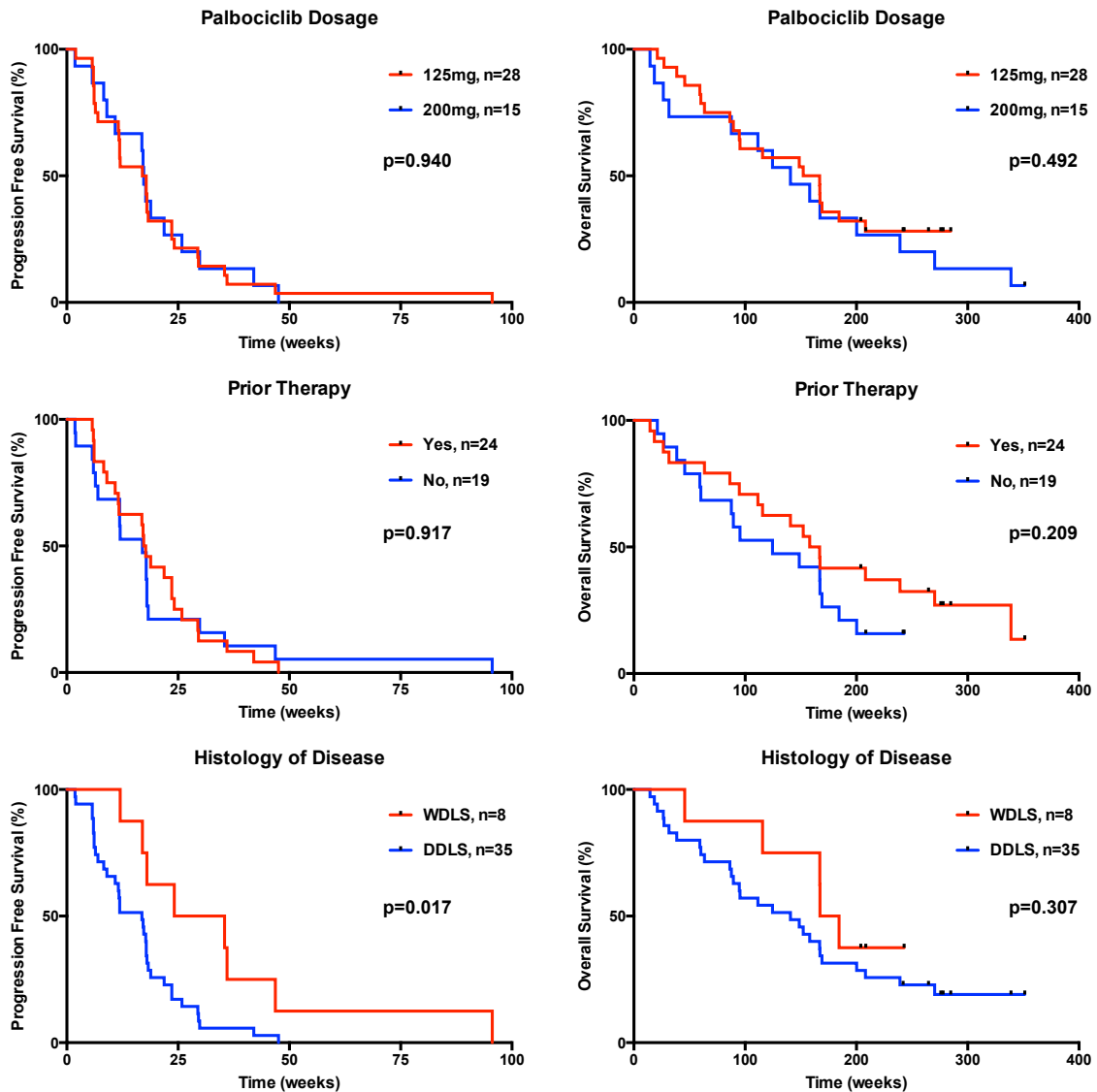


Figure 3.26. Other clinical factors do not stratify patient response to palbociclib monotherapy

Progression free survival and overall survival was plotted for patients based on the characteristics shown. Histology of disease represents patients with WDLs or DDLs at the time palbociclib treatment began, not the histology at the time of surgical resection.

Characteristics	CDH18-	CDH18+	Total
Number	13	30	43
Male	6	15	21
Female	7	15	22
Median Age (range), y	64 (41-83)	63 (35-81)	64 (35-83)
ECOG Score			
0	11	22	33
1	2	8	10
Primary Site			
retroperitoneum	12	30	42
extremity	1	0	1
Histology			
Well-differentiated	0	14	14
Dedifferentiated	13	16	29
Prior Systemic Treatment, No			
0	6	12	18
1	7	13	20
2+	0	5	5
Dosage schedule of palbociclib			
125 mg	9	19	28
200 mg	4	11	15

Table 3.1. Patient characteristics based on CDH18 status

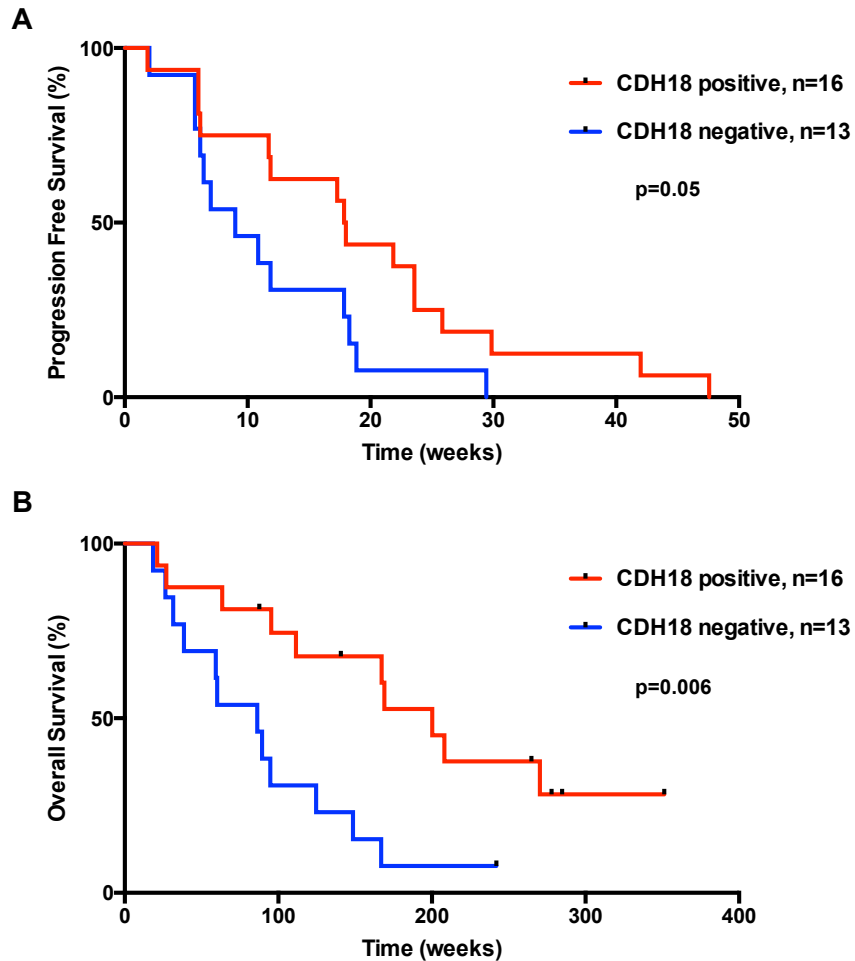


Figure 3.27. CDH18 expression can stratify DDLS patient response to palbociclib monotherapy

(A) Progression free survival was plotted for dedifferentiated liposarcoma patients with CDH18 positive and CDH18 negative tumor samples ($p=0.05$). (B) Overall survival was plotted for patients with CDH18 positive and CDH18 negative tumor samples ($p=0.006$).

months to non-estimable (NE)). For CDH18 negative patients the median PFS was 9.0 weeks (95% confidence interval, 6.1 weeks to NE) and OS was 19.8 months (95% confidence interval, 8.9 months to NE). While the power of the analysis is modest because the sample size is small, it does strengthen the hypothesis that the differential regulation of MDM2 and senescence is a clinically relevant mechanism that underlies the efficacy of this class of drug.

Discussion

When one pathway isn't enough: the context dependent regulation of MDM2

MDM2 (murine double minute 2) is an oncogene whose overexpression has been observed in a wide variety of human tumors [145]. Its structure contains an N-terminal p53-binding domain, a central acidic domain and zinc finger, and a C-terminal ring finger domain that is responsible both for auto-ubiquitination and *trans*-ubiquitination of multiple substrates, the most major of which is p53 [126]. Likely because of MDM2's ability to function as an oncogene and negatively regulate p53 (the 'guardian of the genome'), MDM2 levels are tightly controlled. MDM2 can be regulated transcriptionally, post-transcriptionally, or post-translationally. While the majority of published studies have a singular focus on any one regulator of MDM2, it is likely that in any cell, multiple regulators are involved in fine-tuning MDM2 levels in response to stimuli. These must cooperate to synthesize external signals and modulate MDM2 signaling.

MDM2 down-regulation is necessary for CDK4/6 inhibitor-induced senescence in a variety of cancer cell lines, and the loss of MDM2 is observed post-palbociclib treatment in patients with WD/DDLS who have prolonged periods of progression free survival [57]. Given that senescence is likely a more desirable outcome of cytostatic therapy, I set out to define the mechanism controlling MDM2 down-regulation in response to PD0332991 in cell lines. My ultimate goal was to identify if such regulators of MDM2 could serve as pre-treatment biomarkers of response to CDK4/6 inhibitors or be targeted in combination with CDK4/6 inhibitors to generate positive clinical outcomes.

Here, I illuminated the molecular basis of differential MDM2 regulation in cells that undergo quiescence or senescence after CDK4 inhibitor treatment. Prior work in the Koff lab showed that MDM2 transcription is repressed after treatment with PD0332991, though this occurs uniformly in all cells and the mechanism is not yet understood. CDK4 inhibition also drives the dissociation of HAUSP in all cells, regardless of whether they will become quiescent or senescent. Knockdown of HAUSP in both responder and non-responder cells induces cell cycle exit, but it is only sufficient to induce senescence and MDM2 down-regulation in responder cell lines.

As a deubiquitinase, HAUSP binds to MDM2 and removes ubiquitin from it, stabilizing MDM2 and allowing it to ubiquitinate other substrates [136, 137]. A number of regulators have been identified that can affect the HAUSP-MDM2 interaction including DAXX and RASSF1A [146, 147]. Neither DAXX nor RASSF1A expression changed in our cell lines after PD0332991 treatment, and work by others in the lab has been inconclusive about the effect of DAXX knockdown on CDK4 inhibitor-induced senescence (Kovatcheva and Gleason, unpublished data). Interestingly, DAXX can interact with ATRX [148], and loss of ATRX prevents MDM2 turnover in response to CDK4 inhibition [57]. It is tempting to speculate that ATRX could be required for HAUSP dissociation, but future work remains to determine how ATRX is involved in MDM2 down-regulation and if that mechanism includes the dissociation of HAUSP.

Since the dissociation of HAUSP was not sufficient to induce MDM2 turnover and senescence in all cell lines, I next asked what other factors could be blocking MDM2 turnover. After attempting to knock down five different genes whose proteins had been previously shown to inhibit MDM2 turnover [125], I showed that one, PDLIM7, is needed to stabilize MDM2 and prevent PD0332991 induced senescence. PDLIM7 was previously shown to inhibit MDM2 auto-ubiquitination and allow MDM2 to ubiquitinate p53 [133]. However, there has been scant work done to follow up on this interaction. Perhaps this is because any studies on how PDLIM7 associates with MDM2 would be difficult to perform if two contrasting cell lines (i.e. one where

it binds and one where it does not) were not available. Since PDLIM7 expression was ubiquitous in the cell lines in this study, localization was revealed as the key difference. Furthermore, there is clearly a growth condition component to the interaction between PDLIM7 and MDM2 since serum starvation can ablate PDLIM7 foci and induce an interaction with MDM2 that may not exist in cycling cells. Thus, studying this pathway has allowed me to uncover a context where PDLIM7 regulation of MDM2 plays a critical role.

Importantly, the co-knockdown of PDLIM7 and HAUSP is able to induce senescence even in the absence of CDK4 inhibition. While this does not preclude the possibility that other regulators of MDM2 are also involved in turnover after CDK4 inhibition, especially given the incomplete knockdown of some of the regulators tested, it does suggest that HAUSP and PDLIM7 are two major players in the regulation of MDM2 in response to CDK4 inhibition and that these mechanisms cooperate to achieve MDM2 turnover.

Beyond the plasma membrane: intracellular cadherin expression

PDZ and LIM domain containing proteins have roles in many diverse processes including cytoskeletal organization, neuronal signaling, organ development, and oncogenesis [149]. In addition to the ability of these proteins to bind to actin, PDZ domains have been shown to interact with catenin and with cadherins that are lacking catenin-binding domains [150, 151]. Therefore, I endeavored to understand the composition of the focal complex containing PDLIM7 in responder cells. Given their well-described functions at the cell membrane, I was initially surprised to identify a focal cytoplasmic staining pattern when using an antibody that can recognize type I and II cadherins that co-localized with PDLIM7 [142, 143].

The BD Biosciences ‘pan-cadherin’ antibody (catalog #610182) used in these studies is marketed as an E-cadherin specific antibody. However, in WD/DDLS cells, RNA-seq analysis revealed that E-cadherin is not expressed, shRNAs against E-cadherin had no effect on staining with this antibody, and other antibodies against E-cadherin did not have reactivity. It is worth

noting that other studies have also found differing results between this antibody and an antibody recognizing the extracellular domain of E-cadherin, and have identified perinuclear focal staining with this antibody that they attributed to E-cadherin [152, 153]. While many studies using this antibody are probably identifying E-cadherin specific effects, it is worth proceeding with caution when interpreting results generated with this antibody.

My work has identified that the type II cadherin 18 (CDH18) can be attributed to the perinuclear staining pattern of the pan-cadherin antibody. Knockout of CDH18 causes loss of PDLIM7 foci and blocks CDK4 inhibitor-induced MDM2 turnover and senescence. Furthermore, CDH18 protein expression correlates with whether a cell will undergo quiescence or senescence.

Changes in expression levels of cadherins have been documented in carcinoma and can serve as a determinant of chemotherapeutic response [154, 155]. There have been multiple proposed mechanisms of how cadherins can promote invasion and metastasis, primarily through the epithelial to mesenchymal transition (EMT) [156]. However, I did not see altered levels of other markers that denote EMT in cells correlating with CDH18 expression. To my knowledge, my work on CDH18 is the first time an intracellular cadherin, not linked to EMT, can be associated with therapeutic outcome.

CDH18 was initially identified in a screen for molecules that interact with β -catenin in the central nervous system [157]. However, limited work has been done to study the activity of CDH18 since. There is evidence that similar to other type I and II cadherins, CDH18 may have a role in oncogenesis. CDH18 is upregulated in MCF7 cells upon loss of p53, though the function of this change was not assessed [158]. Additionally, the genomic localization of CDH18 is on the short arm of chromosome 5, a region that is susceptible to loss of heterozygosity in carcinomas and contains a cluster of cadherins [159, 160]. It will be of future interest to determine if there are genomic changes in CDH18 that underlie response to CDK4 inhibition, or if differences in protein expression are driven by other transcriptional or post-transcriptional mechanisms.

Similarly, it will be important to understand what controls the localization of PDLIM7 and CDH18. Is expression of CDH18 alone sufficient to induce this interaction? What domains of PDLIM7 are important for its localization? While we were only able to begin to look at where PDLIM7 and CDH18 are located in the cell, we have preliminary evidence that they are localizing to the lysosome. Thus, the staining pattern I identified could give insight into new cadherin biology beyond the plasma membrane.

From bedside to bench and back again: SAGA is a clinically relevant mechanism

Successful expansion of CDK4/6 inhibitor therapies will require biomarkers that are predictive of response and are applicable in a large number of diverse tumor types [161]. Although large-scale sequencing and gene expression studies carried out so far have failed to identify such markers [50], our data suggests that CDH18 and a deeper understanding of senescence regulation might determine if a patient's tumor would be innately resistant or clinically sensitive to CDK4/6 inhibitors.

In patients with WD/DDLS who received palbociclib, CDH18 is significantly associated with progression free and overall survival. Additionally, it is clear that those patients who are negative for CDH18 are more likely to do poorly. When we model the successful outcome as PFS greater than or equal to 24 weeks, the negative predictive value of CDH18 is 92.3%. In contrast, the positive predictive value is just 33.3%. In line with this, the median PFS of patients who are CDH18 positive is comparable to the median PFS of the entire patient population, whereas the median PFS of CDH18 negative patients is cut in half. This suggests that while CDH18 expression is unable to identify a population that will exclusively have durable responses, it may be able to exclude patients that will not respond. Thus, pre-treatment analysis of CDH18 may identify those patients who would benefit from clinical strategies aimed at augmenting the senescence pathway.

While tumor type can impact on the mechanism underlying response, we believe that a similar mechanism might operate in HR+ HER2- breast cancer patients. MDM2 down-regulation during CDK4 inhibitor-induced senescence is seen in cell lines derived from such breast cancers [57] and we have identified cadherin foci in cell lines derived from multiple tumor types. Furthermore, the two-fold increase in the median PFS in WD/DDLS between CDH18 positive and CDH18 negative populations is comparable in magnitude to the two-fold increase in the duration of response in HR+ HER2- breast cancer patients treated with letrozole and palbociclib [26]. Large-scale retrospective clinical studies in such a disease may ultimately determine whether CDH18 might be an important determinant of response.

Regardless of whether CDH18 expression is predictive, it is worth noting that the association of CDH18 with extended PFS and OS for patients with WD/DDLS treated with palbociclib supports the hypothesis that the regulation of MDM2 and senescence is a clinically relevant mechanism of action for CDK4/6 inhibitors (**Figure 3.28**). As we discover more mechanisms that drive this pathway, perhaps other vulnerabilities will be identified that can further stratify patient response. My work demonstrates the power that a bedside to bench to bedside approach can have, and illustrates how bringing a clinical observation into the laboratory can uncover a new biological mechanism with the potential to influence patient care.

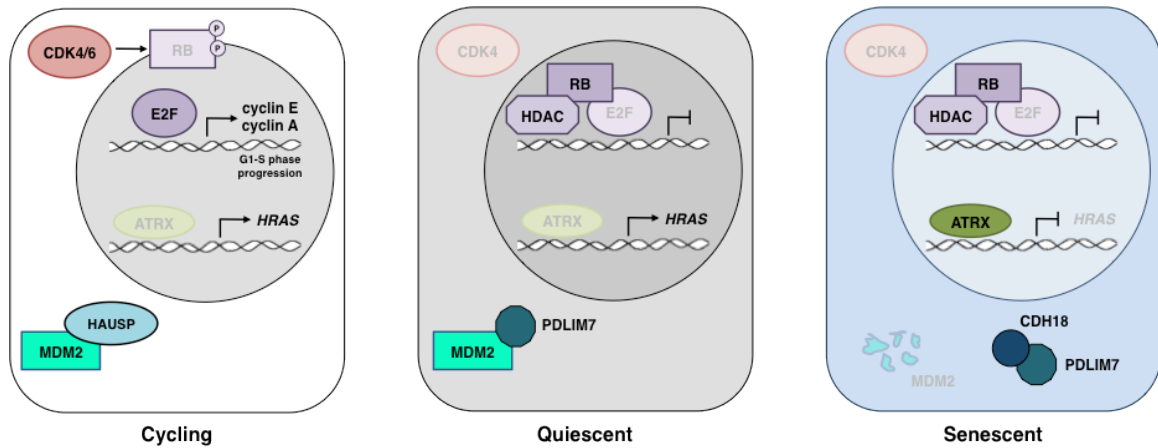


Figure 3.28. Mechanisms underlying CDK4 inhibitor-induced quiescence and senescence

In cycling cells, the transcription factor E2F drives expression of cyclin proteins associated with G₁-S phase progression. After CDK4/6 inhibition, Rb inhibits E2F, causing cells to exit the cell cycle into quiescence or senescence. This decision is dependent upon the ability of ATRX to form nuclear foci and repress transcription of HRAS and the enhanced degradation of MDM2. Specifically, in quiescent cells, MDM2 is stabilized by an interaction with PDLIM7; however, in senescent cells, PDLIM7 is sequestered from MDM2 by an interaction with CDH18 which results in loss of MDM2 and drives senescence.

CHAPTER 4: CDK4 INHIBITORS DRIVE SENESENCE AFTER GROWTH ARREST

Introduction

Quiescence vs. senescence

In parallel to my work on MDM2 regulation, I became interested in the relationship between quiescence and senescence. Quiescent cells are generally characterized by an absence of phenotypes, and quiescence is often thought of as the default state induced in the absence of nutrients or mitogenic signals [162]. However, it is becoming clear that quiescence is an actively regulated program, both transcriptionally and epigenetically [74, 163-166]. Quiescent cells can be identified based on lack of proliferation, lowered RNA content, and the absence of markers of apoptosis, senescence, or differentiation [72]. Critically, once the inducing trigger is removed, or growth factor signaling is reactivated, quiescent cells can return to the cell cycle and proliferate.

Conversely, senescent cells are impervious to growth factor signaling and will not return to the cell cycle, even once the inducing trigger is removed [167]. Similar to quiescent cells, senescent cells exit the cell cycle, often have an enlarged flattened morphology, remain metabolically active, and present no markers of apoptosis or differentiation. Uniquely, depending on the pathway into senescence and cell type, they can also have increased expression of p16 and p53, an increase in DNA damage foci and reactive oxygen species, accumulation of senescence-associated beta-galactosidase (SA- β -Gal), changes in chromatin including the formation of senescence-associated heterochromatic foci (SAHF), an increase in the number of ATRX foci, and the release of a senescence-associated secretory program (SASP) [75, 98, 108, 168].

It has been suggested that the decision between senescence and quiescence is dependent on the presence of growth factor signaling. For example, if p21 or p16 is overexpressed in the presence of growth factors, senescence will occur. But, if growth factors are removed, cells will instead quiesce. Mechanistically, the activity of mTOR, AKT, and/or FoxO3 may underlie this switch [169, 170]. In the case of CDK4 inhibition, the presence of serum is necessary for

senescence, as cells that are first serum starved and then treated with PD0332991 will not undergo senescence (Klein, unpublished data). This may be in part due to the serum dependent regulation of CDH18 and PDLIM7 localization as discussed in Chapter 3. However, the presence of serum is not sufficient for senescence, as many of the cell lines undergo quiescence after treatment with CDK4 inhibitors even when grown in complete serum.

Regardless of what underlies the switch, the decision between quiescence and senescence is often depicted as an either/or decision where cells must choose to exit the cell cycle into either quiescence *or* senescence (**Figure 4.1, A**). In this model, cells must re-enter the mitotic cell cycle from quiescence before exiting into senescence [166, 171-174]. However, it is possible that after CDK4 inhibition, cells exit the cell cycle into quiescence and, if the environment is permissive, can then progress into senescence (**Figure 4.1, B**). Given the finding that HAUSP dissociation can induce all cells to exit into quiescence, but senescence only occurs if the environment is permissive for MDM2 down-regulation, I hypothesized that a sequential pathway exists where cells progress from quiescence into senescence.

Prior work in the Koff lab demonstrated that knockdown of MDM2 in cycling non-responder cells induces cell cycle exit and senescence. On the other hand, enforced expression of MDM2 prevents the ability of CDK4 inhibitors to induce senescence in responder cells, though the cells still exit the cell cycle after drug treatment. In this way, toggling the expression of MDM2 can switch the decision between quiescence and senescence. Importantly, MDM2 is not a cell cycle regulator *per se*, and its expression or loss does not prevent cells from exiting the cell cycle. Loss of MDM2 merely alters the type of exit a cell will undergo. Therefore, by studying CDK4 inhibitor-induced senescence, I had the opportunity to tease apart whether exiting into quiescence is a terminal cell fate or if cells can be induced to undergo progression into senescence after growth arrest is established.

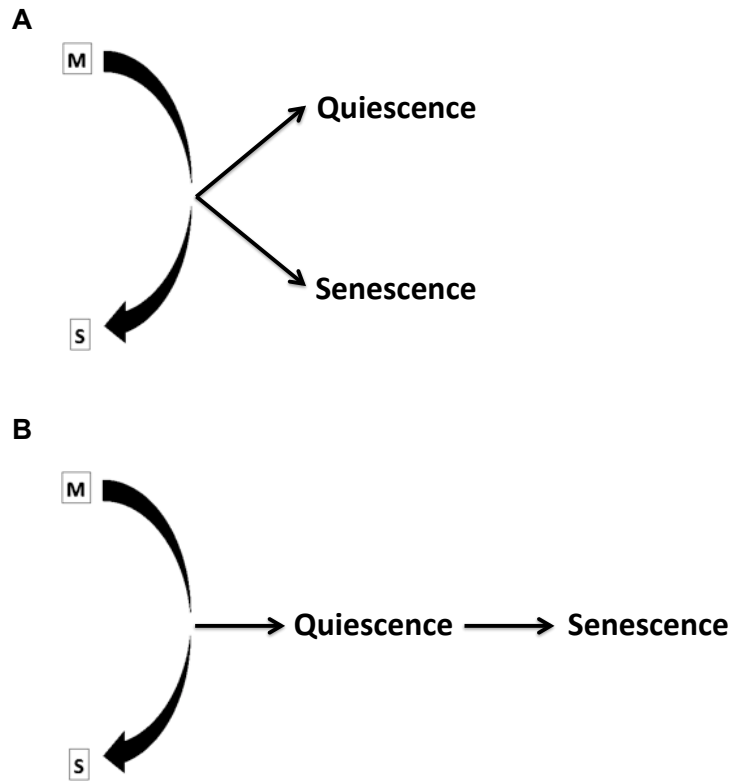


Figure 4.1. Models of the relationship between senescence and quiescence.

In the G_1 phase, cells choose to either exit the cell cycle or commit to another round of genome duplication and division. Cells can exit the cell cycle into different states, and the choice between quiescence and senescence could be a branch point (A), or a sequence of decisions (B).

Results

CDK4 inhibition drives senescence after growth arrest

To evaluate these different possible mechanisms, I took advantage of the knowledge that the non-responder cell line LS8107 undergoes CDK4 inhibitor-induced quiescence, but if MDM2 is knocked down in cycling LS8107 cells they will undergo senescence. I first arrested LS8107 cells in quiescence by treatment with PD0332991 for 2 days. I subsequently transduced these quiescent cells with a lentiviral vector encoding an shRNA targeting MDM2 and performed positive selection with puromycin for 8 days before assaying the effect on senescence markers. Knocking down MDM2 in quiescent cells induced similar levels of senescence markers to those obtained when MDM2 was knocked down in a cycling cell population (**Figure 4.2**). This suggests that quiescence can be converted into senescence by reducing MDM2, and that the decision of a cell to senesce in response to CDK4 inhibition follows the decision of cell cycle exit. We have termed this transition senescence after growth arrest or SAGA.

I next hypothesized that if I stably transduced responder cells with a tetracycline inducible (TetON) MDM2 expression vector, treatment with doxycycline and a CDK4 inhibitor would maintain MDM2 levels and arrest cells in quiescence. Subsequent removal of doxycycline would allow for loss of MDM2, freeing cells to progress into senescence. In collaboration with Scott Dooley, I designed a doxycycline-inducible FLAG-tagged MDM2 (FMDM2) construct and transduced the WD/DDLS responder cell line LS8817 (LS8817^{TetONFMDM2}) (**Figure 4.3, Figure 4.4, A**). In these cells, treatment with 10 μ M doxycycline (dox) was sufficient to induce FMDM2 expression at 48 hours (**Figure 4.4, B**). This expression remained stable when 0.1 μ M PD0332991 (PD) was added in the presence of dox. After removal of dox, while still in the presence of PD, FMDM2 began to decrease after 72 hours (**Figure 4.4, C**).

To test the ability of LS8817^{TetONFMDM2} cells to remain in quiescence or undergo senescence, I treated first with 10 μ M dox for 2 days and then 10 μ M dox + 0.1 μ M PD for 2 additional days (**Figure 4.5**). At this time I either removed dox but maintained the cells in 0.1 μ M

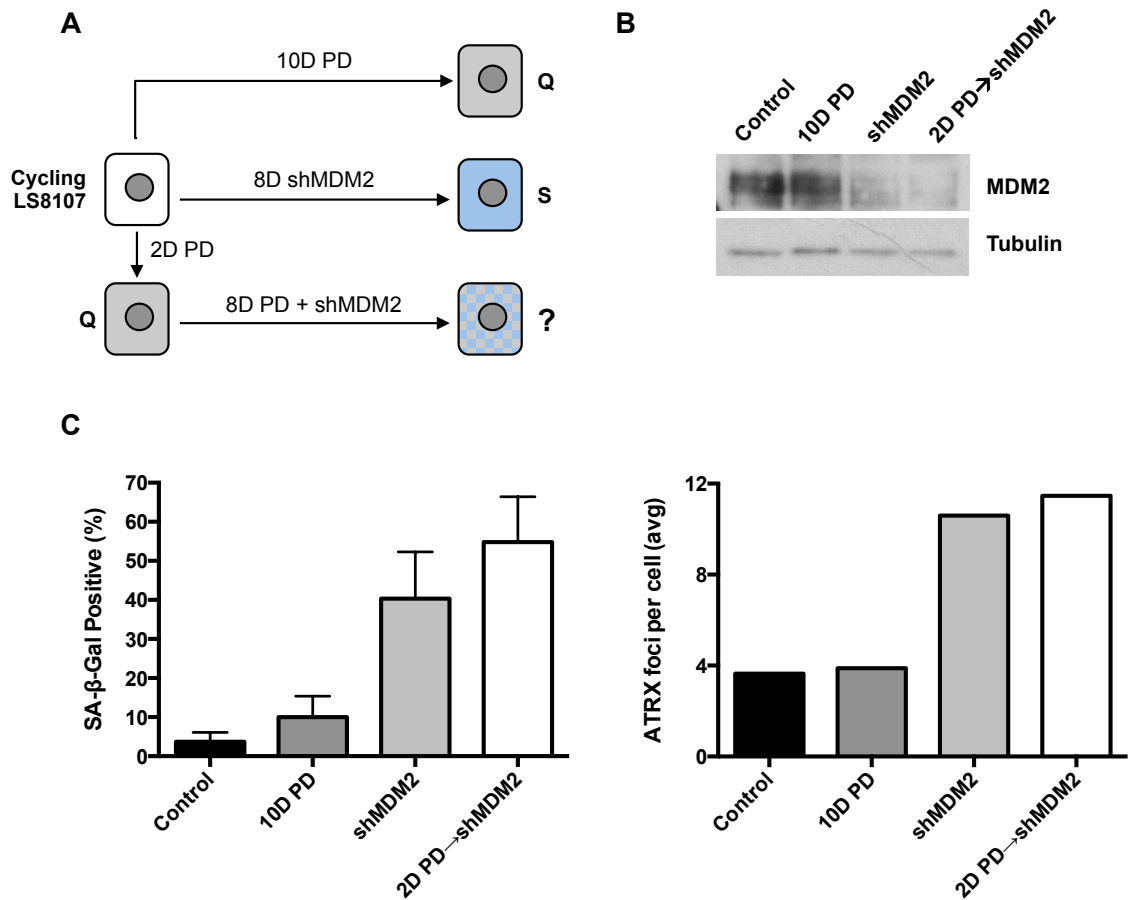


Figure 4.2. Knockdown of MDM2 drives senescence after growth arrest

(A) LS8107 cells were treated with 1 μ M PD0332991 (PD) for 10 days, transduced with a MDM2 knockdown lentiviral vector (shMDM2) and selected in puromycin for 8 days, or treated with 1 μ M PD0332991 for 2 days before being transduced with a MDM2 knockdown lentiviral vector and kept in 1 μ M PD0332991 for a further 8 days. (B) MDM2 protein levels were measured by immunoblot. Tubulin served as a loading control. (C) The number of cells staining for SA- β -Gal and the number of ATRX foci per cell were quantified.

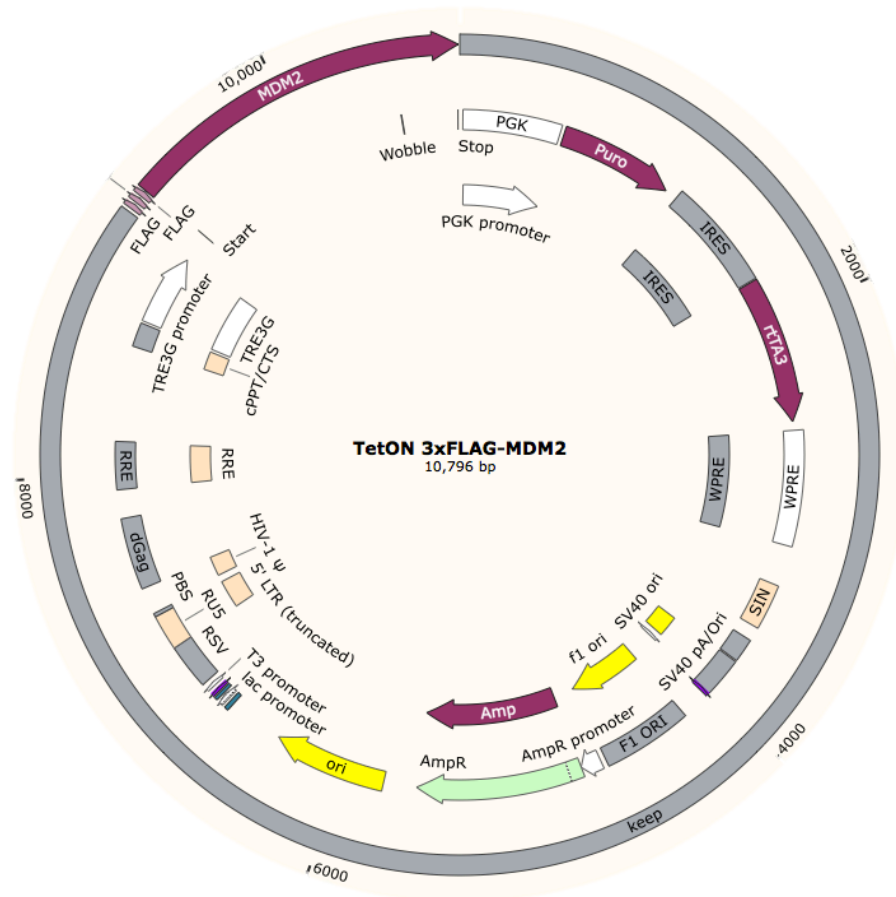


Figure 4.3. Plasmid map of TetON FLAG-MDM2

FLAG-tagged MDM2 was cloned into the LT3 lentiviral vector backbone. Expression of FLAG-MDM2 is driven by the TRE3G promoter in the presence of doxycycline. A selectable marker, puromycin, and the rtTA3 element are constitutively activated by a separate PGK promoter.

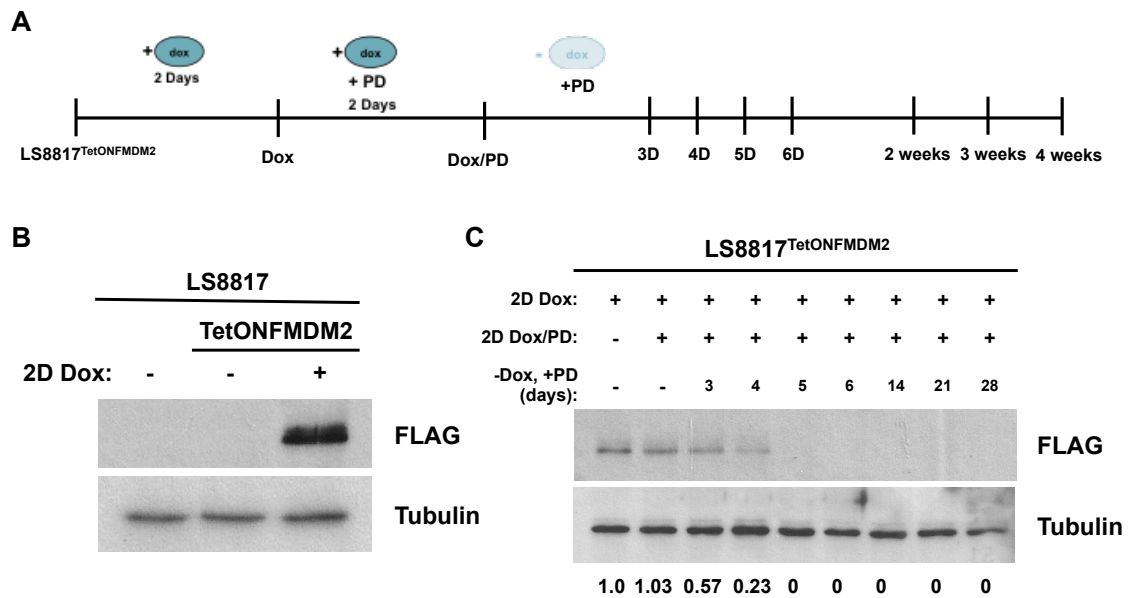


Figure 4.4. Expression of FLAG-MDM2 in LS8817^{TetONFMDM2} cells is controlled by doxycycline

(A) LS8817 cells were transduced with the TetON FLAG-MDM2 construct and selected in puromycin for 7 days (LS8817^{TetONFMDM2}). Cells were initially treated with 10 μ M doxycycline (Dox) for 2 days followed by 10 μ M doxycycline and 0.1 μ M PD0332991 (PD) for a further two days. Cells were then maintained in only 0.1 μ M PD0332991 until protein lysates were harvested at the times indicated. (B, C) FLAG protein levels were detected using immunoblot. Tubulin served as a loading control. Relative quantity was determined by densitometry and is presented below the image.

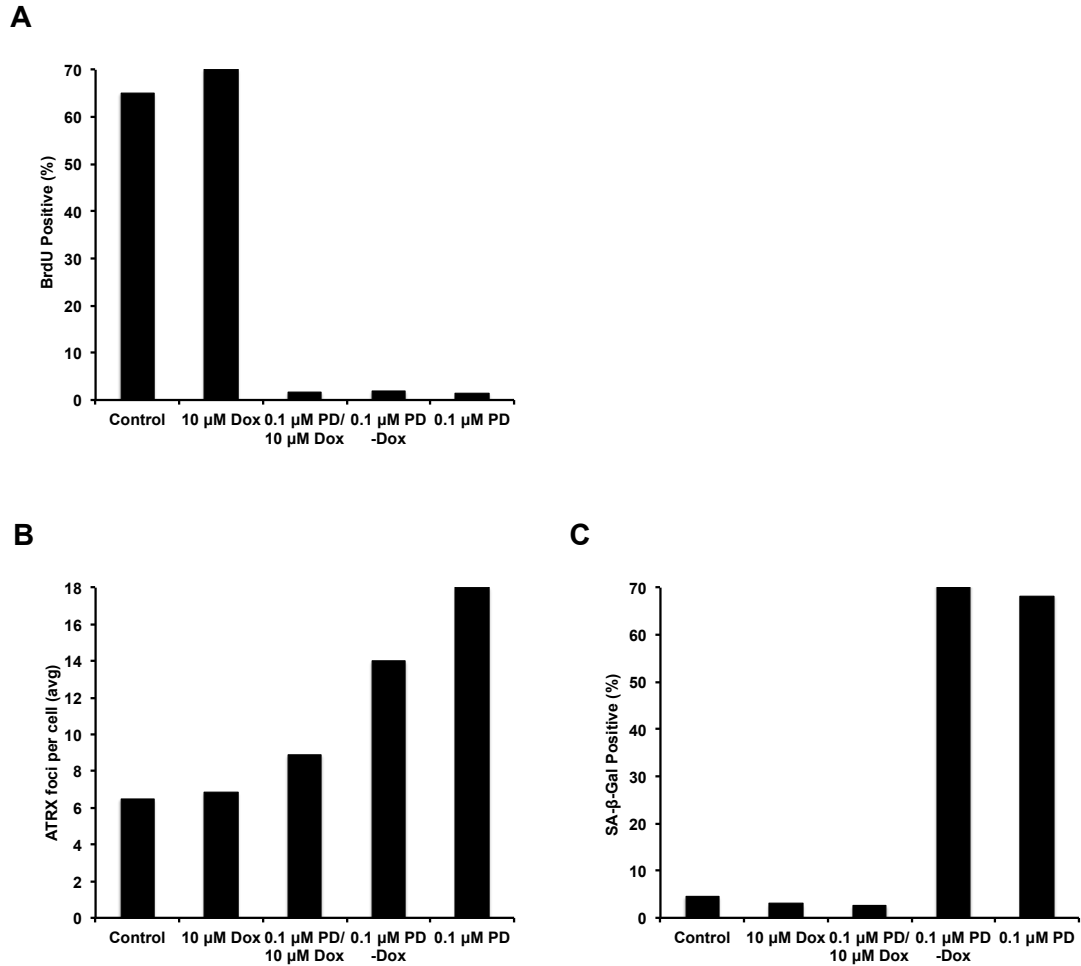


Figure 4.5. LS8817^{TetONFMDM2} cells can be induced to enter a stable quiescent or senescent state by PD0332991

LS8817^{TetONFMDM2} cells were treated with 10 μ M doxycycline (Dox) for 2 days. Cells were then treated with 10 μ M doxycycline and 0.1 μ M PD0332991 (PD) for a further two days. At this time, doxycycline was either removed from the cells and fresh media with only 0.1 μ M PD0332991 was given for a further 6 days (PD -Dox) or doxycycline treatment was continued (PD/Dox). Alternatively, cells that were never treated with doxycycline were treated with 0.1 μ M PD0332991 for 6 days (PD). The number of cells staining for BrdU (A), ATRX foci (B) and SA- β -Gal (C), were quantified.

PD, or continued co-treatment with both drugs for a further 6 days. As a control, I treated cells that had never seen doxycycline with 0.1 μM PD for 8 days. I then assayed markers of growth arrest and senescence. Cells that were treated with both 10 μM dox and 0.1 μM PD (therefore were expressing FMDM2) lost BrdU accumulation but did not acquire SA- β -Gal or ATRX foci. However, removing dox (thus reducing expression of FMDM2) induced similar levels of senescence markers to those obtained when dox naïve cycling cells were treated with 0.1 μM PD.

Similar results were also obtained when LS8817^{TetONFMDM2} cells were treated with abemaciclib, an alternative CDK4 inhibitor (**Figure 4.6, A, B**). Additionally, a responder NSCLC cell line H1975 transduced with the TetON-FMDM2 vector and treated with PD could also be held in quiescence or induced to progress into senescence by toggling the expression of FMDM2 with doxycycline (**Figure 4.6, C, D**). This suggests that senescence after growth arrest is not dependent on cell type or specific to a single CDK4 inhibitor.

LS8817^{TetONFMDM2} system allows for the separation of senescence phenotypes over time

I next wanted to determine the kinetics with which various markers of senescence arise. I treated LS8817^{TetONFMDM2} cells with 10 μM dox + 0.1 μM PD (DoxCDK4i) to induce arrest. After release from dox, I harvested cells daily for a week, followed by weekly for an additional three weeks, and measured ATRX foci, HP1 γ foci, and SA- β -Gal (**Figure 4.7**). Remarkably, not only were the days each phenotype arose extremely reproducible, but also each marker increased from a minimum to a maximum level in a period of 24 hours. The sharp transitions in this system were an improvement over the asynchronous manner in which the senescence phenotypes arose if cycling cells were treated with PD (**Figure 4.8**).

Interestingly, LS8817^{TetONFMDM2} cells were not irreversibly arrested at day 6 of the time course and could return to proliferation upon removal of CDK4 inhibitor, but by day 14 cells were irreversibly arrested and did not proliferate after removal of drug (**Figure 4.9**). Closer investigation revealed growth arrest was still reversible until at least day 12 (**Figure 4.9**).

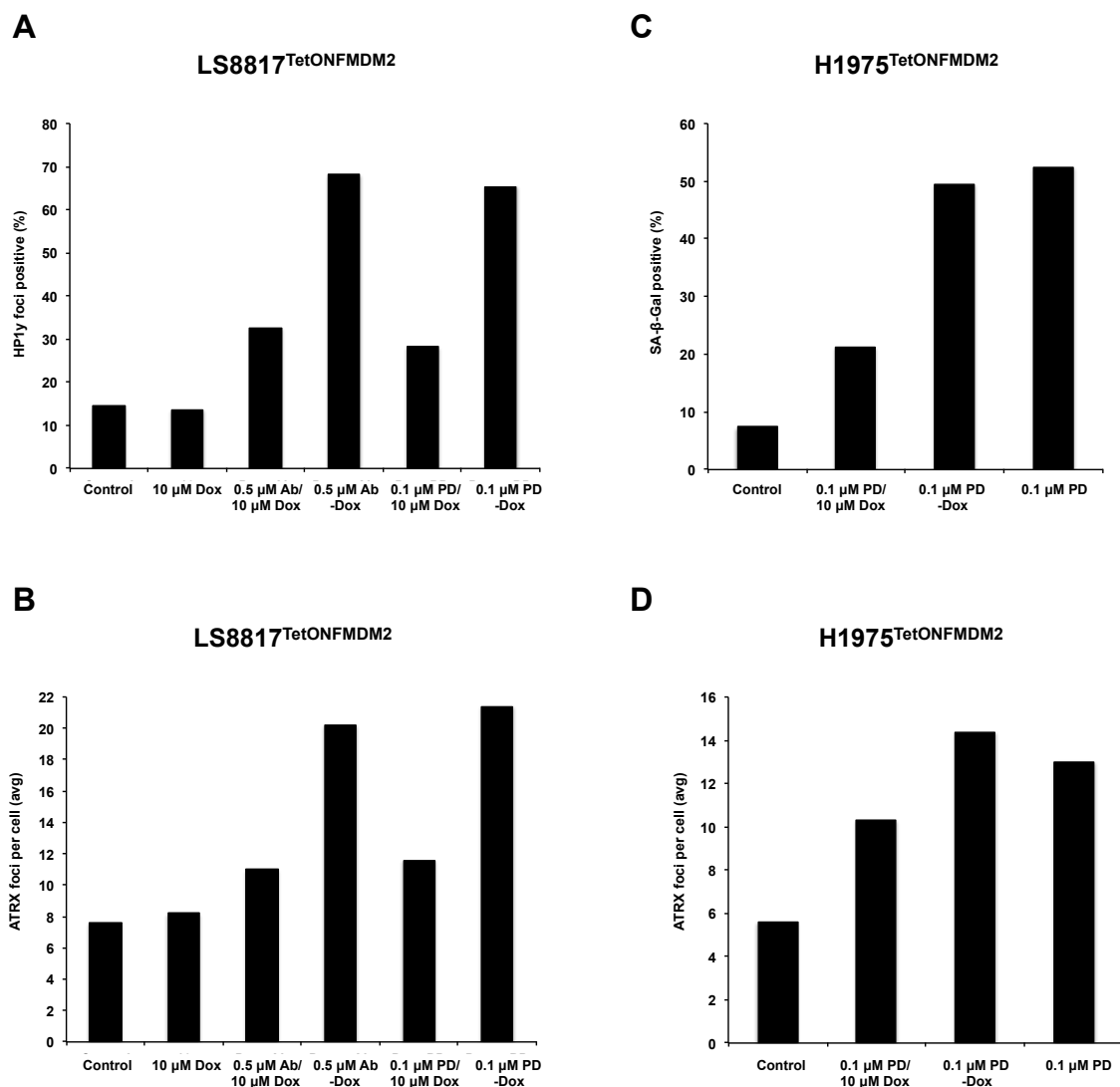


Figure 4.6. The TetONFMDM2 system is not PD0332991 or cell line dependent

(A) Quantification of the number of cells staining for HP1 γ foci and (B) ATRX foci in LS8817^{TetONFMDM2} cells treated as described in Figure 4.3 except they were treated with 0.1 μ M PD0332991 (PD) or 0.5 μ M abemaciclib (Ab) for 14 days. (C) Quantification of the number of cells staining for SA- β -Gal and (D) ATRX foci in H1975^{TetONFMDM2} cells treated as described in Figure 4.3 using 0.1 μ M PD0332991 for 6 days.

LS8817^{TetONFMDM2}

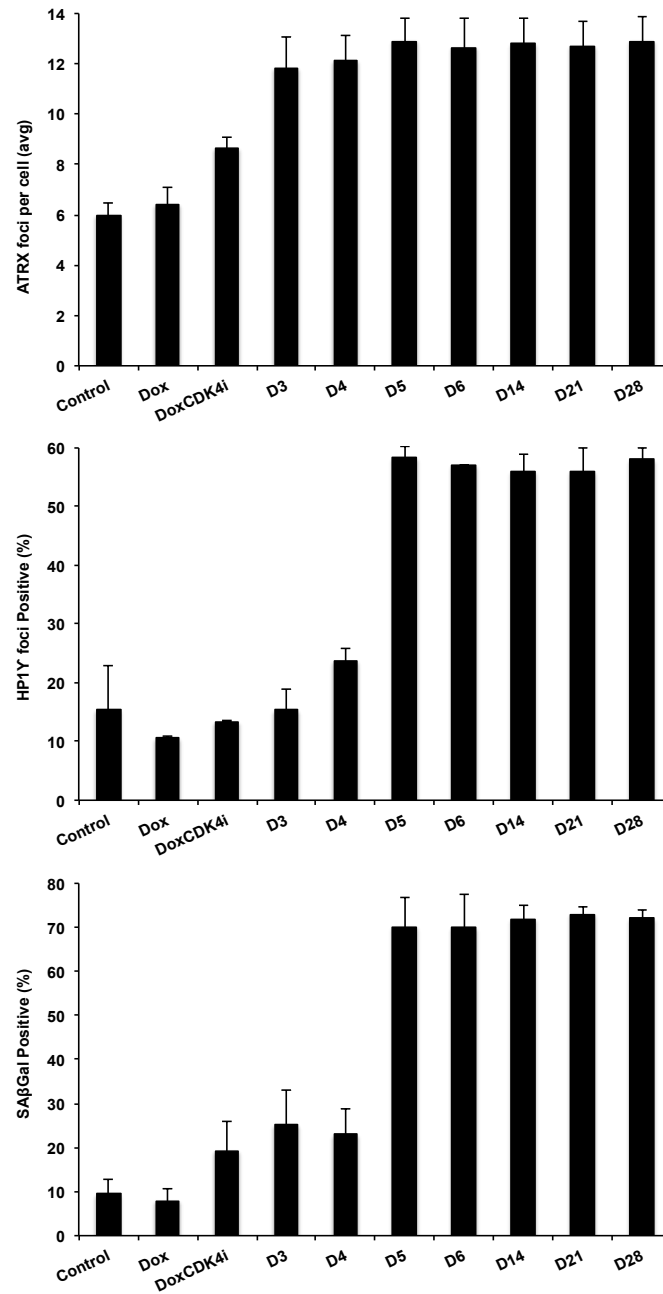


Figure 4.7. LS8817^{TetONFMDM2} cells acquire hallmarks of senescence over time

LS8817^{TetONFMDM2} cells were treated with 10 μ M doxycycline (Dox) for 2 days. Cells were then treated with 10 μ M doxycycline and 0.1 μ M PD0332991 for a further two days (DoxCdk4i). Cells were then maintained in only 0.1 μ M PD0332991 until times indicated. ATRX foci, HP1 γ foci, and SA- β -Gal were quantified, n=6 biological replicates.

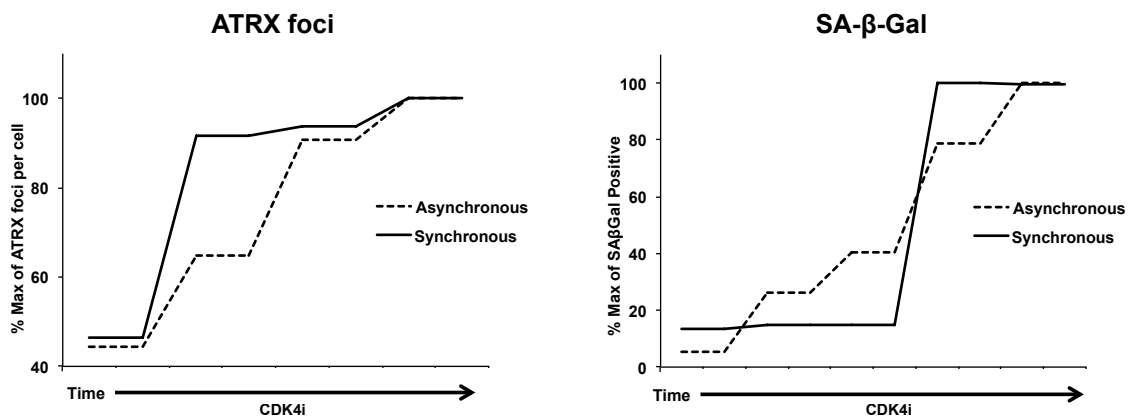


Figure 4.8. $LS8817^{TetONFMDM2}$ system offers sharper resolution of the acquisition of senescence hallmarks

$LS8817^{TetONFMDM2}$ cells were treated with 10 μ M doxycycline for 2 days. Cells were then treated with 10 μ M doxycycline and 0.1 μ M PD0332991 (CDK4i) for a further two days. Cells were then maintained in only 0.1 μ M PD0332991 (synchronous). Alternatively, cycling $LS8817$ cells were treated with 0.1 μ M PD0332991 (asynchronous). The number of cells staining for ATRX foci and SA- β -Gal were quantified and plotted as a function of time.

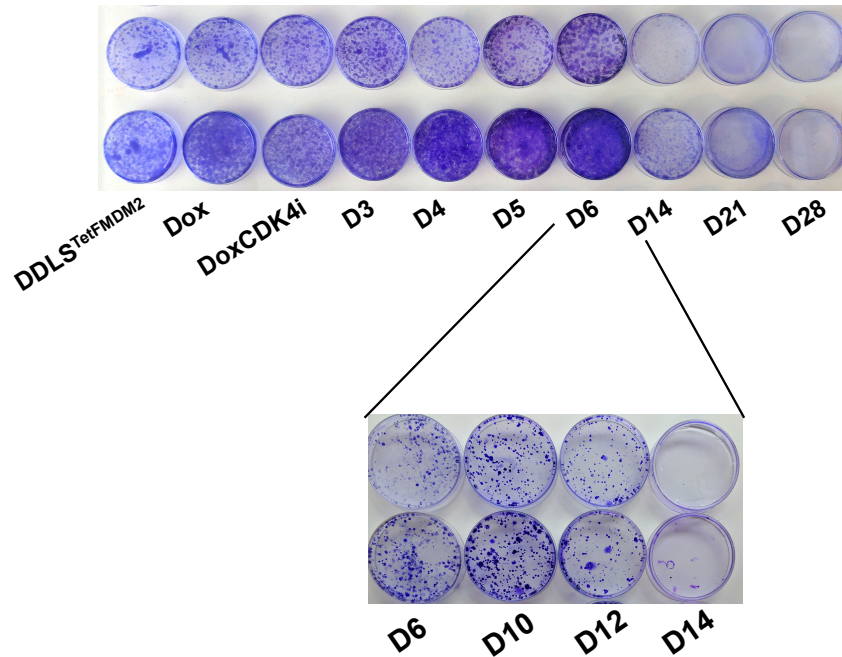


Figure 4.9. LS8817^{Tet}ONFMDM2 cells become irreversibly arrested 14 days after doxycycline removal

LS8817^{Tet}ONFMDM2 cells were treated with 10 μ M doxycycline (Dox) for 2 days. Cells were then treated with 10 μ M doxycycline and 0.1 μ M PD0332991 for a further two days (DoxCDK4i). Cells were then maintained in only 0.1 μ M PD0332991 for the number of days indicated before being plated in drug free media and allowed to grow for 21 days to assess clonogenic growth by the crystal violet assay.

Discussion

SAGA separates cell cycle exit from entry into and deepening of senescence

Quiescence and senescence are often thought of as alternative consequences to cell cycle exit. However, CDK4 inhibitor-induced senescence gave me the opportunity to directly test whether these are independent fates or if cells can progress into senescence after growth arrest. By transducing responder cells with a doxycycline-inducible FMDM2 expression vector, cells could be induced to enter into a quiescent state by the addition of a CDK4 inhibitor and doxycycline. Removal of doxycycline from growth arrested cells, still in the presence of a CDK4 inhibitor, allowed them to progress into senescence and cytological markers of senescence could be profiled at specific points within the time course. I found that there is a linear relationship between senescence and growth arrest such that cells first exit the cell cycle and then progress into senescence.

Senescence itself is not a single endpoint, but rather is the culmination of a dynamic process where numerous phenotypes are acquired over time [75]. Work in the field suggests that further maturation of senescence can occur weeks to months after induction. For example, it has been seen that DNA damage foci become abundant as cells enter into senescence, but diminish as cells remain in culture over long periods of time [175]. A reduced histone content and increased expression of the long interspersed nuclear element retrotransposon L1 have also been observed in senescent fibroblasts weeks after they gained expression of SA- β -Gal [176, 177]. Attempts have been made to separate the triggering events, initiation, entry, and further deepening of senescence. However, to my knowledge there has been no system developed where uniform exit from the cell cycle and synchronous movement into senescence can be monitored. Since cell cycle exit is a pre-requisite to senescence and is a general feature of all senescent cells, it is often difficult to uncouple the roles of inducers such as p16, p21, and Rb in cell cycle exit from their roles in senescence induction. By identifying that CDK4 inhibitors induce senescence after growth arrest, I have been able to develop a system that separates cell cycle exit from senescence.

Furthermore, I found there is temporal separation between the onset of the senescence phenotypes ATRX foci (day 3), SA- β -Gal and HP1 γ foci (day 5), and irreversible growth arrest (day 14) (Figure 4.10).

Potential applications of the LS8817^{TetONFMDM2} system

Based on prior work in the Koff lab, it was not surprising to find ATRX foci occurring early in the path to senescence. ATRX is necessary for the induction of CDK4 inhibitor-induced senescence and, in an asynchronous system, increase in nuclear focal number from days 2 to 7 post treatment. Once senescence is induced, knockdown of ATRX does not affect the irreversibility of the arrest, expression of the SASP, or the accumulation of SA- β -Gal; however, it does cause a decrease in the number of HP1 γ foci, suggesting it remains important for the maintenance of the SAHF [108]. This work left a number of open questions that could be addressed in the future using the LS8817^{TetONFMDM2} system. First, do the chromatin binding sites of ATRX change during the induction of senescence? Unlike in the asynchronous system, ATRX foci are approximately equal in number across the population from day 3 through day 28. However, it is possible that the genomic localization of these foci evolves over time, and identifying those changes through ChIP-seq could give unique insights into further functions of ATRX. Next, is there a point where MDM2 loss is no longer necessary for senescence maintenance similar to ATRX? The advantage of a tetracycline inducible system is MDM2 expression could be restored at any point in the time course. Likely, once senescence is deeply enough induced, the re-expression of MDM2 will not be able to reverse senescence, especially once irreversible arrest is achieved, but it will be interesting to determine if there is such a point where cells can escape and/or which of the phenotypes MDM2 expression can specifically affect.

Finally, the finding that the absence of ATRX will block the induction of all downstream markers, but not reverse permanent growth arrest once it is induced, suggests that while the senescence markers may be temporally and functionally linked during senescence induction, there

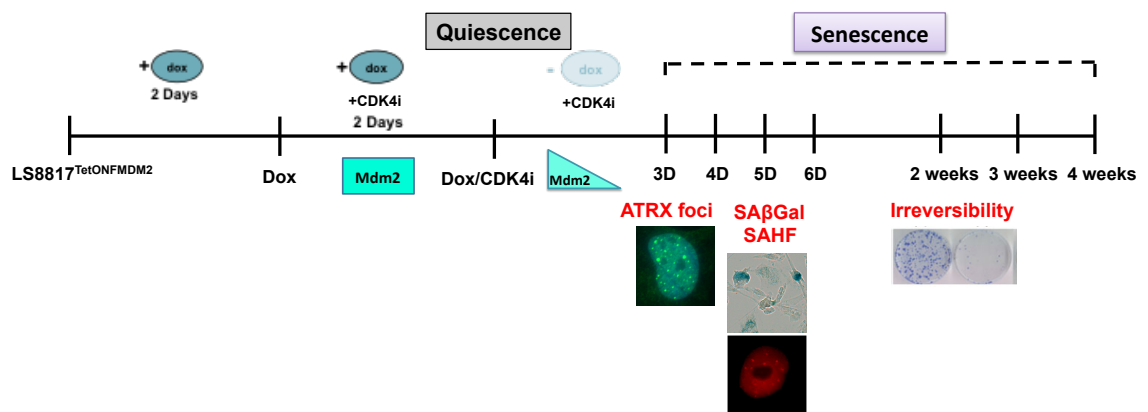


Figure 4.10. Illustration of LS8817^{TetONFMDM2} system and phenotype acquisition over time

are likely multiple feedback pathways to maintain the senescent state later. It stands to reason that the pathway to senescence will require many successful steps, and the absence of one will prevent induction, but once reached redundancies ensure the cell will not escape the state.

Importantly, a system where unique states can be separated and defined provides an opportunity to unravel what gene programs drive each state and what the necessity of one state is for the others. Furthermore, a synchronous system allows monitoring of senescence over time rather than just seeing a snapshot, and changes can be identified that happen early and resolve. Ultimately, by understanding the senescence after growth arrest pathway, we have the opportunity to answer questions about what programs are important for the induction versus the maintenance of the senescent state, and we will hopefully be able to thoroughly elucidate the nuances of senescence biology.

CHAPTER 5: PROFILING THE TEMPORAL DYNAMICS OF GENE TRANSCRIPTION DURING CDK4 INHIBITOR-INDUCED SENESCENCE

Introduction

The tripartite phenotype defining senescence

Senescence is a stable form of cell cycle exit induced by various types of stress. *In vitro*, senescent cells can be identified using a collection of markers including, but not limited to, senescence-associated beta-galactosidase (SA- β -Gal), senescence-associated heterochromatic foci (SAHF), DNA damage foci, increased reactive oxygen species, altered nuclear structures, and increased p16 and p53 [178, 179]. However, none of these markers are specific to senescent cells and not all senescent cells exhibit all markers. Therefore, it is necessary to use multiple markers to define a senescent state [84]. Furthermore, the vast number of triggers that can induce senescence in different cell types introduces a high level of context dependence to the characterization of senescence.

Regardless, there is now consensus in the field that senescence can be defined by a core triad of three functional phenotypes. First, senescent cells are impervious to the re-addition of mitogenic signals and will remain stably growth arrested [83]. Next, senescent cells secrete a variety of cytokines, chemokines, and proteinases known as the senescence-associated secretory phenotype or SASP [180-182]. Finally, senescent cells have increased resistance to apoptosis [86, 183]. However, it has remained unclear how these phenotypes are connected and what the dynamics of these phenotypes are in relation to one another.

Challenges of profiling senescence

Many studies have been performed to understand what changes are necessary for senescence and to identify senescence signatures. However, in these non-synchronous systems, comparisons have been limited to cycling cells vs. SA- β -Gal positive cells vs. 'deep' senescent

cells (weeks to months after induction). Therefore, knowledge gaps exist in the chronology of senescence establishment, the functional relevance of the traditional markers that occur ‘early’ in senescence, and the mechanism by which cells become irreversibly arrested.

One way that has been proposed to close these gaps is single cell sequencing. With the advent of new technology, greater resolution of cellular transcription can be obtained and questions can be asked on a cell-by-cell basis. While single cell sequencing can remove population noise that can come from an asynchronous system, such analyses will still be limited by the lack of a known gene program that defines different cell states on the pathway to senescence. Since the majority of assays used to identify senescent cells are cytological and cannot be duplexed with RNA extraction, the profiles of each cell cannot be assigned based on the individual senescence characteristics such as status of ATRX, SA- β -Gal, SAHF, and irreversible growth arrest. One phenotype that can be compared to these expression profiles is the SASP since there is a transcriptional component to SASP regulation. However, single cell studies have shown marked variability in the expression of SASP genes between cells within an asynchronously-derived senescence population, suggesting that there may be more to understand about the expression of the SASP in different states of senescence [184].

An alternative approach is to use a synchronous system where progression through senescence can be monitored in the population by both cytologic characterization and –omics profiling. Previously in senescence studies, this type of approach has been hampered by the lack of systems where cell cycle arrest can be separated from senescence induction. Instead, cells would begin to exit the cell cycle over a period of 24-48 hours as they reached the appropriate cell cycle phase, leading to gradual and overlapping acquisition of the senescence hallmarks. After discovering that CDK4 inhibitor-induced senescence could follow growth arrest and separate out the acquisition of senescence hallmarks (see Chapter 4), I set out to define genes and pathways along the SAGA transition.

Results

Profiling transcriptional changes as cells progress into senescence

To evaluate what transcriptional changes were occurring as cells progress into senescence, I carried out genome wide RNA sequencing (RNA-seq). While there was variance throughout the dataset, principal component analysis revealed that serum starved and day 28 (D28) senescent cells were the most dissimilar from the rest of the data points (**Figure 5.1**). I then assessed differential gene expression by using R studio and DESeq2 [185]. Using a fold change cutoff of +/- 1.5 and a false discovery rate of 0.5%, I found that 1,780 genes were significantly changed at one or more time points across the time course compared to untreated cells (**Figure 5.2**). There were only 21 genes significantly changed between cycling untreated and cycling doxycycline treated cells, suggesting that the addition of this drug to cells did not cause substantial gene program changes. Hierarchical cluster analysis demonstrated that there was a temporal relationship between the time points we looked at (**Figure 5.2**). As cells were entering into senescence (D3/D4) they were most similar to quiescent cells (DoxCDK4i). Then, as cells were in an early senescent state (D5/D6) and progressing deeper into senescence (D14/D21) there was a branch with two distinct clusters. Finally, when cells were in a late senescent state (D28) they were the most dissimilar from any of these earlier programs. Interestingly, similar to the principle component plot, hierarchical cluster analysis showed that serum starved cells were much more similar to D28 senescent cells than quiescent DoxCDK4i cells. This calls into question whether a serum starvation condition should truly be used as a quiescent control when trying to identify genes that are changed in senescence.

I next probed transcriptional changes as cells move into senescence. In an effort to exclude genes that are affected as cells exit the cell cycle and are not specific to senescence, I compared RNA expression in the time course to quiescent cells (DoxCDK4i). 596 genes were up-regulated at one or more time points along the progression into senescence, and 223 genes were down-regulated. There were multiple gene expression patterns observed over the time course,

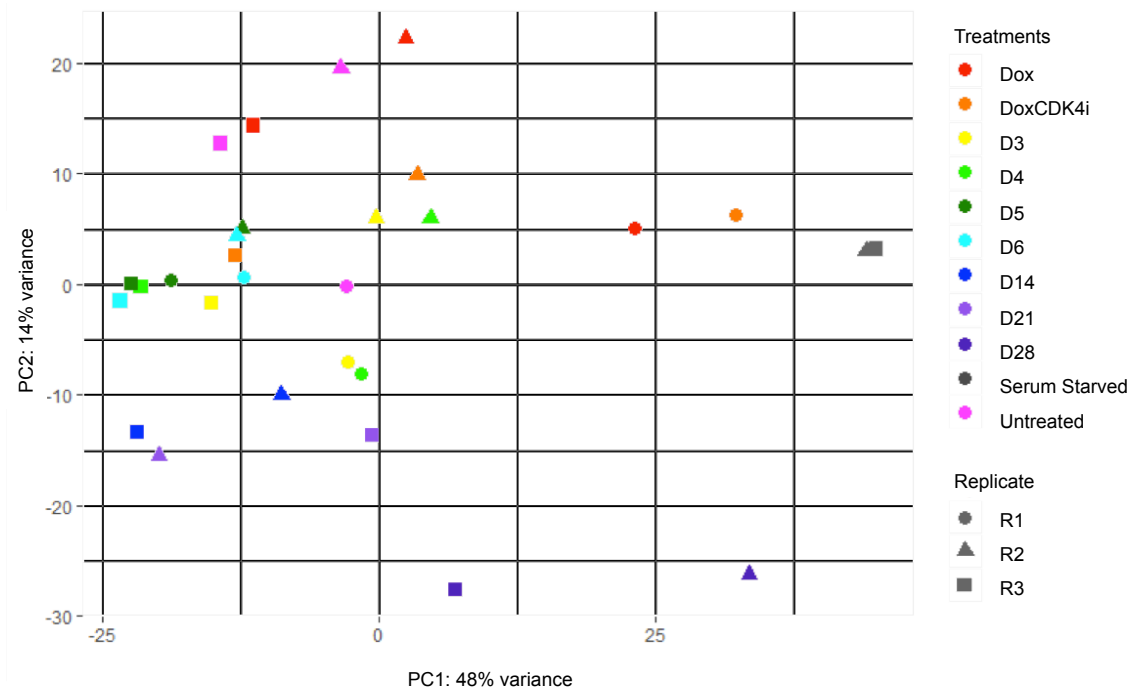


Figure 5.1. Principle component analysis of LS8817^{Tet}ONFMDM2 cells across the time course
 Principle component analysis was performed with Bioconductor DESeq2 on RNA-seq data generated from LS8817^{Tet}ONFMDM2 cells treated as illustrated in 4.10. Treatments are indicated by color and replicates are indicated by shape. 3 biological replicates were analyzed per treatment.

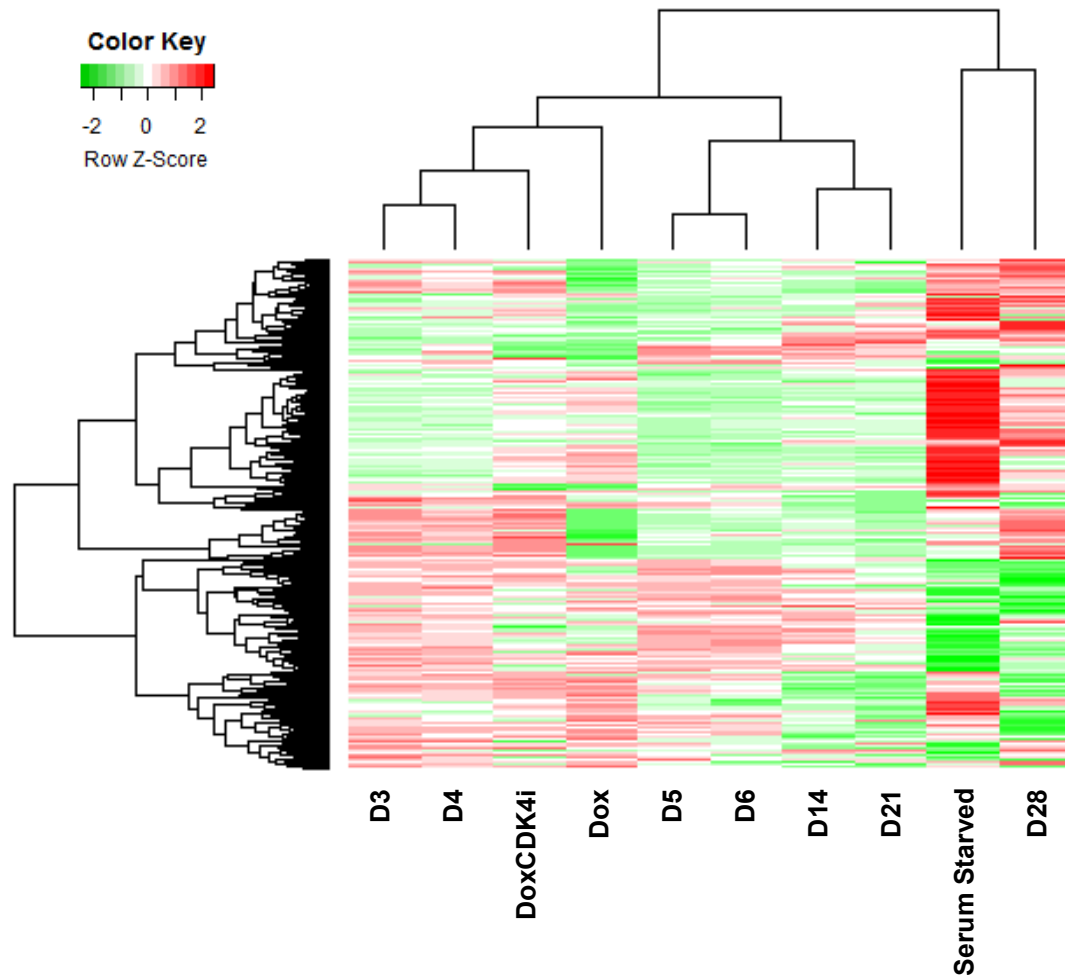


Figure 5.2. Hierarchical cluster analysis of gene expression changes across the time course
 DESeq2 analysis was performed comparing cycling LS8817^{TetON^{FM}DM2} cells to each of the time points indicated and a fold change cutoff of +/- 1.5 and $p_{adj} < 0.005$ was used to assess significance. 1,780 genes were changed at one or more points across the time course. The expression levels of those genes were used to generate a heatmap.

i.e. genes could increase/decrease and hold steady, increase/decrease continuously, or they could increase/decrease and then return to baseline (**Figure 5.3**). However, trends emerged when viewing the data globally. There was a large shift observed at day 5, which correlates with the onset of SA- β -Gal accumulation and HP1 γ foci (early senescence). A further number of expression changes were acquired at day 14, which correlates with the onset of irreversible growth arrest. Finally, at day 28 (late senescence) those changes either increased in intensity or reverted back to an earlier state. Given these broad patterns, I considered if these changes could be classified by using gene set enrichment analysis and the molecular signature database [111, 112] (**Figure 5.4**).

Gene changes associated with entry into and early senescence

I began by evaluating changes in gene expression that occur as cells down-regulate MDM2 and up-regulate ATRX foci. Only 13 genes changed significantly between DoxCDK4i and D3/4 as cells begin to enter into senescence. Interestingly, all of the significant genes identified were down-regulated at these time points, and many were transcription factors or transcriptional regulators. These gene changes may underlie broader alterations in the transcriptional landscape that occur as cells move through senescence.

I next evaluated changes that occur coincident with the onset of SA- β -Gal and HP1 γ foci, the state which we have termed early senescence. At day 5, genes involved in Gene Ontology (GO) processes related to cell cycle progression were activated (**Figure 5.4, A**). These genes are primarily associated with the G₂-M phase including: CDCA5, AURKB, SKA1, and CDK1. By day 28, these genes were no longer significant (**Figure 5.4, E**). While it is somewhat paradoxical that G₂-M cell cycle genes are enhanced while cells are undergoing a G₀-G₁ arrest, other studies profiling senescence have seen similar early upregulation [186, 187]. In my study, the finding of enhanced cell cycle programs may be in part due to the analysis pipeline, as these genes do

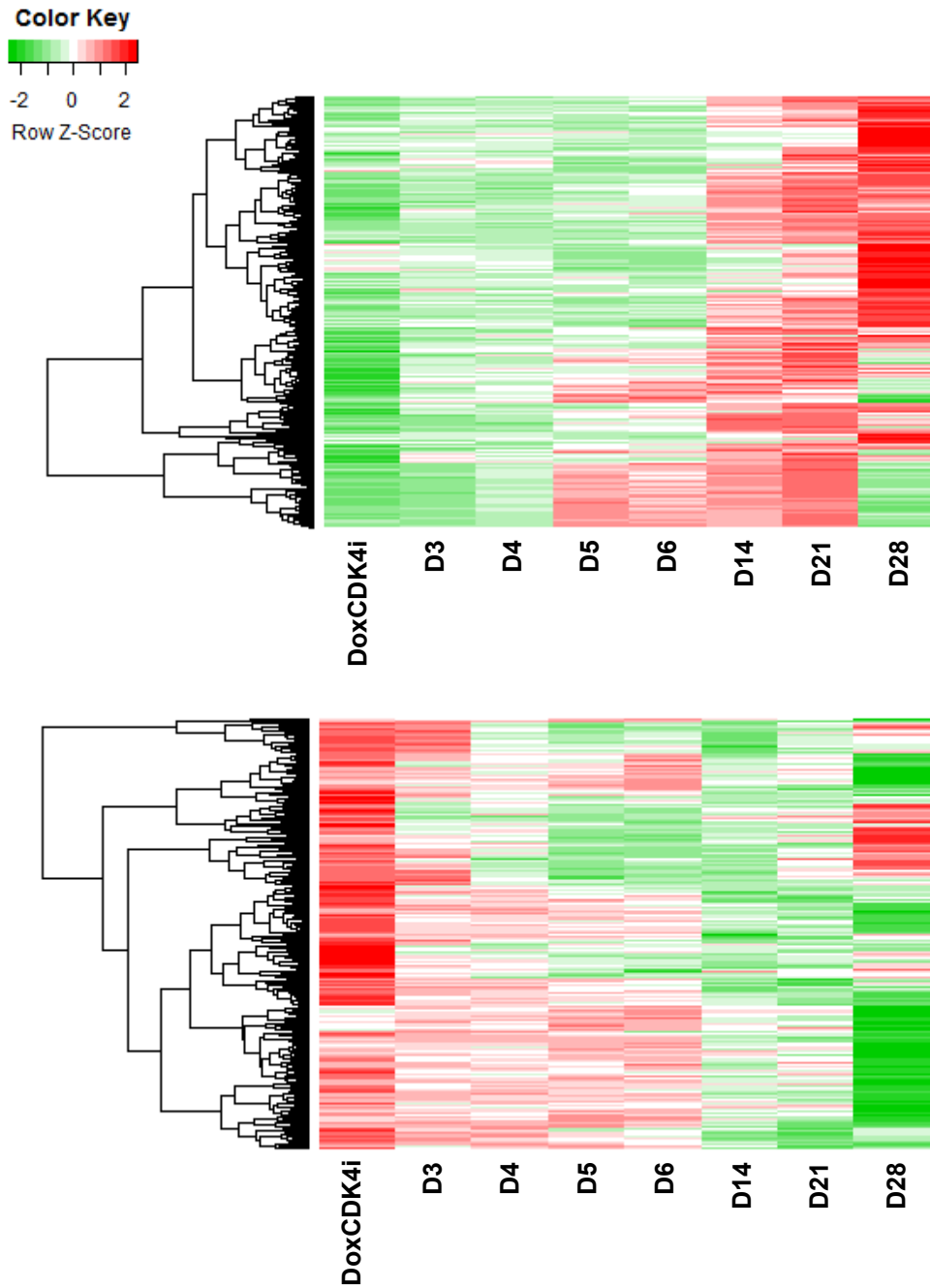


Figure 5.3. Heatmap of gene expression changes during the progression of senescence after growth arrest

DESeq2 analysis was performed comparing growth arrested LS8817^{TetONFMDM2} cells (DoxCDK4i) to each of the time points indicated, and a fold change cutoff of +/- 1.5 and $p_{adj} < 0.005$ was used to assess significance. 596 genes were increased (*upper*) and 223 genes were decreased (*lower*) at one or more points across the time course.

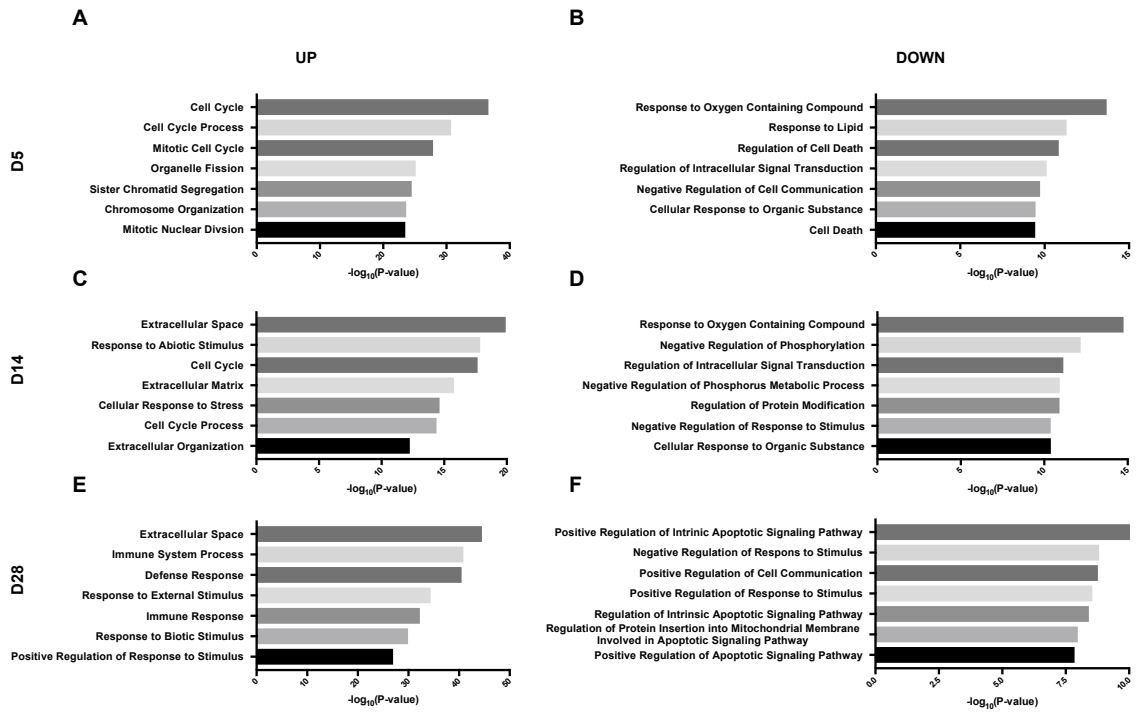


Figure 5.4. Gene ontology terms identified by gene set enrichment analysis across the time course

Genes identified by DESeq2 with a fold change cutoff of +/- 1.5 and $p_{adj} < 0.005$ at days 5, 14, or 28 of the LS8817^{Tet}ONFMDM2 time course were compared against the C5 Gene Ontology (GO) gene sets. The top seven GO terms are shown along with their false discovery rate.

remain repressed compared to cycling cells at all times across the time course despite being significantly increased compared to quiescent cells.

Finally, I looked at processes that are repressed at day 5. Interestingly, while a variety of general signaling pathways emerged, GO terms related to cell death were also enriched (**Figure 5.4, B**). Unlike the cell cycle genes, at day 28 genes involved in apoptosis were still strongly repressed, suggesting that an anti-apoptotic phenotype arise early in the path to senescence and remain important throughout (**Figure 5.4, F**).

A senescence-associated secretory program arises coincident with irreversible growth arrest

One unique facet of my system is the ability to separate irreversible growth arrest from the occurrence of SA- β -Gal and HP1 γ foci. Thus, I wanted to ask what gene changes occur as cells undergo irreversible growth arrest and enter into a deeper senescent state at day 14. At this time point, GO terms related to extracellular space, extracellular matrix, and response to abiotic stimulus were highly enriched (**Figure 5.4, C**). Similar terms were also found enriched at day 28 (**Figure 5.4, E**). This type of profile is often indicative of SASP activation [188]. The SASP can have a multitude of functions for the cell including entry into senescence, maintenance of the senescence state, and immune cell recruitment. Unique factors can contribute to each of these roles. Additionally, while all senescent cells express a SASP, the factors that comprise the secretome is highly dependent on the inducer of senescence and context of the cell. Therefore, I explored if the GO terms identified were indicative of the expression of known SASP factors and determined what happens to the expression of the SASP throughout the time course.

In order to do this, I searched RNA-seq, microarray, and secretome studies published in the literature and compiled a list of 151 genes implicated in the SASP [181, 188-195] (**Table 5.1**). Of the 829 genes that were identified here as significantly changed throughout the time course of senescence, 37 have been previously linked to the SASP (**Figure 5.5, A**). I next plotted the expression of these specific genes over the entire time course (**Figure 5.5, B**). Hierarchical cluster

151 Genes previously implicated in the SASP					
ADIPOQ	CCL8	FGF2	IL12A	IL6ST	PLAUR
AGRP	CD55	FGF7	IL12B	IL7	PTGES
ANG	CD9	FGF9	IL13	IL7R	SERPINE1
ANGPT2	CNTF	FLT3LG	IL13RA2	ITGA2	TGFB1
ANGPTL4	CPE	GABRA2	IL15	ITPKA	TGFB3
AREG	CSF1	GDNF	IL16	KITLG	THPO
Axl	CSF2	GEM	IL17D	LEP	TIMP1
AXL	CSF3	GMFG	IL17RB	LTA	TIMP2
BDNF	CX3CL1	HGF	IL18BP	MIF	TIMP3
BMP4	CXCL1	ICAM1	IL1A	MMP1	TIMP4
BMP6	CXCL10	ICAM3	IL1b	MMP11	TNF
BTC	CXCL11	IFNG	IL1B	MMP2	TNFRSF10C
CCL1	CXCL13	IGF1	IL1R1	MMP3	TNFRSF10D
CCL11	CXCL16	IGF1R	IL1RL1	MST1	TNFRSF11B
CCL13	CXCL2	IGF2	IL1RN	NFKB1	TNFRSF18
CCL17	CXCL5	IGF2R	IL2	NFKBIE	TNFRSF1A
CCL19	CXCL6	IGFBP1	IL20RB	NR4A2	TNFRSF1B
CCL2	CXCL8	IGFBP2	IL27RA	NTF3	TNFSF14
CCL20	CXCL9	IGFBP3	IL2RA	OSM	TNFSF18
CCL22	CXCR2	IGFBP4	IL3	PCNX1	TUBGCP2
CCL24	EGF	IGFBP5	IL4	PDGFA	TYRO3
CCL25	EGFR	IGFBP6	IL4R	PDGFB	VEGFA
CCL26	FAM131A	IGFBP7	IL5	PIGF	VEGF
CCL28	Fas	IL10	IL6	PLAT	WNT2
CCL7	FAS	IL11	IL6R	PLAU	XCL1

Table 5.1. Genes implicated previously in the SASP

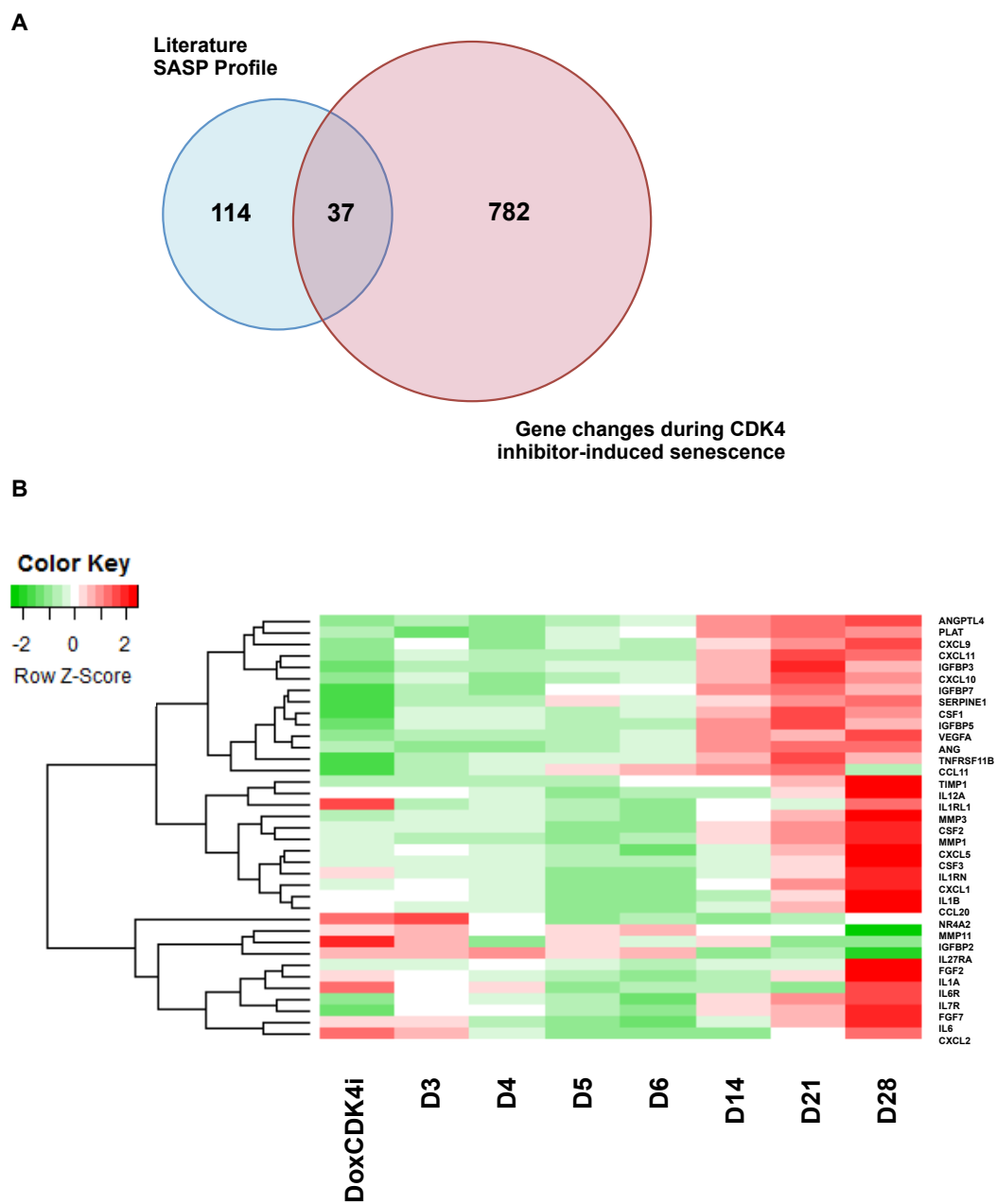


Figure 5.5. Hierarchical cluster analysis of SASP genes across the time course
 (A) The 819 total genes identified in figure 5.3 were compared to a literature SASP profile, and an overlap of 37 genes was identified. (B) The expression of only the 37 genes was isolated from the DESeq2 data and used to generate a more specific heat map with cluster analysis.

analysis revealed three distinct gene clusters, one of which arose at day 14 coincident with the onset of irreversible growth arrest, hereafter Cluster 1.

Two major transcriptional pathways through which SASP genes are activated are GATA4-NF κ B and C/EBP β . Thus, I asked if these clusters could be classified not only temporally, but also based on gene regulation by specific transcription factors. I used TRANSFAC to find genes with common consensus binding sequences for these transcription factors within 4kb of their transcription start site, as well as Gene Set Enrichment Analysis to identify transcription factor targets that were enriched in these 37 genes in an unbiased manner. There were no obvious correlations between transcription factor binding sites present in the first hierarchical cluster and other clusters (**Figure 5.6**). Interestingly, BACH1 binding sites were only found in the second hierarchical cluster and ETS2 sites were found in the second and third. Both transcription factors have been implicated in oncogene-induced senescence and may be important for the activation of later SASP genes [196, 197].

Given that the expression of the SASP and irreversible growth arrest are both part of the triad of senescence, I focused on the relationship between the SASP genes that arose at day 14 and irreversible growth arrest. To expand my studies to other mechanisms of senescence, I analyzed the genes in Cluster 1 in two previously published independent RNA-seq data sets from our lab: asynchronously growing LS8817 cells treated with 1 μ M PD0332991 for 7 days and LS8817 cells treated with 100 nM doxorubicin for 7 days [108]. In addition, I performed RT-qPCR using RNA from another responder liposarcoma cell line (LS141) treated with 1 μ M PD0332991 for 7 days, and from the human fibroblast cell line WI38 treated with doxorubicin, irradiated, or grown to replicative senescence at passage 21. Three genes, IGFBP3, ANGPTL4, and IGFBP7, were consistently upregulated in all seven data sets and one gene, PLAT, was upregulated in all conditions except for replicative senescence (**Figure 5.7**).

		NFKB	GATA	CEBPB	ISRE	TGGAAA NFAT	TGGNNNN NNKCCAR UNKNOWN	TGANTCA AP1	CAGGTG E12	BACH1	RYTTCCTG ETS2	
Cluster 1	CXCL9	■										
	CXCL11	■			■							
	CXCL10	■				■						
	IGFBP3				■							
	IGFBP7				■							
	TNFRSF11B				■							
	IGFBP5		■		■		■		■			
	VEGFA				■			■				
	ANGPTL4				■			■				
	PLAT						■					
	ANG											
	CSF1											
	SERPINE1											
	Cluster 2	IL12A	■									
CSF3			■					■		■		
CXCL5			■					■				
CSF2			■								■	
IL1RN		■			■			■		■		
MMP3					■			■		■		
TIMP1											■	
MMP1								■		■		
IL1RL1			■									
IL1B				■								
CCL11												
CXCL1												
Cluster 3		IL27RA	■									
		IL1A	■									
	CXCL2	■										
	MMP11							■				
	IL6R											
	CCL20										■	
	FGF7				■	■						
	NR4A2				■	■			■			
	IL7R				■	■		■			■	
	IL6				■	■	■	■				
	FGF2											
	IGFBP2											

Figure 5.6. TRANSFAC analysis of the 37 SASP genes

The publicly available TRANSFAC database was used to assess NFκB, GATA, and C/EBPβ transcription factor binding sites in the promoters of the 37 SASP genes identified in this study. Clusters 1, 2, and 3 were identified in the previous figure. Additional transcription factors were identified by gene set enrichment analysis for each cluster and binding sites were cross-referenced to the other clusters. Grey shading indicates the presence of a transcription factor binding site.

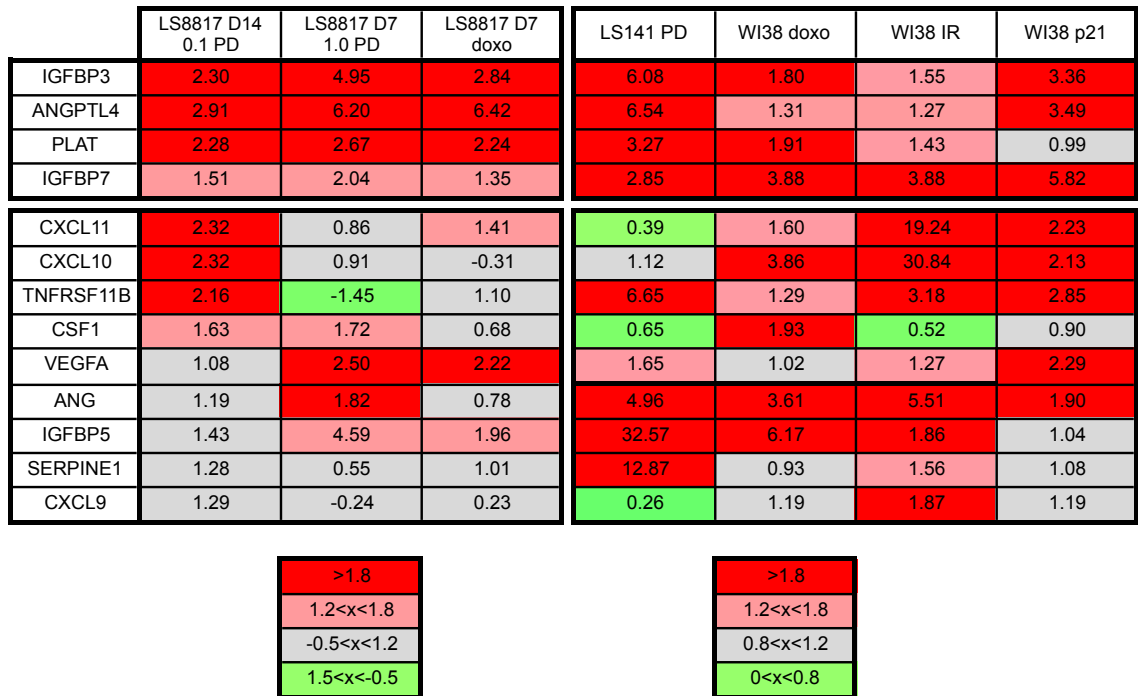


Figure 5.7. Expression levels of 13 SASP genes from Cluster 1 in additional senescence data sets

Expression of the 13 genes from Cluster 1 in Figure 5.6, which demonstrated an increase in expression at day 14 compared to early time points, were analyzed in additional senescence-induction systems. *Left*, RNA-seq was used to analyze gene expression changes in LS8817^{TetONFMDM2} at day 14 from the time course. These genes were also assessed in previously published senescence data sets (Kovatcheva et al., 2017). *Right*, RT-qPCR in LS141 and WI38 cells. WI38 are a human primary fibroblast cell line with 3 mechanisms to senescence: doxorubicin (therapy-induced), gamma-irradiation (DNA damage-induced), or after 21 passages (replication-induced). Doxo, doxorubicin; IR, γ -irradiation; PD, PD0332991.

Knockdown of ANGPTL4 blocks CDK4 inhibitor induced irreversible cell cycle exit

I next designed an experiment to investigate the effect of knocking down these four genes on the induction of senescence (**Figure 5.8, A**). In short, cells were growth arrested by treating with doxycycline and 0.1 μ M PD0332991, transduced with lentiviral vectors encoding short hairpin RNA, and selected in puromycin. Two independent short hairpin RNA lentiviral vectors were employed for each gene. After selection, doxycycline was removed from the cells and they were allowed to progress into senescence. At day 21, cells were harvested for RNA and senescence assays.

Knockdown of each gene was generally effective, with 3/4 of the genes having both hairpins that achieved greater than 70% reduction (**Figure 5.8, B**). None of the knockdowns had a significant affect on the formation of ATRX foci (**Figure 5.8, C**). The hairpin with more efficient knockdown of PLAT had a slight reduction in the accumulation of SA- β -Gal (**Figure 5.8, D**). Interestingly, knockdown of ANGPTL4 by both hairpins and IGFBP3 by one hairpin allowed the cells to reenter the cell cycle following removal of CDK4 inhibition as measured by BrdU incorporation over the next 48 hours (**Figure 5.8, E**). Of these, knockdown of ANGPTL4 was able to sustain cycling over the next 3 weeks and achieved colony formation after being plated at a low density in drug free media (**Figure 5.8, F**). Cumulatively, this suggests that knockdown of ANGPTL4 can block CDK4 inhibitor-induced irreversible growth arrest without affecting the induction of other earlier senescence hallmarks.

Knockdown of ANGPTL4 suggests the presence of multiple, parallel SASP pathways

SASP factors are generally thought to function in four main areas: (1) they can reinforce the development of senescence in an autocrine manner, (2) they can drive senescence within surrounding cells through a paracrine mechanism, (3) they can have a pro-oncogenic effect on surrounding cells, or (4) they can drive infiltration of immune cells. One of the ways in which they cooperate to achieve such diverse tasks is through regulating the expression of other SASP

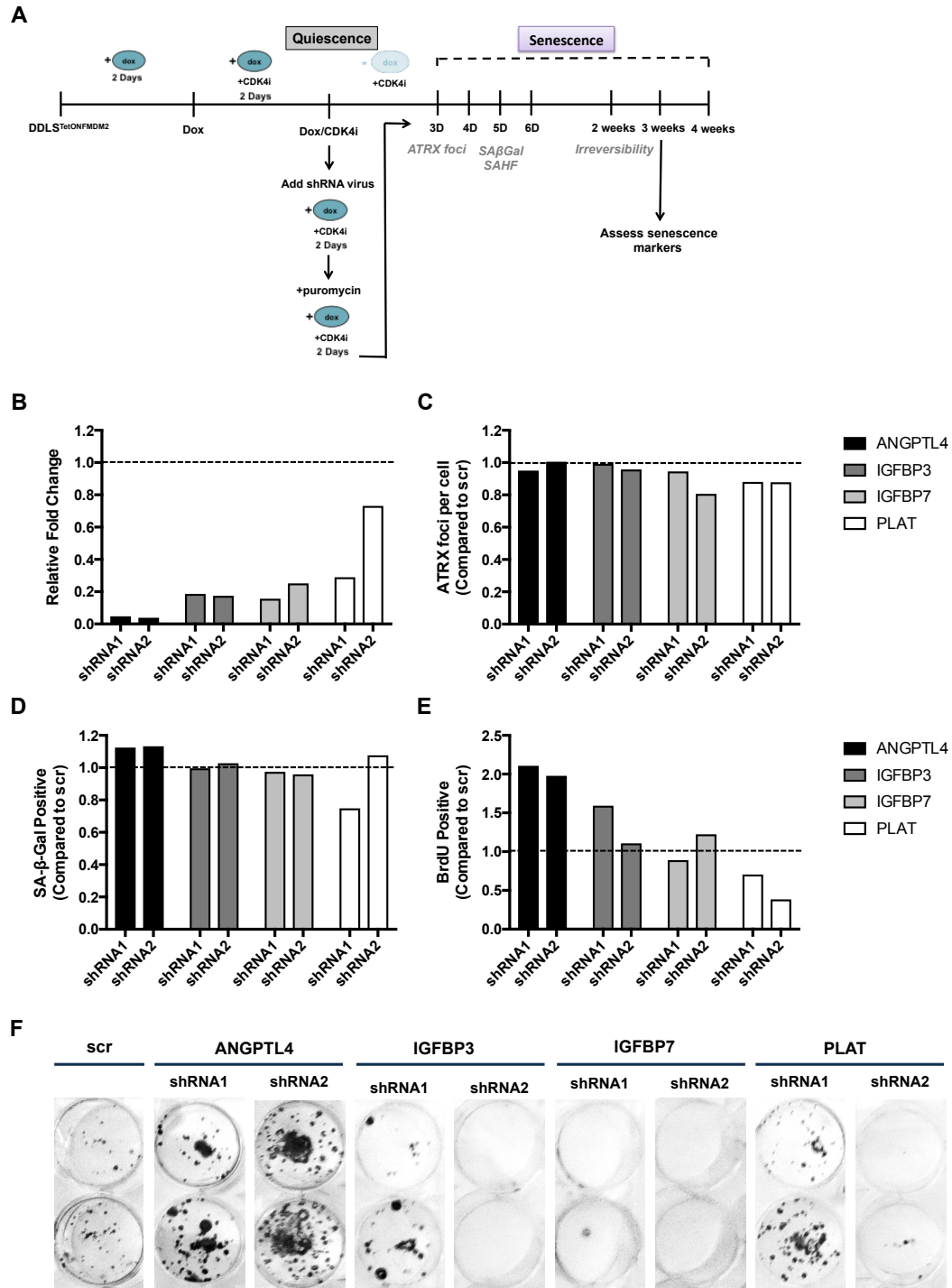


Figure 5.8 Evaluating senescence hallmarks after knockdown of conserved SASP

(A) Illustration of LS8817^{TetONFMDM2} time course with shRNA knockdown by lentiviral vectors. Phenotypes were assessed at 21 days (3 weeks) post-doxycycline removal. (B) RT-qPCR for the genes as indicated following shRNA knockdown. Two shRNA sequences were tested for each gene. (C) Quantification of ATRX foci and (D) percent of cells positive for SA-β-Gal. (E) Quantification of BrdU incorporation following a 48 hour pulse in drug-free media. (F) Clonogenicity assay following 21 days in drug free media.

factors. For example, it has been shown that depletion of IL6 prevents the induction of oncogene induced senescence and elaboration of a further inflammatory network [181]. Even further upstream, IL1 α can control the expression of IL6 [198]. Therefore I asked if knockdown of ANGPTL4 would prevent the elaboration of other cytokines. To accomplish this I selected a number of genes from each of the three clusters and used RT-qPCR to assess their expression in cells transduced with a scrambled shRNA control vector at day 21 post doxycycline removal and compared these to quiescent DoxCDK4i cells. I also compared this expression to cells infected with either shRNA against ANGPTL4. I only assessed the affect of knockdown on genes that were at minimum 5-fold increased in the control scramble cells at day 21 compared to quiescence. I found that approximately 60% of the genes tested were attenuated in the knockdown conditions, suggesting that ANGPTL4 is necessary for their expression (**Figure 4.9, Upper**). On the other hand, approximately 40% of the genes tested were still able to increase after doxycycline was removed to a similar level as the control (**Figure 4.9, Lower**). The distribution of ANGPTL4-connected genes was not correlated with what cluster they existed in or the presence of transcription factor binding sites at their promoters. This suggests that there are at least two parallel pathways that control the expression of SASP genes: one that requires expression of ANGPTL4 and one that does not.

Discussion

Transcriptional changes: an evolution over time

The description of senescence as a tripartite phenotype, in which all senescent cells are irreversibly growth arrested, secrete a SASP program, and are resistant to apoptosis, allows for the senescent state to be defined functionally. However, knowledge of the molecular mechanisms that underlie these phenotypes, and the relationship between these and other markers of senescence, is still lacking. After developing a doxycycline-inducible system where I could

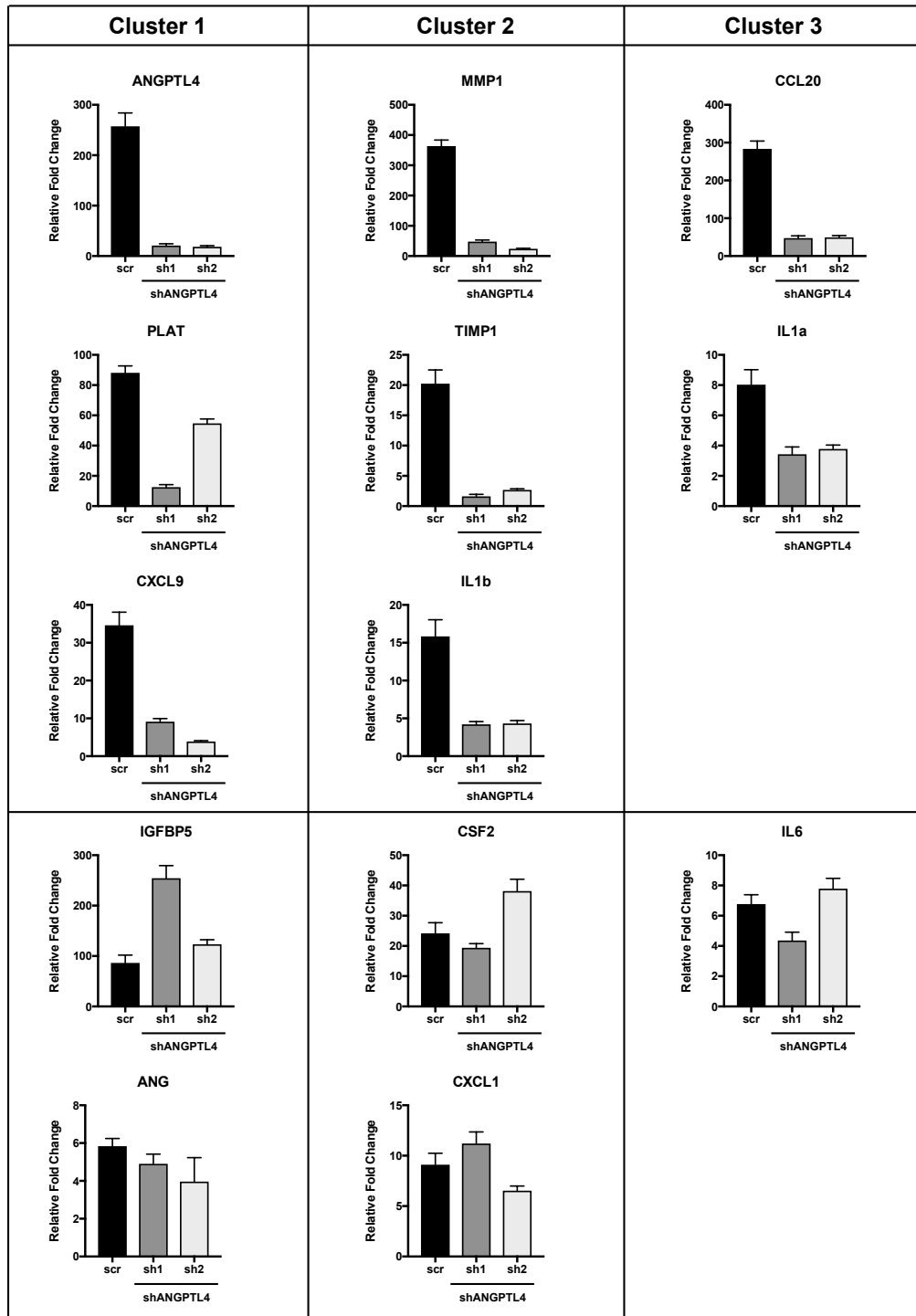


Figure 5.9 RT-qPCR of SASP genes after knockdown of ANGPTL4 reveals a bimodal response

The expression levels of twelve SASP genes up-regulated by at least 5-fold over quiescent DoxCDK4i cells were evaluated in cDNA from LS8817^{Tet^{ON}FMDM2} shANGPTL4 cells (see Figure 5.8). Genes are shown whose expression was attenuated (*Upper*) or unaffected (*Lower*) following ANGPTL4 knockdown.

monitor the synchronous progression of cells into senescence, I wanted to understand what transcriptional changes occur as cells move through the SAGA pathway.

Early during entry into senescence I found there is an upregulation of G₂-M genes that is lost at late time points. It has been proposed that senescence occurs in response to a futile period of growth. In the case of mTOR signaling, senescence occurs when growth factor pathways remain active in the presence of signals that block cell proliferation. In this way, blocking the cell cycle (i.e. through induction of p21) in the presence of serum will cause senescence, but blocking the cell cycle in the absence of serum will lead to quiescence [199, 200]. Although CDK4 inhibitor-induced senescence is not dependent on mTOR, I have similarly found that serum-starving cells before adding CDK4 inhibitors will block senescence. This leads to the question of whether the up-regulation of these cell cycle genes is required for cells to progress into senescence and why they are repressed again once irreversible arrest is achieved and maintained.

Another pattern I identified in my data are genes involved in death signaling pathways. Senescent cells are known to be resistant to apoptosis; however, it was surprising that genes involved in cell death were repressed as early as day 5, much earlier than the onset of irreversibility, and even further down-regulated later in senescence. Mechanisms of resistance to apoptosis are not well understood, though this phenotype is thought to be driven by a shift in the balance of pro- and anti-apoptotic proteins including increased BCL-2 and decreased BAX [183, 201, 202]. Underlying these changes may be modifications in the epigenetic landscape, or it has been proposed that SASP factor signaling can crosstalk with the apoptosis pathway [188, 202, 203]. It will be important in the future to ask if modulating the SASP genes identified in this study can impact on not only irreversible growth arrest, but also apoptosis resistance.

The complex actions and regulation of the SASP

While it is clear that there are many questions this system allows us to ask, I decided to focus on the relationship between the SASP and irreversible growth arrest. As with the context

dependence of the other markers of senescence, the specific combination of factors that comprise each SASP is thought to depend on the inducer and cell type undergoing senescence. SASP factors, including IGFBP3, IGFBP7, and CXCL2 have been previously linked to irreversible growth arrest [189, 204-208]. However, in these studies modulating these factors impacts the occurrence of all senescence phenotypes. Uniquely in my system, knockdown of ANGPTL4 only affects clonogenic growth arrest and not the other phenotypes that we have looked at. Knockdown of IGFBP3 only had a modest affect on irreversible growth arrest, and knockdown of IGFBP7 did not affect any senescence markers. Despite the prior publications, it is not surprising that we did not see large effects with IGFBP3 or IGFBP7 knockdown because it is clear that different SASP factors are required for senescence depending on the inducer of senescence. It remains to be seen if ANGPTL4 is required for senescence in other systems.

Besides irreversible growth arrest, different components of the SASP are known to have varying, context dependent functions. In tumorigenesis, secretion of the SASP can promote the clearance of tumor cells by the immune system or activate a paracrine senescence program in adjacent cells [88-90, 209, 210]. On the other hand, senescent cells can stimulate the division of neighboring cells, both tumor and epithelial, generating a pro-inflammatory environment and promoting angiogenesis [75, 211]. The SASP has also been demonstrated to promote cellular reprogramming [212-215]. During development, senescent cells have been reported to be key for appropriate tissue architecture formation [77, 78]. During wound healing, senescent cells accumulate in the skin and are necessary for the restoration of tissue architecture [216, 217]. Specifically in this context, the temporal regulation of the SASP seems to be crucial as secretion of early SASP factors promotes wound closure and later they drive their own immune mediated clearance. Finally, inappropriate occurrence, or persistence, of senescent cells has the detrimental effect of disrupting tissue structures and creating a pro-inflammatory environment that can contribute to aging [168].

Therefore, I wanted to ask what might explain how the three SASP clusters I identified are grouped temporally. First, they could be clustered by their functional similarity [188]; however, no differences in functional GO terms were immediately clear between the clusters.

Transcriptionally, key pathways could regulate each class separately [180, 181, 189] or epigenetic changes could underlie their differential regulation [190, 218-221]. TRANSFAC sequence consensus analysis did not reveal clear differences in the three programs outside of BACH1 and ETS2 activity. It is worth noting that such an analysis would miss transcription factors that may have weak binding at core promoters but strong binding at upstream enhancer regions as has been shown for C/EBP β and IL1A [222, 223]. In the future, techniques such as ATAC-seq, ChIP-seq, and methylation profiling may be able to garner insights into the regulation of the SASP genes, and it will be interesting to probe how the epigenetic landscape changes more generally as cells progress into senescence.

Finally, the expression of the early SASP genes could be required for later activation of the other clusters [181, 189, 198, 209]. It does appear that there are at least two parallel SASP signaling pathways since knockdown of ANGPTL4 dampens the expression of some, but not all, SASP genes. Surprisingly, this is not seemingly related to the time at which the gene expression occurs. Future studies will be necessary to dissect the intricate relationship between these factors.

Functions of ANGPTL4

Here, I demonstrated that ANGPTL4 is required for CDK4 inhibitor induced senescence in the liposarcoma cell line LS8817. To my knowledge, my study is the first time ANGPTL4 has been implicated in the onset of irreversible growth arrest. ANGPTL4 is a secreted factor whose expression has been seen to increase in a variety of senescent states including mesenchymal stromal cells undergoing replicative senescence, human endothelial cells with c-Myc knockdown, and oncogene-induced senescence in human fibroblasts [190, 224, 225]. I further showed that its expression was increased in cancer cells undergoing therapy-induced senescence, as well as

human fibroblasts undergoing replicative and DNA damage-induced senescence. Other SASP factors I tested were not as conserved between all systems, so it is possible that ANGPTL4 is important for irreversible growth arrest in other mechanisms of senescence, but that remains to be tested.

Transcriptionally, ANGPTL4 can be regulated through a variety of mechanisms including being repressed by macroH2A1 or promoter methylation and activated by the glucocorticoid receptor or HIF-1 α [190, 226-228]. Since ATRX is necessary for irreversible growth arrest and can act as a negative regulator of macroH2A localization, this is a particularly interesting mechanism to explore in the future and may be involved in how ATRX controls senescence, either by regulating the ANGPTL4 locus or others [108, 229]. However, this mechanism will likely not be sufficient as U2OS cells, which lack a functional ATRX and undergo quiescence in response to CDK4 inhibition, still up-regulate ANGPTL4 after treatment (Klein, unpublished data). This experiment suggests that while ANGPTL4 may be necessary for irreversible growth arrest, its expression may not be sufficient, and there are likely multiple pathways necessary to achieve a durable senescent state.

ANGPTL4 has multiple functions attributed to it and the way in which ANGPTL4 could be contributing to the senescence state is multifold. First, ANGPTL4 has been shown to act as a negative regulator of apoptosis, so it could be conferring part of the anti-apoptotic phenotype of senescent cells [230, 231]. Next, ANGPTL4 has been implicated in a variety of metabolic pathways including glycolysis and lipid metabolism [232, 233]. Given that senescent cells have different energy requirements and are known to have altered metabolism, there could be crosstalk between the SASP and these pathways. Finally, there are conflicting reports on the ability of ANGPTL4 to induce tumor growth, angiogenesis, and metastasis [234-239], and these are all phenotypes that can also be consequences of the double-edged sword of SASP (see Chapter 6). One of the hypotheses behind the conflicting reports regarding the function of ANGPTL4 is the number of possible cleavage products of this protein. The N-terminus has been attributed to

metabolic functions whereas the C-terminus seems to be important for cancer promoting effects [240]. Furthermore, ANGPTL4 can be regulated post-translationally through glycosylation, oligomerization, and cleavage prior to secretion [233]. Uncovering which component of ANGPTL4 can contribute to its senescence promoting effects will help generate hypotheses about which function of this protein is important for senescence and what signaling pathways it can activate.

Senescence: one state or many pathways?

It has been suggested that because there are so many triggers that induce senescence, the corresponding senescent states will always be different. This hypothesis is supported by work on the bookends of senescence. Clearly, the pathways that induce senescence are very diverse. Commonly, p16 and p53 are increased in senescent cells, but they are not required for many forms of therapy-induced senescence, including CDK4 inhibitor-induced, which is both p16 and p53 independent. On the other end, the markers of senescence are equally diverse. Even one of the triad of hallmarks, the elaboration of a SASP, has context dependent regulation to its components. However, it is still unclear whether there are similarities that exist between all senescent states in the black box between induction of and late senescence (**Figure 5.10, A**).

A similar problem faced the cell cycle community 30 years ago. Many growth factor signaling pathways can induce progression through the cell cycle, all of which are highly context and tissue dependent. However, it is now accepted that at the core, a small number of proteins are required for faithful progression through the mitotic cell cycle and numerous regulators support the activities of these proteins [241, 242]. Therefore, it stands to reason that a few core genes may be discovered in senescence.

Perhaps one way to discover a core senescence program is to uncover what molecular mechanisms underpin the core trio of phenotypes. Research trying to find such regulators of the SASP has found two primary transcription factors, NF κ B and C/EBP β , so there is reason for

belief in such a strategy. By separating senescence progression from growth arrest and stratifying the phenotypes of senescence, the TetONFMDM2 system described here has the potential to identify more genes that could be exclusively involved in senescence. The Koff lab has shown that ATRX is required for the induction of senescence and so far ATRX foci formation has been seen in all senescent and no quiescent cells tested (Kovatcheva and Gleason, unpublished data). My work has nominated ANGPTL4 as another gene required to reach irreversible growth arrest. These likely act in parallel pathways as ANGPTL4 can be increased in the absence of ATRX and ATRX foci can form in the absence of ANGPTL4. There is also likely at least one more parallel SASP pathway since knockdown of ANGPTL4 is sufficient to block the induction of some, but not all SASP factors. This data supports the hypothesis that a number of effector pathways are necessary to enter into a deep senescent state (**Figure 5.10, B**).

However, this still does not address the problem of defining *a* senescent state. If senescence at its core requires resistance to apoptosis, irreversible growth arrest, and elaboration of a SASP, then is a cell not senescent until all three requirements are met? Clearly in my system, canonical markers of senescence arise before many of these phenotypes. Additionally, once these three requirements are met (minimally so at day 14), the transcriptional landscape continues to evolve over the next 14 days. If this study were to extend for longer gene changes may continue, as there is no evidence to suggest that we have reached a plateau, or in fact that there is ever a plateau in senescent cells. Is it fair then to just call each of these cells ‘senescent’ when they are clearly each distinct in their transcriptional profiles? Here I have labeled my senescence states entry, early, deepening, and late but such labels would not translate to non-synchronous systems. Whether or not a core program of senescence is found, it is clear that the context dependence of senescence will always require explicit definition of how a cell was made senescent, how long it has been senescent, and what markers were used to define this state. While studies like the one performed here can begin to provide clarity about mechanisms of progression through senescence, they also demonstrate the complexity of how different ‘senescent’ cells can be.

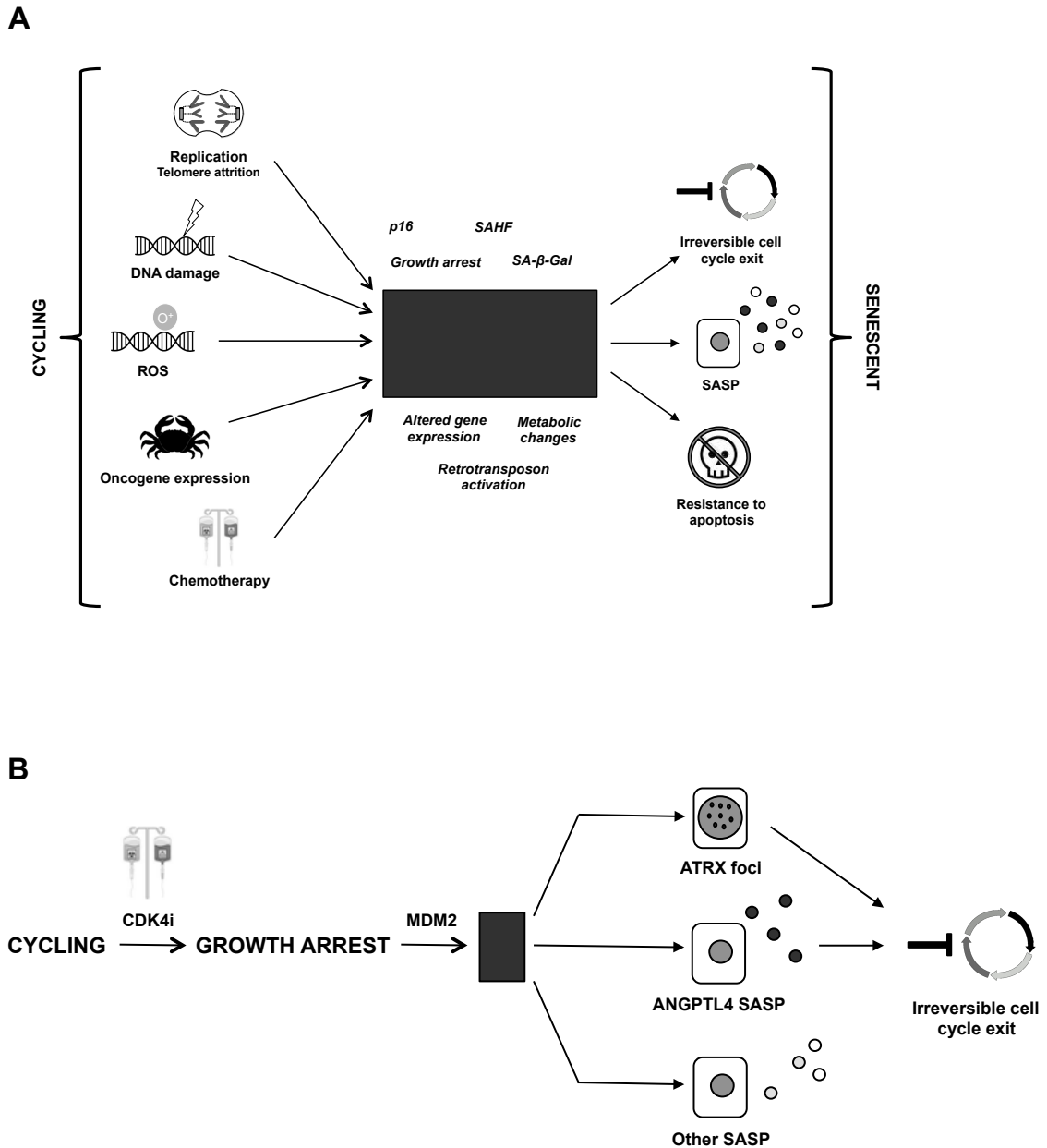


Figure 5.10. Illustration of the pathways to senescence

(A) There are diverse triggers and numerous phenotypes associated with the progression of a cycling cell into the senescent state, but a dearth of knowledge exists over the molecular mechanism that controls this transition. (B) Therapy induced senescence after growth arrest (SAGA) is beginning to shrink this black box by identifying pathways that are required for irreversible growth arrest and uncovering relationships between the hallmarks of senescence.

CHAPTER 6: DISCUSSION

Throughout the 20th century there were great medical advances that expanded human longevity worldwide. However, now in the 21st century, we are faced with an increased ailing population that is susceptible to diseases of old age, including cancer. Public initiatives like Cancer Moonshot and Stand Up To Cancer have led to a renewed push to understand the molecular mechanisms that drive tumorigenesis and develop novel therapies.

My thesis work has focused on understanding how cells respond to one relatively new class of drugs, CDK4/6 inhibitors. In clinical trials these inhibitors have shown great promise for the treatment of a variety of neoplasms, both as single agents and in combination with other therapies. However, a subset of patients do not respond to these inhibitors and, despite large-scale efforts, biomarkers that underlie response *in vivo* have escaped detection. Prior work in the Koff laboratory demonstrated that when cell lines derived from well-differentiated and dedifferentiated liposarcoma are treated with CDK4 inhibitors, some exit the cell cycle into senescence while others exit into quiescence. This decision is dependent on the down-regulation of MDM2.

I have expanded on this finding by demonstrating that the response to CDK4 inhibitors is driven by senescence after growth arrest (SAGA). After treatment with CDK4 inhibitors cells exit the cell cycle into a reversible quiescent state and HAUSP dissociates from MDM2. Then, if the environment is permissive, MDM2 will be turned over and cells will progress into senescence. This turnover is able to occur if CDH18 is present in focal loci and interacting with PDLIM7. In the absence of CDH18, PDLIM7 can interact with MDM2 and prevent its turnover, leaving cells unable to progress into senescence. Furthermore, the expression of CDH18 is associated with extended progression free and overall survival in well-differentiated and dedifferentiated liposarcoma (WD/DDLS) patients treated with the CDK4 inhibitor palbociclib in a Phase II trial, suggesting that SAGA is a clinically relevant mechanism of action for CDK4 inhibitors.

To begin to understand what other molecular events occur during the pathway into senescence, I developed a system that could take advantage of SAGA. By modulating the expression of MDM2, I demonstrated that by forcing cells to accumulate in quiescence and then releasing them into senescence I could monitor the progression into senescence and observe cells accumulating known markers of senescence in a highly synchronous manner. Further, I was able to temporally separate these markers, giving an unprecedented opportunity to identify gene expression changes that may be important for the acquisition of individual senescence phenotypes, including a new link between the senescence-associated secretory program (SASP) and irreversible growth arrest. In this chapter, I will reflect on the consequences these findings may have *in vivo* and discuss the promise my data holds for understanding the broader biological significance of senescence after growth arrest.

Senescence after growth arrest links MDM2 regulation to therapeutic outcomes in cancer

Between senescence and quiescence, senescence is generally thought to be the preferred outcome of therapy. In part, this hypothesis came from studies on oncogene-induced senescence, where senescence is a barrier to unchecked proliferation and tumorigenesis [95, 243]. Certainly with a clinical treatment like palbociclib, where patients are cycled off the drug to give their immune system a chance to recover, it stands to reason that in the off period a cell that is merely quiescent could return to the cell cycle and proliferate, whereas a senescent cell would remain durably growth arrested. However, given the lack of markers for identifying senescent cells *in vivo*, it has never been formally tested if senescence is the clinically preferred outcome.

The Koff lab has two lines of evidence to suggest that patients that can reach senescence will perform better when treated with palbociclib. First, in a pilot study of 7 patients who consented to pre- and post- treatment biopsies while on trial, MDM2 levels are down-regulated in patients who perform well and stable in patients who have limited clinical responses [57]. Secondly, my work on CDH18 suggests that expression of this protein correlates with patient

response to palbociclib and that modulation of CDH18 *in vitro* affects the outcome to CDK4 inhibition, *vis a vis* quiescence or senescence (Klein et al, *Oncogene* in press).

Currently studies are ongoing to determine if senescence is preferable to durable quiescence in a mouse model of lung cancer (Gleason, unpublished data). Additionally, a phase II clinical trial with abemaciclib is being conducted for WD/DDLS patients at Memorial Sloan Kettering. Excitingly, as a part of this trial, pre-treatment and on-treatment frozen and formalin-fixed paraffin embedded biopsies are being collected for all patients. This is an excellent opportunity to test the importance of CDH18 in pre-treatment specimens. Furthermore, gene expression analyses can be performed on these samples and compared to existing data sets in the laboratory (both my time course study and others) to ask if there are changes in senescence programs that are associated with response. Since CDH18 has strong negative predictive value but a weak positive predictive value, it is likely that there are other requirements for response along the senescence pathway that will hopefully be unmasked as we continue to discover what changes underlie the senescence response in cell lines. Unlike palbociclib, abemaciclib is dosed continuously, so it will be interesting to determine if there is a similar stratification of patient response as is seen with palbociclib. If senescence can be associated with an improved outcome in these patients, it suggests that other facets of senescence besides irreversible arrest alone may contribute to the benefits of this state.

One possibility is that the elaboration of the SASP also contributes to improved clinical outcomes. The SASP can sculpt immune response and induce the recruitment of immune cells that mediate tumor clearance or promote paracrine senescence [88, 209, 244]. This suggests that combining drugs that induce senescence with those that sculpt the immune system could improve cancer therapies. For example, treating PTEN-null tumors with docetaxel induces senescence but gives little overall benefit until a JAK2 inhibitor is added, which reprograms the SASP and triggers an antitumor immune response *in vivo* [245].

On the other hand, secretion of the SASP can create a pro-tumorigenic environment [182, 211, 246-248] and induce cellular plasticity, allowing cancer cells that escape senescence to have a more aggressive, cancer stem cell-like identity [215, 249]. This has led to the SASP often being referred to as a double-edged sword. Ultimately the most effective approach may be to first induce senescence and then eliminate the persistent senescent cells. Evidence that BCL-2 inhibitors can directly eliminate senescent cells [250, 251] suggests that combining this with other cancer therapies in a sequential manner might be useful. Preliminary data suggests that CDK4 inhibitor-induced senescence is accompanied by increased metabolic flux through the glycolytic pathway, leading to senescent cells being uniquely vulnerable to killing by glycolysis pathway inhibitors (Klein unpublished data). Hopefully in the future, my time course data can be mined to find additional unique susceptibilities within the senescent cell.

However, there are still a large percentage of patients that would not benefit from such therapies since they do not reach senescence with CDK4 inhibition alone. When I began studying the regulation of MDM2, I was hopeful that uncovering this pathway would lead to rational combination therapies that could improve treatments for patients. Unfortunately, the discovery of a number of understudied proteins like PDLIM7 and CDH18, while scientifically exciting, limits such options. Therefore, I turned my attention to what could be learned from the pathways downstream of MDM2. While the exact target of MDM2 in the senescence pathway is not yet discovered, MDM2's function in suppressing senescence is dependent on its E3 ligase domain [57]. Thus, a strong and selective inhibitor of MDM2's E3 ligase activity could potentially convert quiescence to senescence. Unfortunately, such MDM2 inhibitors that are currently available are weak at best and have struggled to reach the clinic [252, 253].

The discovery of senescence after growth arrest offers new hope for developing combination therapies. If quiescence and senescence were terminal fates, it would be difficult to combine CDK4/6 inhibitors with other drugs and improve response. On the other hand, since quiescence can be converted in to senescence, patients could hypothetically be treated first with a

CDK4/6 inhibitor to induce growth arrest and secondly with another inhibitor that pushes cells into senescence. To determine if data existed in my time course that could lead to rationale combination therapies, I analyzed what hallmark gene sets were being down-regulated to determine if there were signaling pathways that could perhaps be targeted to induce senescence. I found repression of a number of genes that can be up-regulated by mitogen activated kinase pathway (MAPK) components including HRAS, EGF, and KRAS. Prior work in the lab also implicated ATRX's repression of HRAS as necessary for CDK4-inhibitor induced senescence [108]. Therefore, I obtained a number of drugs against the Ras pathway and its effectors including HRAS, MEK, PI3K, and AKT inhibitors. Preliminary data suggests inhibitors against both the farnesyltransferase of HRAS (tipifarnib) and MEK (trametenib) are able to push LS8107 cells into senescence (Klein, unpublished data). This is not the first time MEK inhibitors have been seen to cooperate with CDK4 inhibitors and drive senescence [38]. It was initially surprising that tipifarnib had an effect on senescence, as this drug is generally ineffective as a single agent when treating cycling cells [254-256]. However, my findings support the hypothesis that the cooperation of CDK4/6 inhibitors and signaling pathway inhibitors may be affecting sequential decisions in the tumor cell. Therefore, inhibitors that have minimal effect in cycling tumor cells may have more of an impact in non-cycling CDK4/6 inhibitor treated cells. As we begin to understand more players on the SAGA pathway, hopefully we will identify other combinations that can improve patient outcomes.

Finally, it is tempting to speculate that the mechanisms of response to CDK4/6 inhibitors discussed in this thesis are not completely separate: the ability of these drugs to drive tumor cells into senescence may drive changes in the immune response (perhaps through the SASP) *and* cellular metabolism, thus yielding a unified mechanistic cellular response that is initiated by the simple act of inhibiting CDK4/6 kinases in normal and tumor cells.

Quiescence is an actively inactive state

The discovery of SAGA has clear implications for the treatment of cancer, but also leads one to wonder if there are other biological contexts in which this pathway is important. At any given time many of the cells in an organism are not proliferating and exist in a growth arrested state. Therefore, an understanding of the importance of this quiescent state could give insight into where SAGA plays a role.

The proliferation capacity of cells can be generally classified into three categories: (1) differentiated cells that never divide again, (2) cells that regularly proliferate, and (3) cells that are generally quiescent but can resume proliferation upon appropriate stimulation [257]. For example, there are some differentiated cells, such as cardiac muscle cells, that are long lived and have no ability to proliferate [258]. If they are lost they cannot be regenerated. On the other extreme, there are cells that proliferate regularly such as stem cells that give rise to differentiated blood cells, skin epithelial cells, and the epithelial cells lining the gut [259-262]. Throughout the organism's lifespan, these cells continually replenish cells that are lost and turned over [263]. However, even hematopoietic stem cells have a small population, 5-10% of cells, that divide at a much slower rate [264, 265] and similar 'active' and 'dormant' populations of stem cells can be labeled and identified in the gut and hair follicles [266]. Finally, many cells exist in a quiescent state where there is a tight balance between maintaining the capacity to proliferate and remaining appropriately arrested (**Figure 6.1, homeostasis**).

Cells need to maintain the ability to re-enter the cell cycle so that proliferation can be appropriately induced upon a stimulus or injury (**Figure 6.1, after injury**). Memory B-cells can remain in quiescence for years waiting for an antigen stimulus that induces them to proliferate and mature [267]. After damage, skin fibroblasts, liver epithelial cells, vascular smooth muscle cells, and muscle satellite stem cells can all resume proliferation to repair the tissue [268-273]. However, cells also need to be able to re-exit the cell cycle at the appropriate time. If muscle satellite stem cells fail to return to quiescence, premature differentiation and stem cell pool

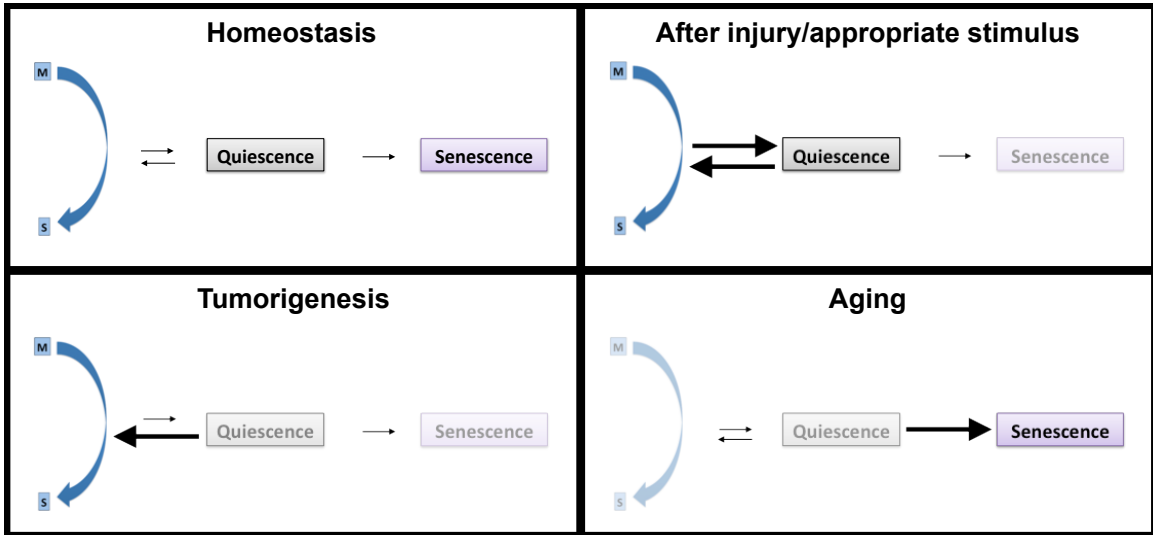


Figure 6.1. Possible physiological consequences of exiting quiescence

Many cells exist in a quiescent state where there is a tight balance between maintaining the capacity to proliferate and remaining appropriately arrested. Cells need to be able to respond to appropriate cues and return to the cell cycle after injury, but inappropriate activation can lead to tumorigenesis. On the other hand, losing the capacity to return to the cell cycle and undergoing senescence can contribute to aging.

exhaustion occurs [274]. If B cells cannot enter into quiescence they will not accomplish variable-diversity-joining recombination, as RAG2 expression is required and restricted to the G₀-G₁ phase of the cell cycle [275]. Finally, it has been suggested that the maintenance of stem cells in a ‘dormant’ state may contribute to their longevity, either by minimizing replicative stress or by down-regulating antigen presentation machinery allowing them to escape killing by T cell immunity [276, 277].

The other consequence of not re-exiting the cell cycle is unchecked proliferation, one of the hallmarks of cancer (**Figure 6.1, tumorigenesis**). Interestingly, despite being highly proliferative, tumor cells can also maintain themselves in an advantageous growth arrested state. For example, disseminated tumor cells can exist in a dormant state for years before later giving rise to metastases [278]. This arrest can be driven by the absence of growth factor or adhesion signaling at the new tissue site and can allow tumor cells to survive and return to proliferation later while also garnering resistance to cytotoxic therapies [279]. Understanding how these cells maintain themselves in quiescence and return to the cell cycle may yield new clinical options to prevent later metastatic disease. The other alternative is to identify ways to push quiescent cells into senescence. By discovering and populating the SAGA pathway, we can hopefully nominate therapies that will employ this strategy, as discussed previously.

Given the necessity to be able to return to the cell cycle, what happens if cells achieve cell cycle exit but lose their ability to respond to proliferation inducing signals? Reversibility is likely not an innate property of non-dividing cells. In yeast, glucose removal will initiate a G₁ arrest that is reversible as long as Xbp1 is present, but failure to repress Xbp1 targets will lead to senescence [280]. Similarly in mammalian fibroblasts, enforced cell cycle arrest in culture will initiate senescence unless HES1 is expressed, allowing growth arrest to remain reversible [281]. There are physiological consequences to such changes. In mice, muscle satellite stem cells have increases in p16 associated with age, which switches these cells from quiescence into an irreversible senescent state and prevents muscle regeneration [282]. Likewise, immunosenescence

leads to a diminished production of adaptive immune cells and a decrease in the functional capacity of these cells with age, though there are conflicting reports if p16-driven senescence specifically contributes to these declining phenotypes [283-287]. Therefore, failure to maintain quiescence may lead to a shift into senescence, and be associated with aging (**Figure 6.1, aging**). Such a pathway is modeled similarly to SAGA, so I wondered if SAGA could be implicated in aging.

Exploiting senescence after growth arrest to combat age-associated pathologies

Senescent cells have been found to accumulate in pathologies associated with age including glaucoma, diabetes, and osteoarthritis [288-290]. Likely the inability of senescent cells to return to the cell cycle and proliferate, coupled with the release of factors in the SASP that can increase local inflammation and create further tissue damage, can drive age associated pathologies [291, 292]. Formative work by Baker et al in 2011 demonstrated that continual clearance of p16 positive cells in a progeria transgenic mouse model delayed age-related pathologies in the adipose tissue, skeletal muscle, and eye [293]. This work has been further extrapolated to wild-type mice where clearance of senescent cells preserved the function of multiple organs including the kidney, heart, and fat [294].

The finding that senescence can be causally linked to aging has led to the founding of multiple companies dedicated to finding mechanisms to kill or hinder senescent cells, collectively known as senotherapies. The ultimate goal of a successful senotherapy is to prevent disease and extend healthy lifespan. The three primary strategies being employed are: (1) identifying what makes a cell resistant to apoptosis and targeting those survival strategies, (2) developing therapies that interfere with SASP production or the inflammatory environment they promote, and (3) augmenting the immune system to enhance the clearance of senescent cells [291, 295, 296].

However, so far strategies 1 and 2 seem to be hampered by a lack of specificity. Unlike senescence which can be induced through multiple triggers and have multiple pathways in,

apoptosis is a relatively linear effector pathway. While this makes it quite clear what pathways should be targeted to induce apoptosis, these pathways are very important in many cells. Therefore, one concern of a senolytic therapy, like a BCL-2 or p53 inhibitor is broad off-target effects by inducing apoptosis in unintended cells. Similarly, key signaling pathways that have been found to underlie the secretion of inflammatory cytokines, including NF κ B and mTOR, are important for a multitude of functions within the cell. One future possibility is by understanding which specific SASP factors contribute to pathologies, more targeted therapies can be developed.

Perhaps the greatest hope at this time comes from modulating the immune system. However, it is known that the immune system itself ages over time, giving rise to immunosenescence [297-299]. Unlike in a young organism, where the appropriate and inappropriate arousal of senescent cells can be balanced through immune clearance, this ability is lost as the organism ages. As more senescent cells are generated and fewer are cleared, the proportion of senescent cells increases (**Figure 6.2**). Finding therapeutics that successfully modulate the effect of the immune system will have to overcome both the dulled recognition of pathogens and the compromised ability to clear senescent cells.

The identification of SAGA suggests that another strategy exists to correct this balance. While the appearance of some of these senescent cells is likely a consequence of replication or DNA damage stress, post-mitotic cells such as neurons can also become senescent. If we could slow the accumulation of senescent cells as we age, this will allow for an appropriate balance to be maintained even in the absence of a fully functional immune response (**Figure 6.2**). This approach is referred to as *seno-suppression*.

How then can we exploit the knowledge that we have garnered by studying CDK4 inhibitor induced senescence after growth arrest to combat aging? One approach is to take the gene changes I have found as cells progress into senescence and ask if they are also increased in aging (Gleason, unpublished data). Future work will hopefully illuminate whether the changes I have identified in therapy induced SAGA are conserved in other forms of senescence and aged

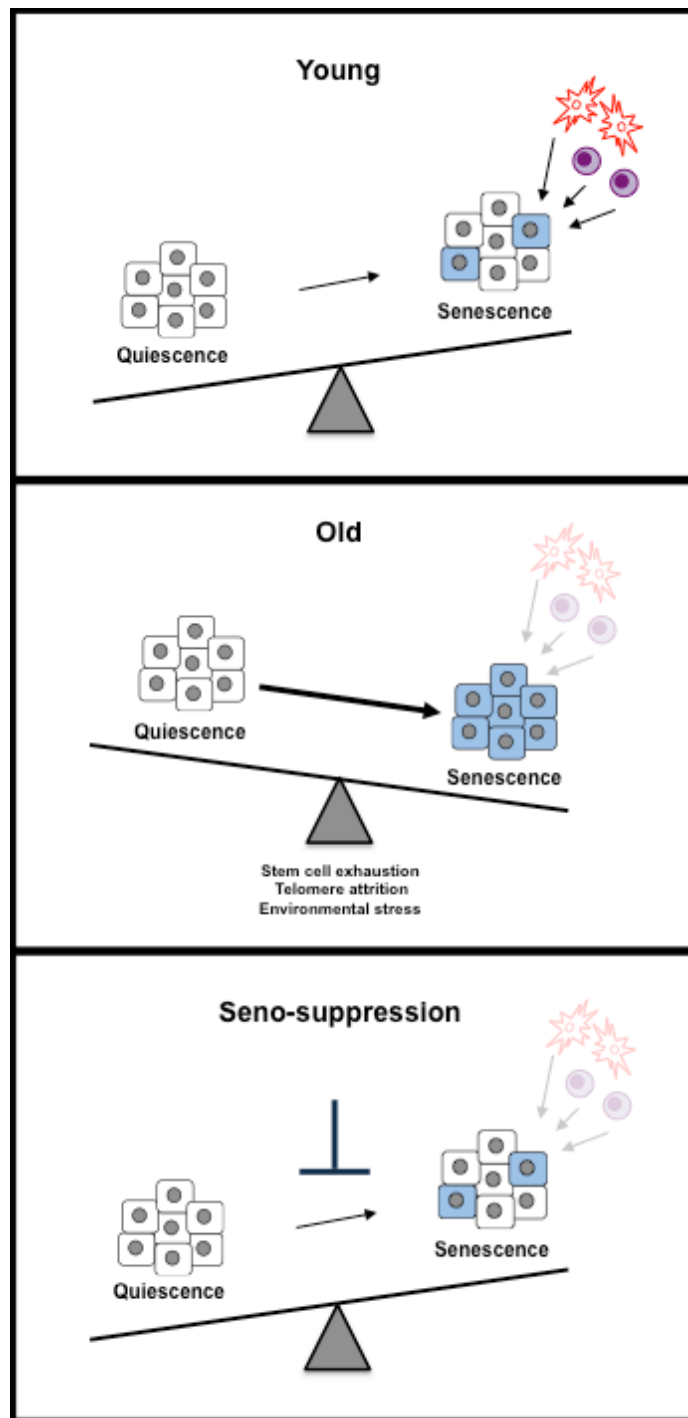


Figure 6.2. Countering the senescence burden by preventing SAGA

In young organisms, the gradual appearance of senescent cells is countered by an active immune system. With time, decreased immune system function coupled with increases in the appearance of senescent cells may conspire to drive age related phenotypes. Using seno-suppressants to block senescence after growth arrest (SAGA) may slow the accumulation of senescent cells and delay pathologies associated with age.

tissues. Once it is clear what the overlap between these systems is we will have a better idea if there are signaling pathways or molecules we could strive to target.

We already know of one such molecule that appears highly conserved throughout all senescent states, the formation of ATRX foci. Importantly, ATRX foci occur early in the time course, suggesting if we could find therapeutics that halt ATRX foci formation we could halt many of the gene and phenotype changes that happen as cells progress into senescence, including irreversible growth arrest and the release of a SASP. Such a therapy could be given without concerns of killing healthy senescent cells and, without inducing apoptosis, tissue architecture will be preserved and there will not be off target inflammatory responses. Though much work remains to determine if SAGA is important for, and can be manipulated in, aging, such a strategy may delay the onset of aging by extending healthspan and preserving youthful tissue characteristics.

Collectively, my work has demonstrated how molecular pathways identified in the lab can have broad affects physiologically. A beside to bench to bedside approach like the one I employed has great promise to improve cancer therapies and beyond. I eagerly anticipate the results of future work that will help determine if senescence after growth arrest can be exploited to treat a multitude of diseases.

REFERENCES

1. Breasted, J.H. and New-York Historical Society. Library., *The Edwin Smith surgical papyrus*. 1930, Chicago, Ill.: The University of Chicago Press.
2. Hajdu, S.I., *Greco-Roman thought about cancer*. *Cancer*, 2004. **100**(10): p. 2048-51.
3. DeVita, V.T., Jr. and E. Chu, *A history of cancer chemotherapy*. *Cancer Res*, 2008. **68**(21): p. 8643-53.
4. Jones, D.S., S.H. Podolsky, and J.A. Greene, *The burden of disease and the changing task of medicine*. *N Engl J Med*, 2012. **366**(25): p. 2333-8.
5. Hanahan, D. and R.A. Weinberg, *Hallmarks of cancer: the next generation*. *Cell*, 2011. **144**(5): p. 646-74.
6. Goodman, L., *Targeting oncogenes*. *J Clin Invest*, 2004. **114**(10): p. 1362.
7. Morris, L.G. and T.A. Chan, *Therapeutic targeting of tumor suppressor genes*. *Cancer*, 2015. **121**(9): p. 1357-68.
8. Allegranza, M.J. and J.R. Conejo-Garcia, *Targeted Therapy and Immunosuppression in the Tumor Microenvironment*. *Trends Cancer*, 2017. **3**(1): p. 19-27.
9. Martin, M., H. Wei, and T. Lu, *Targeting microenvironment in cancer therapeutics*. *Oncotarget*, 2016. **7**(32): p. 52575-52583.
10. Asghar, U., et al., *The history and future of targeting cyclin-dependent kinases in cancer therapy*. *Nat Rev Drug Discov*, 2015. **14**(2): p. 130-46.
11. Sherr, C.J. and J.M. Roberts, *CDK inhibitors: positive and negative regulators of G1-phase progression*. *Genes Dev*, 1999. **13**(12): p. 1501-12.
12. Classon, M. and E. Harlow, *The retinoblastoma tumour suppressor in development and cancer*. *Nat Rev Cancer*, 2002. **2**(12): p. 910-7.
13. Harbour, J.W. and D.C. Dean, *The Rb/E2F pathway: expanding roles and emerging paradigms*. *Genes Dev*, 2000. **14**(19): p. 2393-409.
14. Stevaux, O. and N.J. Dyson, *A revised picture of the E2F transcriptional network and RB function*. *Curr Opin Cell Biol*, 2002. **14**(6): p. 684-91.
15. Harbour, J.W., et al., *Cdk phosphorylation triggers sequential intramolecular interactions that progressively block Rb functions as cells move through G1*. *Cell*, 1999. **98**(6): p. 859-69.
16. Lundberg, A.S. and R.A. Weinberg, *Functional inactivation of the retinoblastoma protein requires sequential modification by at least two distinct cyclin-cdk complexes*. *Mol Cell Biol*, 1998. **18**(2): p. 753-61.
17. Rane, S.G., et al., *Loss of Cdk4 expression causes insulin-deficient diabetes and Cdk4 activation results in beta-islet cell hyperplasia*. *Nat Genet*, 1999. **22**(1): p. 44-52.
18. Tsutsui, T., et al., *Targeted disruption of CDK4 delays cell cycle entry with enhanced p27(Kip1) activity*. *Mol Cell Biol*, 1999. **19**(10): p. 7011-9.
19. Moons, D.S., et al., *Pituitary hypoplasia and lactotroph dysfunction in mice deficient for cyclin-dependent kinase-4*. *Endocrinology*, 2002. **143**(8): p. 3001-8.
20. Moons, D.S., et al., *Intact follicular maturation and defective luteal function in mice deficient for cyclin-dependent kinase-4*. *Endocrinology*, 2002. **143**(2): p. 647-54.
21. Martin, J., et al., *Genetic rescue of Cdk4 null mice restores pancreatic beta-cell proliferation but not homeostatic cell number*. *Oncogene*, 2003. **22**(34): p. 5261-9.
22. Sherr, C.J. and J.M. Roberts, *Living with or without cyclins and cyclin-dependent kinases*. *Genes Dev*, 2004. **18**(22): p. 2699-711.
23. Landis, M.W., et al., *Cyclin D1-dependent kinase activity in murine development and mammary tumorigenesis*. *Cancer Cell*, 2006. **9**(1): p. 13-22.
24. Choi, Y.J., et al., *The requirement for cyclin D function in tumor maintenance*. *Cancer Cell*, 2012. **22**(4): p. 438-51.

25. Puyol, M., et al., *A synthetic lethal interaction between K-Ras oncogenes and Cdk4 unveils a therapeutic strategy for non-small cell lung carcinoma*. *Cancer Cell*, 2010. **18**(1): p. 63-73.
26. Finn, R.S., et al., *Palbociclib and Letrozole in Advanced Breast Cancer*. *N Engl J Med*, 2016. **375**(20): p. 1925-1936.
27. Fry, D.W., et al., *Specific inhibition of cyclin-dependent kinase 4/6 by PD 0332991 and associated antitumor activity in human tumor xenografts*. *Mol Cancer Ther*, 2004. **3**(11): p. 1427-38.
28. Gelbert, L.M., et al., *Preclinical characterization of the CDK4/6 inhibitor LY2835219: in-vivo cell cycle-dependent/independent anti-tumor activities alone/in combination with gemcitabine*. *Invest New Drugs*, 2014. **32**(5): p. 825-37.
29. Tripathy, D., A. Bardia, and W.R. Sellers, *Ribociclib (LEE011): Mechanism of Action and Clinical Impact of This Selective Cyclin-Dependent Kinase 4/6 Inhibitor in Various Solid Tumors*. *Clin Cancer Res*, 2017. **23**(13): p. 3251-3262.
30. Knudsen, E.S., et al., *Biological specificity of CDK4/6 inhibitors: dose response relationship, in vivo signaling, and composite response signature*. *Oncotarget*, 2017. **8**(27): p. 43678-43691.
31. Johnson, N. and G.I. Shapiro, *Cyclin-dependent kinases (cdks) and the DNA damage response: rationale for cdk inhibitor-chemotherapy combinations as an anticancer strategy for solid tumors*. *Expert Opin Ther Targets*, 2010. **14**(11): p. 1199-212.
32. DiPippo, A.J., N.K. Patel, and C.M. Barnett, *Cyclin-Dependent Kinase Inhibitors for the Treatment of Breast Cancer: Past, Present, and Future*. *Pharmacotherapy*, 2016. **36**(6): p. 652-67.
33. Raub, T.J., et al., *Brain Exposure of Two Selective Dual CDK4 and CDK6 Inhibitors and the Antitumor Activity of CDK4 and CDK6 Inhibition in Combination with Temozolomide in an Intracranial Glioblastoma Xenograft*. *Drug Metab Dispos*, 2015. **43**(9): p. 1360-71.
34. Yin, L., et al., *A highly potent CDK4/6 inhibitor was rationally designed to overcome blood brain barrier in glioblastoma therapy*. *Eur J Med Chem*, 2017. **144**: p. 1-28.
35. Hortobagyi, G.N., et al., *Ribociclib as First-Line Therapy for HR-Positive, Advanced Breast Cancer*. *N Engl J Med*, 2016. **375**(18): p. 1738-1748.
36. Knudsen, E.S. and A.K. Witkiewicz, *The Strange Case of CDK4/6 Inhibitors: Mechanisms, Resistance, and Combination Strategies*. *Trends Cancer*, 2017. **3**(1): p. 39-55.
37. Herrera-Abreu, M.T., et al., *Early Adaptation and Acquired Resistance to CDK4/6 Inhibition in Estrogen Receptor-Positive Breast Cancer*. *Cancer Res*, 2016. **76**(8): p. 2301-13.
38. Franco, J., A.K. Witkiewicz, and E.S. Knudsen, *CDK4/6 inhibitors have potent activity in combination with pathway selective therapeutic agents in models of pancreatic cancer*. *Oncotarget*, 2014. **5**(15): p. 6512-25.
39. Heilmann, A.M., et al., *CDK4/6 and IGF1 receptor inhibitors synergize to suppress the growth of p16INK4A-deficient pancreatic cancers*. *Cancer Res*, 2014. **74**(14): p. 3947-58.
40. Yang, C., et al., *Acquired CDK6 amplification promotes breast cancer resistance to CDK4/6 inhibitors and loss of ER signaling and dependence*. *Oncogene*, 2017. **36**(16): p. 2255-2264.
41. Gong, X., et al., *Genomic Aberrations that Activate D-type Cyclins Are Associated with Enhanced Sensitivity to the CDK4 and CDK6 Inhibitor Abemaciclib*. *Cancer Cell*, 2017. **32**(6): p. 761-776 e6.
42. Jiang, J., et al., *Coexistence of p16/CDKN2A homozygous deletions and activating EGFR mutations in lung adenocarcinoma patients signifies a poor response to EGFR-TKIs*. *Lung Cancer*, 2016. **102**: p. 101-107.

43. Long, G.V., et al., *Increased MAPK reactivation in early resistance to dabrafenib/trametinib combination therapy of BRAF-mutant metastatic melanoma*. Nat Commun, 2014. **5**: p. 5694.
44. Yadav, V., et al., *The CDK4/6 inhibitor LY2835219 overcomes vemurafenib resistance resulting from MAPK reactivation and cyclin D1 upregulation*. Mol Cancer Ther, 2014. **13**(10): p. 2253-63.
45. Finn, R.S., et al., *PD 0332991, a selective cyclin D kinase 4/6 inhibitor, preferentially inhibits proliferation of luminal estrogen receptor-positive human breast cancer cell lines in vitro*. Breast Cancer Res, 2009. **11**(5): p. R77.
46. Goel, S., et al., *Overcoming Therapeutic Resistance in HER2-Positive Breast Cancers with CDK4/6 Inhibitors*. Cancer Cell, 2016. **29**(3): p. 255-69.
47. Kwong, L.N., et al., *Oncogenic NRAS signaling differentially regulates survival and proliferation in melanoma*. Nat Med, 2012. **18**(10): p. 1503-10.
48. Vora, S.R., et al., *CDK 4/6 inhibitors sensitize PIK3CA mutant breast cancer to PI3K inhibitors*. Cancer Cell, 2014. **26**(1): p. 136-49.
49. Zhou, J., et al., *CDK4/6 or MAPK blockade enhances efficacy of EGFR inhibition in oesophageal squamous cell carcinoma*. Nat Commun, 2017. **8**: p. 13897.
50. Polk, A., et al., *Specific CDK4/6 inhibition in breast cancer: a systematic review of current clinical evidence*. ESMO Open, 2016. **1**(6): p. e000093.
51. Georger, B., et al., *A Phase I Study of the CDK4/6 Inhibitor Ribociclib (LEE011) in Pediatric Patients with Malignant Rhabdoid Tumors, Neuroblastoma, and Other Solid Tumors*. Clin Cancer Res, 2017. **23**(10): p. 2433-2441.
52. Michel, L., et al., *Phase I trial of palbociclib, a selective cyclin dependent kinase 4/6 inhibitor, in combination with cetuximab in patients with recurrent/metastatic head and neck squamous cell carcinoma*. Oral Oncol, 2016. **58**: p. 41-8.
53. Niesvizky, R., et al., *Phase 1/2 study of cyclin-dependent kinase (CDK)4/6 inhibitor palbociclib (PD-0332991) with bortezomib and dexamethasone in relapsed/refractory multiple myeloma*. Leuk Lymphoma, 2015. **56**(12): p. 3320-8.
54. Doi, T., et al., *Phase I study of single-agent ribociclib in Japanese patients with advanced solid tumors*. Cancer Sci, 2018. **109**(1): p. 193-198.
55. Dickson, M.A., et al., *Phase II trial of the CDK4 inhibitor PD0332991 in patients with advanced CDK4-amplified well-differentiated or dedifferentiated liposarcoma*. J Clin Oncol, 2013. **31**(16): p. 2024-8.
56. Dickson, M.A., et al., *Progression-Free Survival Among Patients With Well-Differentiated or Dedifferentiated Liposarcoma Treated With CDK4 Inhibitor Palbociclib: A Phase 2 Clinical Trial*. JAMA Oncol, 2016. **2**(7): p. 937-40.
57. Kovatcheva, M., et al., *MDM2 turnover and expression of ATRX determine the choice between quiescence and senescence in response to CDK4 inhibition*. Oncotarget, 2015. **6**(10): p. 8226-43.
58. Finn, R.S., et al., *The cyclin-dependent kinase 4/6 inhibitor palbociclib in combination with letrozole versus letrozole alone as first-line treatment of oestrogen receptor-positive, HER2-negative, advanced breast cancer (PALOMA-1/TRIO-18): a randomised phase 2 study*. Lancet Oncol, 2015. **16**(1): p. 25-35.
59. Patnaik, A., et al., *Efficacy and Safety of Abemaciclib, an Inhibitor of CDK4 and CDK6, for Patients with Breast Cancer, Non-Small Cell Lung Cancer, and Other Solid Tumors*. Cancer Discov, 2016. **6**(7): p. 740-53.
60. Ciznadija, D., et al., *Cyclin D1 and cdk4 mediate development of neurologically destructive oligodendroglioma*. Cancer Res, 2011. **71**(19): p. 6174-83.
61. Goel, S., et al., *CDK4/6 inhibition triggers anti-tumour immunity*. Nature, 2017. **548**(7668): p. 471-475.

62. Chow, Y.H., et al., *Role of Cdk4 in lymphocyte function and allergen response*. Cell Cycle, 2010. **9**(24): p. 4922-30.
63. Lopez-Mejia, I.C., et al., *CDK4 Phosphorylates AMPKalpha2 to Inhibit Its Activity and Repress Fatty Acid Oxidation*. Mol Cell, 2017. **68**(2): p. 336-349 e6.
64. Lee, Y., et al., *Cyclin D1-Cdk4 controls glucose metabolism independently of cell cycle progression*. Nature, 2014. **510**(7506): p. 547-51.
65. Franco, J., et al., *Metabolic Reprogramming of Pancreatic Cancer Mediated by CDK4/6 Inhibition Elicits Unique Vulnerabilities*. Cell Rep, 2016. **14**(5): p. 979-990.
66. Michaud, K., et al., *Pharmacologic inhibition of cyclin-dependent kinases 4 and 6 arrests the growth of glioblastoma multiforme intracranial xenografts*. Cancer Res, 2010. **70**(8): p. 3228-38.
67. Sawai, C.M., et al., *Therapeutic targeting of the cyclin D3:CDK4/6 complex in T cell leukemia*. Cancer Cell, 2012. **22**(4): p. 452-65.
68. Wolowiec, D., et al., *Differential expression of cell proliferation regulatory proteins in B- and T-lineage acute lymphoblastic leukaemias*. Br J Haematol, 1996. **95**(3): p. 518-23.
69. Wang, H., et al., *The metabolic function of cyclin D3-CDK6 kinase in cancer cell survival*. Nature, 2017. **546**(7658): p. 426-430.
70. Baughn, L.B., et al., *A novel orally active small molecule potently induces G1 arrest in primary myeloma cells and prevents tumor growth by specific inhibition of cyclin-dependent kinase 4/6*. Cancer Res, 2006. **66**(15): p. 7661-7.
71. Yoshida, A., E.K. Lee, and J.A. Diehl, *Induction of Therapeutic Senescence in Vemurafenib-Resistant Melanoma by Extended Inhibition of CDK4/6*. Cancer Res, 2016. **76**(10): p. 2990-3002.
72. Collier, H.A., *Cell biology. The essence of quiescence*. Science, 2011. **334**(6059): p. 1074-5.
73. Baisch, H., *Different quiescence states of three culture cell lines detected by acridine orange staining of cellular RNA*. Cytometry, 1988. **9**(4): p. 325-31.
74. Collier, H.A., L. Sang, and J.M. Roberts, *A new description of cellular quiescence*. PLoS Biol, 2006. **4**(3): p. e83.
75. Rodier, F. and J. Campisi, *Four faces of cellular senescence*. J Cell Biol, 2011. **192**(4): p. 547-56.
76. Hayflick, L., *The Limited in Vitro Lifetime of Human Diploid Cell Strains*. Exp Cell Res, 1965. **37**: p. 614-36.
77. Munoz-Espin, D., et al., *Programmed cell senescence during mammalian embryonic development*. Cell, 2013. **155**(5): p. 1104-18.
78. Storer, M., et al., *Senescence is a developmental mechanism that contributes to embryonic growth and patterning*. Cell, 2013. **155**(5): p. 1119-30.
79. van Deursen, J.M., *The role of senescent cells in ageing*. Nature, 2014. **509**(7501): p. 439-46.
80. Munoz-Espin, D. and M. Serrano, *Cellular senescence: from physiology to pathology*. Nat Rev Mol Cell Biol, 2014. **15**(7): p. 482-96.
81. Baker, D.J. and J.M. Sedivy, *Probing the depths of cellular senescence*. J Cell Biol, 2013. **202**(1): p. 11-3.
82. Nelson, D.M., et al., *A comparison of oncogene-induced senescence and replicative senescence: implications for tumor suppression and aging*. Age (Dordr), 2014. **36**(3): p. 9637.
83. Kuilman, T., et al., *The essence of senescence*. Genes Dev, 2010. **24**(22): p. 2463-79.
84. Sharpless, N.E. and C.J. Sherr, *Forging a signature of in vivo senescence*. Nat Rev Cancer, 2015. **15**(7): p. 397-408.
85. Neves, J., et al., *Of flies, mice, and men: evolutionarily conserved tissue damage responses and aging*. Dev Cell, 2015. **32**(1): p. 9-18.

86. Pasillas, M.P., et al., *Proteomic analysis reveals a role for Bcl2-associated athanogene 3 and major vault protein in resistance to apoptosis in senescent cells by regulating ERK1/2 activation*. Mol Cell Proteomics, 2015. **14**(1): p. 1-14.
87. Ryu, S.J. and S.C. Park, *Targeting major vault protein in senescence-associated apoptosis resistance*. Expert Opin Ther Targets, 2009. **13**(4): p. 479-84.
88. Xue, W., et al., *Senescence and tumour clearance is triggered by p53 restoration in murine liver carcinomas*. Nature, 2007. **445**(7128): p. 656-60.
89. Krizhanovsky, V., et al., *Senescence of activated stellate cells limits liver fibrosis*. Cell, 2008. **134**(4): p. 657-67.
90. Lujambio, A., et al., *Non-cell-autonomous tumor suppression by p53*. Cell, 2013. **153**(2): p. 449-60.
91. Fumagalli, M., et al., *Telomeric DNA damage is irreparable and causes persistent DNA-damage-response activation*. Nat Cell Biol, 2012. **14**(4): p. 355-65.
92. Hewitt, G., et al., *Telomeres are favoured targets of a persistent DNA damage response in ageing and stress-induced senescence*. Nat Commun, 2012. **3**: p. 708.
93. Chen, J.H., S.E. Ozanne, and C.N. Hales, *Methods of cellular senescence induction using oxidative stress*. Methods Mol Biol, 2007. **371**: p. 179-89.
94. d'Adda di Fagagna, F., *Living on a break: cellular senescence as a DNA-damage response*. Nat Rev Cancer, 2008. **8**(7): p. 512-22.
95. Courtois-Cox, S., S.L. Jones, and K. Cichowski, *Many roads lead to oncogene-induced senescence*. Oncogene, 2008. **27**(20): p. 2801-9.
96. te Poele, R.H., et al., *DNA damage is able to induce senescence in tumor cells in vitro and in vivo*. Cancer Res, 2002. **62**(6): p. 1876-83.
97. Zou, X., et al., *Cdk4 disruption renders primary mouse cells resistant to oncogenic transformation, leading to Arf/p53-independent senescence*. Genes Dev, 2002. **16**(22): p. 2923-34.
98. Campisi, J. and F. d'Adda di Fagagna, *Cellular senescence: when bad things happen to good cells*. Nat Rev Mol Cell Biol, 2007. **8**(9): p. 729-40.
99. Chang, B.D., et al., *Role of p53 and p21waf1/cip1 in senescence-like terminal proliferation arrest induced in human tumor cells by chemotherapeutic drugs*. Oncogene, 1999. **18**(34): p. 4808-18.
100. Rebbaa, A., et al., *Caspase inhibition switches doxorubicin-induced apoptosis to senescence*. Oncogene, 2003. **22**(18): p. 2805-11.
101. Paek, A.L., et al., *Cell-to-Cell Variation in p53 Dynamics Leads to Fractional Killing*. Cell, 2016. **165**(3): p. 631-42.
102. Purvis, J.E., et al., *p53 dynamics control cell fate*. Science, 2012. **336**(6087): p. 1440-4.
103. Wu, M., et al., *p53 dynamics orchestrates with binding affinity to target genes for cell fate decision*. Cell Death Dis, 2017. **8**(10): p. e3130.
104. Ventura, A., et al., *Restoration of p53 function leads to tumour regression in vivo*. Nature, 2007. **445**(7128): p. 661-5.
105. Khoo, K.H., C.S. Verma, and D.P. Lane, *Drugging the p53 pathway: understanding the route to clinical efficacy*. Nat Rev Drug Discov, 2014. **13**(3): p. 217-36.
106. Schmitt, E., et al., *DNA-damage response network at the crossroads of cell-cycle checkpoints, cellular senescence and apoptosis*. J Zhejiang Univ Sci B, 2007. **8**(6): p. 377-97.
107. Barretina, J., et al., *Subtype-specific genomic alterations define new targets for soft-tissue sarcoma therapy*. Nat Genet, 2010. **42**(8): p. 715-21.
108. Kovatcheva, M., et al., *ATRX is a regulator of therapy induced senescence in human cells*. Nat Commun, 2017. **8**(1): p. 386.
109. Guschin, D.Y., et al., *A rapid and general assay for monitoring endogenous gene modification*. Methods Mol Biol, 2010. **649**: p. 247-56.

110. Dobin, A., et al., *STAR: ultrafast universal RNA-seq aligner*. Bioinformatics, 2013. **29**(1): p. 15-21.
111. Subramanian, A., et al., *Gene set enrichment analysis: a knowledge-based approach for interpreting genome-wide expression profiles*. Proc Natl Acad Sci U S A, 2005. **102**(43): p. 15545-50.
112. Mootha, V.K., et al., *PGC-1alpha-responsive genes involved in oxidative phosphorylation are coordinately downregulated in human diabetes*. Nat Genet, 2003. **34**(3): p. 267-73.
113. Conyers, R., S. Young, and D.M. Thomas, *Liposarcoma: molecular genetics and therapeutics*. Sarcoma, 2011. **2011**: p. 483154.
114. Italiano, A., et al., *Clinical and biological significance of CDK4 amplification in well-differentiated and dedifferentiated liposarcomas*. Clin Cancer Res, 2009. **15**(18): p. 5696-703.
115. Italiano, A., et al., *Advanced well-differentiated/dedifferentiated liposarcomas: role of chemotherapy and survival*. Ann Oncol, 2012. **23**(6): p. 1601-7.
116. Van Glabbeke, M., et al., *Progression-free rate as the principal end-point for phase II trials in soft-tissue sarcomas*. Eur J Cancer, 2002. **38**(4): p. 543-9.
117. Singer, S., et al., *Histologic subtype and margin of resection predict pattern of recurrence and survival for retroperitoneal liposarcoma*. Ann Surg, 2003. **238**(3): p. 358-70; discussion 370-1.
118. Fakhrazadeh, S.S., S.P. Trusko, and D.L. George, *Tumorigenic potential associated with enhanced expression of a gene that is amplified in a mouse tumor cell line*. EMBO J, 1991. **10**(6): p. 1565-9.
119. Momand, J., et al., *The mdm-2 oncogene product forms a complex with the p53 protein and inhibits p53-mediated transactivation*. Cell, 1992. **69**(7): p. 1237-45.
120. Marchenko, N.D., et al., *Monoubiquitylation promotes mitochondrial p53 translocation*. EMBO J, 2007. **26**(4): p. 923-34.
121. Poyurovsky, M.V., et al., *The Mdm2 RING domain C-terminus is required for supramolecular assembly and ubiquitin ligase activity*. EMBO J, 2007. **26**(1): p. 90-101.
122. Boddy, M.N., P.S. Freemont, and K.L. Borden, *The p53-associated protein MDM2 contains a newly characterized zinc-binding domain called the RING finger*. Trends Biochem Sci, 1994. **19**(5): p. 198-9.
123. Fang, S., et al., *Mdm2 is a RING finger-dependent ubiquitin protein ligase for itself and p53*. J Biol Chem, 2000. **275**(12): p. 8945-51.
124. Levine, A.J., *p53, the cellular gatekeeper for growth and division*. Cell, 1997. **88**(3): p. 323-31.
125. Riley, M.F. and G. Lozano, *The Many Faces of MDM2 Binding Partners*. Genes Cancer, 2012. **3**(3-4): p. 226-39.
126. Zhao, Y., H. Yu, and W. Hu, *The regulation of MDM2 oncogene and its impact on human cancers*. Acta Biochim Biophys Sin (Shanghai), 2014. **46**(3): p. 180-9.
127. Mendrysa, S.M. and M.E. Perry, *The p53 tumor suppressor protein does not regulate expression of its own inhibitor, MDM2, except under conditions of stress*. Mol Cell Biol, 2000. **20**(6): p. 2023-30.
128. Roth, J., et al., *Nucleo-cytoplasmic shuttling of the hdm2 oncoprotein regulates the levels of the p53 protein via a pathway used by the human immunodeficiency virus rev protein*. EMBO J, 1998. **17**(2): p. 554-64.
129. Nihira, N.T., et al., *Acetylation-dependent regulation of MDM2 E3 ligase activity dictates its oncogenic function*. Sci Signal, 2017. **10**(466).
130. Inuzuka, H., et al., *Phosphorylation by casein kinase I promotes the turnover of the Mdm2 oncoprotein via the SCF(beta-TRCP) ubiquitin ligase*. Cancer Cell, 2010. **18**(2): p. 147-59.

131. Cummins, J.M. and B. Vogelstein, *HAUSP is required for p53 destabilization*. Cell Cycle, 2004. **3**(6): p. 689-92.
132. Linares, L.K., et al., *Intrinsic ubiquitination activity of PCAF controls the stability of the oncoprotein Hdm2*. Nat Cell Biol, 2007. **9**(3): p. 331-8.
133. Jung, C.R., et al., *Enigma negatively regulates p53 through MDM2 and promotes tumor cell survival in mice*. J Clin Invest, 2010. **120**(12): p. 4493-506.
134. Higashitsuji, H., et al., *The oncoprotein gankyrin binds to MDM2/HDM2, enhancing ubiquitylation and degradation of p53*. Cancer Cell, 2005. **8**(1): p. 75-87.
135. Xu, C., C.D. Fan, and X. Wang, *Regulation of Mdm2 protein stability and the p53 response by NEDD4-1 E3 ligase*. Oncogene, 2015. **34**(3): p. 281-9.
136. Li, M., et al., *A dynamic role of HAUSP in the p53-Mdm2 pathway*. Mol Cell, 2004. **13**(6): p. 879-86.
137. Brooks, C.L., et al., *The p53--Mdm2--HAUSP complex is involved in p53 stabilization by HAUSP*. Oncogene, 2007. **26**(51): p. 7262-6.
138. Fanning, A.S. and J.M. Anderson, *Protein-protein interactions: PDZ domain networks*. Curr Biol, 1996. **6**(11): p. 1385-8.
139. Krcmery, J., et al., *Nucleocytoplasmic functions of the PDZ-LIM protein family: new insights into organ development*. Bioessays, 2010. **32**(2): p. 100-8.
140. Urban, A.E., et al., *Pdlim7 Regulates Arf6-Dependent Actin Dynamics and Is Required for Platelet-Mediated Thrombosis in Mice*. PLoS One, 2016. **11**(10): p. e0164042.
141. Gullberg, M. and A.-C. Andersson, *Visualization and quantification of protein-protein interactions in cells and tissues*. Nature Methods, 2010. **7**.
142. Halbleib, J.M. and W.J. Nelson, *Cadherins in development: cell adhesion, sorting, and tissue morphogenesis*. Genes Dev, 2006. **20**(23): p. 3199-214.
143. van Roy, F., *Beyond E-cadherin: roles of other cadherin superfamily members in cancer*. Nat Rev Cancer, 2014. **14**(2): p. 121-34.
144. Kanojia, D., et al., *Genomic landscape of liposarcoma*. Oncotarget, 2015. **6**(40): p. 42429-44.
145. Momand, J., et al., *The MDM2 gene amplification database*. Nucleic Acids Res, 1998. **26**(15): p. 3453-9.
146. Song, M.S., et al., *The tumour suppressor RASSF1A promotes MDM2 self-ubiquitination by disrupting the MDM2-DAXX-HAUSP complex*. EMBO J, 2008. **27**(13): p. 1863-74.
147. Tang, J., et al., *Critical role for Daxx in regulating Mdm2*. Nat Cell Biol, 2006. **8**(8): p. 855-62.
148. Tang, J., et al., *A novel transcription regulatory complex containing death domain-associated protein and the ATR-X syndrome protein*. J Biol Chem, 2004. **279**(19): p. 20369-77.
149. te Velthuis, A.J. and C.P. Bagowski, *PDZ and LIM domain-encoding genes: molecular interactions and their role in development*. ScientificWorldJournal, 2007. **7**: p. 1470-92.
150. Demontis, F., B. Habermann, and C. Dahmann, *PDZ-domain-binding sites are common among cadherins*. Dev Genes Evol, 2006. **216**(11): p. 737-41.
151. Gujral, T.S., et al., *Family-wide investigation of PDZ domain-mediated protein-protein interactions implicates beta-catenin in maintaining the integrity of tight junctions*. Chem Biol, 2013. **20**(6): p. 816-27.
152. Chetty, R. and S. Serra, *Membrane loss and aberrant nuclear localization of E-cadherin are consistent features of solid pseudopapillary tumour of the pancreas. An immunohistochemical study using two antibodies recognizing different domains of the E-cadherin molecule*. Histopathology, 2008. **52**(3): p. 325-30.
153. Takauji, S.R., et al., *Expression and subcellular localization of E-cadherin, alpha-catenin, and beta-catenin in 8 feline mammary tumor cell lines*. J Vet Med Sci, 2007. **69**(8): p. 831-4.

154. Berx, G. and F. van Roy, *Involvement of members of the cadherin superfamily in cancer*. Cold Spring Harb Perspect Biol, 2009. **1**(6): p. a003129.
155. Zhou, P., et al., *The epithelial to mesenchymal transition (EMT) and cancer stem cells: implication for treatment resistance in pancreatic cancer*. Mol Cancer, 2017. **16**(1): p. 52.
156. Jeanes, A., C.J. Gottardi, and A.S. Yap, *Cadherins and cancer: how does cadherin dysfunction promote tumor progression?* Oncogene, 2008. **27**(55): p. 6920-9.
157. Shibata, T., et al., *Identification of human cadherin-14, a novel neurally specific type II cadherin, by protein interaction cloning*. J Biol Chem, 1997. **272**(8): p. 5236-40.
158. D'Assoro, A.B., et al., *Abrogation of p53 function leads to metastatic transcriptome networks that typify tumor progression in human breast cancer xenografts*. Int J Oncol, 2010. **37**(5): p. 1167-76.
159. Weiland L, B.M., Arden KC, Ammermuller T, Bogatz S, Viars CS, and Rajewsky MF, *Allelic deletion mapping on chromosome 5 in human lung carcinomas*. Oncogene, 1996. **12**: p. 97-102.
160. Chalmers, I.J., H. Hofler, and M.J. Atkinson, *Mapping of a cadherin gene cluster to a region of chromosome 5 subject to frequent allelic loss in carcinoma*. Genomics, 1999. **57**(1): p. 160-3.
161. O'Leary, B., R.S. Finn, and N.C. Turner, *Treating cancer with selective CDK4/6 inhibitors*. Nat Rev Clin Oncol, 2016. **13**(7): p. 417-30.
162. Gray, J.V., et al., *"Sleeping beauty": quiescence in Saccharomyces cerevisiae*. Microbiol Mol Biol Rev, 2004. **68**(2): p. 187-206.
163. Subramaniam, S., et al., *Distinct transcriptional networks in quiescent myoblasts: a role for Wnt signaling in reversible vs. irreversible arrest*. PLoS One, 2014. **8**(6): p. e65097.
164. Evertts, A.G., et al., *H4K20 methylation regulates quiescence and chromatin compaction*. Mol Biol Cell, 2013. **24**(19): p. 3025-37.
165. Srivastava, S., et al., *Distinguishing States of Arrest: Genome-Wide Descriptions of Cellular Quiescence Using ChIP-Seq and RNA-Seq Analysis*. Methods Mol Biol, 2018. **1686**: p. 215-239.
166. Yao, G., *Modelling mammalian cellular quiescence*. Interface Focus, 2014. **4**(3): p. 20130074.
167. Sharpless, N.E. and R.A. DePinho, *Telomeres, stem cells, senescence, and cancer*. J Clin Invest, 2004. **113**(2): p. 160-8.
168. Campisi, J., *Aging, cellular senescence, and cancer*. Annu Rev Physiol, 2013. **75**: p. 685-705.
169. Blagosklonny, M.V., *Cell cycle arrest is not yet senescence, which is not just cell cycle arrest: terminology for TOR-driven aging*. Aging (Albany NY), 2012. **4**(3): p. 159-65.
170. Imai, Y., et al., *Crosstalk between the Rb pathway and AKT signaling forms a quiescence-senescence switch*. Cell Rep, 2014. **7**(1): p. 194-207.
171. Cheung, T.H. and T.A. Rando, *Molecular regulation of stem cell quiescence*. Nat Rev Mol Cell Biol, 2013. **14**(6): p. 329-40.
172. Schug, T.T., *mTOR favors senescence over quiescence in p53-arrested cells*. Aging (Albany NY), 2010. **2**(6): p. 327-8.
173. Terzi, M.Y., M. Izmirlı, and B. Gogebakan, *The cell fate: senescence or quiescence*. Mol Biol Rep, 2016. **43**(11): p. 1213-1220.
174. Dulic, V., *Senescence regulation by mTOR*. Methods Mol Biol, 2013. **965**: p. 15-35.
175. Chen, J.H. and S.E. Ozanne, *Deep senescent human fibroblasts show diminished DNA damage foci but retain checkpoint capacity to oxidative stress*. FEBS Lett, 2006. **580**(28-29): p. 6669-73.
176. Ivanov, A., et al., *Lysosome-mediated processing of chromatin in senescence*. J Cell Biol, 2013. **202**(1): p. 129-43.

177. De Cecco, M., et al., *Genomes of replicatively senescent cells undergo global epigenetic changes leading to gene silencing and activation of transposable elements*. *Aging Cell*, 2013. **12**(2): p. 247-56.
178. Carnero, A., *Markers of cellular senescence*. *Methods Mol Biol*, 2013. **965**: p. 63-81.
179. Hernandez-Segura, A., J. Nehme, and M. Demaria, *Hallmarks of Cellular Senescence*. *Trends Cell Biol*, 2018.
180. Chien, Y., et al., *Control of the senescence-associated secretory phenotype by NF-kappaB promotes senescence and enhances chemosensitivity*. *Genes Dev*, 2011. **25**(20): p. 2125-36.
181. Kuilman, T., et al., *Oncogene-induced senescence relayed by an interleukin-dependent inflammatory network*. *Cell*, 2008. **133**(6): p. 1019-31.
182. Coppe, J.P., et al., *The senescence-associated secretory phenotype: the dark side of tumor suppression*. *Annu Rev Pathol*, 2010. **5**: p. 99-118.
183. Ryu, S.J., Y.S. Oh, and S.C. Park, *Failure of stress-induced downregulation of Bcl-2 contributes to apoptosis resistance in senescent human diploid fibroblasts*. *Cell Death Differ*, 2007. **14**(5): p. 1020-8.
184. Wiley, C.D., et al., *Analysis of individual cells identifies cell-to-cell variability following induction of cellular senescence*. *Aging Cell*, 2017. **16**(5): p. 1043-1050.
185. Love, M.I., W. Huber, and S. Anders, *Moderated estimation of fold change and dispersion for RNA-seq data with DESeq2*. *Genome Biol*, 2014. **15**(12): p. 550.
186. Bunt, J., et al., *Regulation of cell cycle genes and induction of senescence by overexpression of OTX2 in medulloblastoma cell lines*. *Mol Cancer Res*, 2010. **8**(10): p. 1344-57.
187. Blagosklonny, M.V., *Aging and immortality: quasi-programmed senescence and its pharmacologic inhibition*. *Cell Cycle*, 2006. **5**(18): p. 2087-102.
188. Ozcan, S., et al., *Unbiased analysis of senescence-associated secretory phenotype (SASP) to identify common components following different genotoxic stresses*. *Aging (Albany NY)*, 2016. **8**(7): p. 1316-29.
189. Acosta, J.C., et al., *Chemokine signaling via the CXCR2 receptor reinforces senescence*. *Cell*, 2008. **133**(6): p. 1006-18.
190. Chen, H., et al., *MacroH2A1 and ATM Play Opposing Roles in Paracrine Senescence and the Senescence-Associated Secretory Phenotype*. *Mol Cell*, 2015. **59**(5): p. 719-31.
191. Coppe, J.P., et al., *A human-like senescence-associated secretory phenotype is conserved in mouse cells dependent on physiological oxygen*. *PLoS One*, 2010. **5**(2): p. e9188.
192. Coppe, J.P., et al., *Senescence-associated secretory phenotypes reveal cell-nonautonomous functions of oncogenic RAS and the p53 tumor suppressor*. *PLoS Biol*, 2008. **6**(12): p. 2853-68.
193. Kuilman, T. and D.S. Peeper, *Senescence-messaging secretome: SMS-ing cellular stress*. *Nat Rev Cancer*, 2009. **9**(2): p. 81-94.
194. Lackner, D.H., et al., *A genomics approach identifies senescence-specific gene expression regulation*. *Aging Cell*, 2014. **13**(5): p. 946-50.
195. Pribluda, A., et al., *A senescence-inflammatory switch from cancer-inhibitory to cancer-promoting mechanism*. *Cancer Cell*, 2013. **24**(2): p. 242-56.
196. Dohi, Y., et al., *Bach1 inhibits oxidative stress-induced cellular senescence by impeding p53 function on chromatin*. *Nat Struct Mol Biol*, 2008. **15**(12): p. 1246-54.
197. Ohtani, N., et al., *Opposing effects of Ets and Id proteins on p16INK4a expression during cellular senescence*. *Nature*, 2001. **409**(6823): p. 1067-70.
198. Orjalo, A.V., et al., *Cell surface-bound IL-1alpha is an upstream regulator of the senescence-associated IL-6/IL-8 cytokine network*. *Proc Natl Acad Sci U S A*, 2009. **106**(40): p. 17031-6.

199. Demidenko, Z.N. and M.V. Blagosklonny, *Growth stimulation leads to cellular senescence when the cell cycle is blocked*. Cell Cycle, 2008. **7**(21): p. 3355-61.
200. Blagosklonny, M.V., *Geroconversion: irreversible step to cellular senescence*. Cell Cycle, 2014. **13**(23): p. 3628-35.
201. Rochette, P.J. and D.E. Brash, *Progressive apoptosis resistance prior to senescence and control by the anti-apoptotic protein BCL-xL*. Mech Ageing Dev, 2008. **129**(4): p. 207-14.
202. Sanders, Y.Y., et al., *Histone modifications in senescence-associated resistance to apoptosis by oxidative stress*. Redox Biol, 2013. **1**: p. 8-16.
203. Hampel, B., et al., *Apoptosis resistance of senescent human fibroblasts is correlated with the absence of nuclear IGFBP-3*. Aging Cell, 2005. **4**(6): p. 325-30.
204. Severino, V., et al., *Insulin-like growth factor binding proteins 4 and 7 released by senescent cells promote premature senescence in mesenchymal stem cells*. Cell Death Dis, 2013. **4**: p. e911.
205. Wajapeyee, N., et al., *Oncogenic BRAF induces senescence and apoptosis through pathways mediated by the secreted protein IGFBP7*. Cell, 2008. **132**(3): p. 363-74.
206. Benatar, T., et al., *IGFBP7 reduces breast tumor growth by induction of senescence and apoptosis pathways*. Breast Cancer Res Treat, 2012. **133**(2): p. 563-73.
207. Kim, K.S., et al., *Regulation of replicative senescence by insulin-like growth factor-binding protein 3 in human umbilical vein endothelial cells*. Aging Cell, 2007. **6**(4): p. 535-45.
208. Elzi, D.J., et al., *Plasminogen activator inhibitor 1--insulin-like growth factor binding protein 3 cascade regulates stress-induced senescence*. Proc Natl Acad Sci U S A, 2012. **109**(30): p. 12052-7.
209. Acosta, J.C., et al., *A complex secretory program orchestrated by the inflammasome controls paracrine senescence*. Nat Cell Biol, 2013. **15**(8): p. 978-90.
210. Tasmimir, N. and S.W. Lowe, *Senescent cells spread the word: non-cell autonomous propagation of cellular senescence*. EMBO J, 2013. **32**(14): p. 1975-6.
211. Krtolica, A., et al., *Senescent fibroblasts promote epithelial cell growth and tumorigenesis: a link between cancer and aging*. Proc Natl Acad Sci U S A, 2001. **98**(21): p. 12072-7.
212. Mosteiro, L., et al., *Tissue damage and senescence provide critical signals for cellular reprogramming in vivo*. Science, 2016. **354**(6315).
213. Ocampo, A., et al., *In Vivo Amelioration of Age-Associated Hallmarks by Partial Reprogramming*. Cell, 2016. **167**(7): p. 1719-1733 e12.
214. Chiche, A., et al., *Injury-Induced Senescence Enables In Vivo Reprogramming in Skeletal Muscle*. Cell Stem Cell, 2017. **20**(3): p. 407-414 e4.
215. Ritschka, B., et al., *The senescence-associated secretory phenotype induces cellular plasticity and tissue regeneration*. Genes Dev, 2017. **31**(2): p. 172-183.
216. Jun, J.I. and L.F. Lau, *The matricellular protein CCN1 induces fibroblast senescence and restricts fibrosis in cutaneous wound healing*. Nat Cell Biol, 2010. **12**(7): p. 676-85.
217. Demaria, M., et al., *An essential role for senescent cells in optimal wound healing through secretion of PDGF-AA*. Dev Cell, 2014. **31**(6): p. 722-33.
218. Tasmimir, N., et al., *BRD4 Connects Enhancer Remodeling to Senescence Immune Surveillance*. Cancer Discov, 2016. **6**(6): p. 612-29.
219. Takahashi, A., et al., *DNA damage signaling triggers degradation of histone methyltransferases through APC/C(Cdh1) in senescent cells*. Mol Cell, 2012. **45**(1): p. 123-31.
220. Contrepois, K., et al., *Histone variant H2A.J accumulates in senescent cells and promotes inflammatory gene expression*. Nat Commun, 2017. **8**: p. 14995.

221. Aird, K.M., et al., *HMGB2 orchestrates the chromatin landscape of senescence-associated secretory phenotype gene loci*. J Cell Biol, 2016. **215**(3): p. 325-334.
222. Jin, F., et al., *A high-resolution map of the three-dimensional chromatin interactome in human cells*. Nature, 2013. **503**(7475): p. 290-4.
223. Hoare, M., et al., *NOTCH1 mediates a switch between two distinct secretomes during senescence*. Nat Cell Biol, 2016. **18**(9): p. 979-92.
224. Andre, T., et al., *Evidences of early senescence in multiple myeloma bone marrow mesenchymal stromal cells*. PLoS One, 2013. **8**(3): p. e59756.
225. Florea, V., et al., *c-Myc is essential to prevent endothelial pro-inflammatory senescent phenotype*. PLoS One, 2013. **8**(9): p. e73146.
226. Nakamoto, M., et al., *The Glucocorticoid Receptor Regulates the ANGPTL4 Gene in a CTCF-Mediated Chromatin Context in Human Hepatic Cells*. PLoS One, 2017. **12**(1): p. e0169225.
227. Hsieh, H.Y., et al., *Epigenetic silencing of the dual-role signal mediator, ANGPTL4 in tumor tissues and its overexpression in the urothelial carcinoma microenvironment*. Oncogene, 2018. **37**(5): p. 673-686.
228. Inoue, T., et al., *Cross-enhancement of ANGPTL4 transcription by HIF1 alpha and PPAR beta/delta is the result of the conformational proximity of two response elements*. Genome Biol, 2014. **15**(4): p. R63.
229. Ratnakumar, K., et al., *ATRX-mediated chromatin association of histone variant macroH2A1 regulates alpha-globin expression*. Genes Dev, 2012. **26**(5): p. 433-8.
230. Kim, I., et al., *Hepatic expression, synthesis and secretion of a novel fibrinogen/angiopoietin-related protein that prevents endothelial-cell apoptosis*. Biochem J, 2000. **346 Pt 3**: p. 603-10.
231. Zhu, P., et al., *Angiopoietin-like 4 protein elevates the prosurvival intracellular O2(-):H2O2 ratio and confers anoikis resistance to tumors*. Cancer Cell, 2011. **19**(3): p. 401-15.
232. Tan, Z.W., et al., *ANGPTL4 T266M variant is associated with reduced cancer invasiveness*. Biochim Biophys Acta, 2017. **1864**(10): p. 1525-1536.
233. La Paglia, L., et al., *Potential Role of ANGPTL4 in the Cross Talk between Metabolism and Cancer through PPAR Signaling Pathway*. PPAR Res, 2017. **2017**: p. 8187235.
234. Kim, S.H., et al., *ANGPTL4 induction by prostaglandin E2 under hypoxic conditions promotes colorectal cancer progression*. Cancer Res, 2011. **71**(22): p. 7010-20.
235. Le Jan, S., et al., *Angiopoietin-like 4 is a proangiogenic factor produced during ischemia and in conventional renal cell carcinoma*. Am J Pathol, 2003. **162**(5): p. 1521-8.
236. Ito, Y., et al., *Inhibition of angiogenesis and vascular leakiness by angiopoietin-related protein 4*. Cancer Res, 2003. **63**(20): p. 6651-7.
237. Padua, D., et al., *TGFbeta primes breast tumors for lung metastasis seeding through angiopoietin-like 4*. Cell, 2008. **133**(1): p. 66-77.
238. Huang, R.L., et al., *ANGPTL4 modulates vascular junction integrity by integrin signaling and disruption of intercellular VE-cadherin and claudin-5 clusters*. Blood, 2011. **118**(14): p. 3990-4002.
239. Galaup, A., et al., *Angiopoietin-like 4 prevents metastasis through inhibition of vascular permeability and tumor cell motility and invasiveness*. Proc Natl Acad Sci U S A, 2006. **103**(49): p. 18721-6.
240. Tan, M.J., et al., *Emerging roles of angiopoietin-like 4 in human cancer*. Mol Cancer Res, 2012. **10**(6): p. 677-88.
241. Morgan, D.O., *SnapShot: Cell-cycle regulators II*. Cell, 2008. **135**(5): p. 974-974 e1.
242. Morgan, D.O., *SnapShot: cell-cycle regulators I*. Cell, 2008. **135**(4): p. 764-764 e1.
243. Braig, M. and C.A. Schmitt, *Oncogene-induced senescence: putting the brakes on tumor development*. Cancer Res, 2006. **66**(6): p. 2881-4.

244. Ohtani, N. and E. Hara, *Roles and mechanisms of cellular senescence in regulation of tissue homeostasis*. *Cancer Sci*, 2013. **104**(5): p. 525-30.
245. Toso, A., et al., *Enhancing chemotherapy efficacy in Pten-deficient prostate tumors by activating the senescence-associated antitumor immunity*. *Cell Rep*, 2014. **9**(1): p. 75-89.
246. Davalos, A.R., et al., *Senescent cells as a source of inflammatory factors for tumor progression*. *Cancer Metastasis Rev*, 2010. **29**(2): p. 273-83.
247. Ruhland, M.K., et al., *Stromal senescence establishes an immunosuppressive microenvironment that drives tumorigenesis*. *Nat Commun*, 2016. **7**: p. 11762.
248. Ruhland, M.K., L.M. Coussens, and S.A. Stewart, *Senescence and cancer: An evolving inflammatory paradox*. *Biochim Biophys Acta*, 2016. **1865**(1): p. 14-22.
249. Milanovic, M., et al., *Senescence-associated reprogramming promotes cancer stemness*. *Nature*, 2018. **553**(7686): p. 96-100.
250. Chang, J., et al., *Clearance of senescent cells by ABT263 rejuvenates aged hematopoietic stem cells in mice*. *Nat Med*, 2016. **22**(1): p. 78-83.
251. Yosef, R., et al., *Directed elimination of senescent cells by inhibition of BCL-W and BCL-XL*. *Nat Commun*, 2016. **7**: p. 11190.
252. Herman, A.G., et al., *Discovery of Mdm2-MdmX E3 ligase inhibitors using a cell-based ubiquitination assay*. *Cancer Discov*, 2011. **1**(4): p. 312-25.
253. Wade, M., et al., *Functional analysis and consequences of Mdm2 E3 ligase inhibition in human tumor cells*. *Oncogene*, 2012. **31**(45): p. 4789-97.
254. Appels, N.M., J.H. Beijnen, and J.H. Schellens, *Development of farnesyl transferase inhibitors: a review*. *Oncologist*, 2005. **10**(8): p. 565-78.
255. Dehghan-Paz, I., et al., *Tipifarnib and farnesyltransferase inhibitors in the treatment of inflammatory breast cancer: is the story over? A review*. *Orphan Drugs: Research and Reviews*, 2013. **3**: p. 11-21.
256. Mesa, R.A., *Tipifarnib: farnesyl transferase inhibition at a crossroads*. *Expert Review of Anticancer Therapy*, 2014(3): p. 313-319.
257. GM, C., *Cell Proliferation in Development and Differentiation*, in *The Cell: A Molecular Approach*. 2000, Sinauer Associates: Sunderland, MA.
258. Claycomb, W.C., *Control of cardiac muscle cell division*. *Trends Cardiovasc Med*, 1992. **2**(6): p. 231-6.
259. Boulais, P.E. and P.S. Frenette, *Making sense of hematopoietic stem cell niches*. *Blood*, 2015. **125**(17): p. 2621-9.
260. Weinstein, G.D., J.L. McCullough, and P. Ross, *Cell proliferation in normal epidermis*. *J Invest Dermatol*, 1984. **82**(6): p. 623-8.
261. Vermeulen, L. and H.J. Snippert, *Stem cell dynamics in homeostasis and cancer of the intestine*. *Nat Rev Cancer*, 2014. **14**(7): p. 468-80.
262. Umar, S., *Intestinal stem cells*. *Curr Gastroenterol Rep*, 2010. **12**(5): p. 340-8.
263. Pietras, E.M., M.R. Warr, and E. Passegue, *Cell cycle regulation in hematopoietic stem cells*. *J Cell Biol*, 2011. **195**(5): p. 709-20.
264. Foudi, A., et al., *Analysis of histone 2B-GFP retention reveals slowly cycling hematopoietic stem cells*. *Nat Biotechnol*, 2009. **27**(1): p. 84-90.
265. Wilson, A., et al., *Hematopoietic stem cells reversibly switch from dormancy to self-renewal during homeostasis and repair*. *Cell*, 2008. **135**(6): p. 1118-29.
266. Li, L. and H. Clevers, *Coexistence of quiescent and active adult stem cells in mammals*. *Science*, 2010. **327**(5965): p. 542-5.
267. Galloway, A., et al., *RNA-binding proteins ZFP36L1 and ZFP36L2 promote cell quiescence*. *Science*, 2016. **352**(6284): p. 453-9.
268. Darby, I.A., et al., *Fibroblasts and myofibroblasts in wound healing*. *Clin Cosmet Investig Dermatol*, 2014. **7**: p. 301-11.

269. Singer, A.J. and R.A. Clark, *Cutaneous wound healing*. N Engl J Med, 1999. **341**(10): p. 738-46.
270. Miyaoka, Y. and A. Miyajima, *To divide or not to divide: revisiting liver regeneration*. Cell Div, 2013. **8**(1): p. 8.
271. Jeremy, J.Y., et al., *Nitric oxide and the proliferation of vascular smooth muscle cells*. Cardiovasc Res, 1999. **43**(3): p. 580-94.
272. Siegel, A.L., P.K. Kuhlmann, and D.D. Cornelison, *Muscle satellite cell proliferation and association: new insights from myofiber time-lapse imaging*. Skelet Muscle, 2011. **1**(1): p. 7.
273. Adams, G.R., *Satellite cell proliferation and skeletal muscle hypertrophy*. Appl Physiol Nutr Metab, 2006. **31**(6): p. 782-90.
274. Yue, F., et al., *Pten is necessary for the quiescence and maintenance of adult muscle stem cells*. Nat Commun, 2017. **8**: p. 14328.
275. Johnson, K., et al., *IL-7 functionally segregates the pro-B cell stage by regulating transcription of recombination mediators across cell cycle*. J Immunol, 2012. **188**(12): p. 6084-92.
276. Eliasson, P. and J.I. Jonsson, *The hematopoietic stem cell niche: low in oxygen but a nice place to be*. J Cell Physiol, 2010. **222**(1): p. 17-22.
277. Agudo, J., et al., *Quiescent Tissue Stem Cells Evade Immune Surveillance*. Immunity, 2018. **48**(2): p. 271-285 e5.
278. Aguirre-Ghiso, J.A., *Models, mechanisms and clinical evidence for cancer dormancy*. Nat Rev Cancer, 2007. **7**(11): p. 834-46.
279. Ghajar, C.M., *Metastasis prevention by targeting the dormant niche*. Nat Rev Cancer, 2015. **15**(4): p. 238-47.
280. Miles, S., et al., *Xbp1 directs global repression of budding yeast transcription during the transition to quiescence and is important for the longevity and reversibility of the quiescent state*. PLoS Genet, 2013. **9**(10): p. e1003854.
281. Sang, L., H.A. Collier, and J.M. Roberts, *Control of the reversibility of cellular quiescence by the transcriptional repressor HES1*. Science, 2008. **321**(5892): p. 1095-100.
282. Sousa-Victor, P., et al., *Geriatric muscle stem cells switch reversible quiescence into senescence*. Nature, 2014. **506**(7488): p. 316-21.
283. Beerman, I., et al., *Stem cells and the aging hematopoietic system*. Curr Opin Immunol, 2010. **22**(4): p. 500-6.
284. Rossi, D.J., et al., *Cell intrinsic alterations underlie hematopoietic stem cell aging*. Proc Natl Acad Sci U S A, 2005. **102**(26): p. 9194-9.
285. Janzen, V., et al., *Stem-cell ageing modified by the cyclin-dependent kinase inhibitor p16INK4a*. Nature, 2006. **443**(7110): p. 421-6.
286. Attema, J.L., et al., *Hematopoietic stem cell ageing is uncoupled from p16 INK4A-mediated senescence*. Oncogene, 2009. **28**(22): p. 2238-43.
287. Crespo, J., et al., *T cell anergy, exhaustion, senescence, and stemness in the tumor microenvironment*. Curr Opin Immunol, 2013. **25**(2): p. 214-21.
288. Liton, P.B., et al., *Cellular senescence in the glaucomatous outflow pathway*. Exp Gerontol, 2005. **40**(8-9): p. 745-8.
289. Martin, J.A. and J.A. Buckwalter, *Aging, articular cartilage chondrocyte senescence and osteoarthritis*. Biogerontology, 2002. **3**(5): p. 257-64.
290. Palmer, A.K., et al., *Cellular Senescence in Type 2 Diabetes: A Therapeutic Opportunity*. Diabetes, 2015. **64**(7): p. 2289-98.
291. Childs, B.G., et al., *Cellular senescence in aging and age-related disease: from mechanisms to therapy*. Nat Med, 2015. **21**(12): p. 1424-35.

292. McHugh, D. and J. Gil, *Senescence and aging: Causes, consequences, and therapeutic avenues*. J Cell Biol, 2018. **217**(1): p. 65-77.
293. Baker, D.J., et al., *Clearance of p16Ink4a-positive senescent cells delays ageing-associated disorders*. Nature, 2011. **479**(7372): p. 232-6.
294. Baker, D.J., et al., *Naturally occurring p16(Ink4a)-positive cells shorten healthy lifespan*. Nature, 2016. **530**(7589): p. 184-9.
295. Soto-Gamez, A. and M. Demaria, *Therapeutic interventions for aging: the case of cellular senescence*. Drug Discov Today, 2017. **22**(5): p. 786-795.
296. Burton, D.G.A. and A. Stolzing, *Cellular senescence: Immunosurveillance and future immunotherapy*. Ageing Res Rev, 2018. **43**: p. 17-25.
297. Aw, D., A.B. Silva, and D.B. Palmer, *Immunosenescence: emerging challenges for an ageing population*. Immunology, 2007. **120**(4): p. 435-46.
298. Ventura, M.T., et al., *Immunosenescence in aging: between immune cells depletion and cytokines up-regulation*. Clin Mol Allergy, 2017. **15**: p. 21.
299. Pawelec, G., *Age and immunity: What is "immunosenescence"?* Exp Gerontol, 2018. **105**: p. 4-9.